

Fall 2010

## A Three-Year Study of the Magnetic Field Fluctuations in the Magnetospheric Cusp

Christina Seiman Chu

*Embry-Riddle Aeronautical University - Daytona Beach*

Follow this and additional works at: <https://commons.erau.edu/db-theses>



Part of the [Physical Sciences and Mathematics Commons](#)

---

### Scholarly Commons Citation

Chu, Christina Seiman, "A Three-Year Study of the Magnetic Field Fluctuations in the Magnetospheric Cusp" (2010). *Theses - Daytona Beach*. 32.

<https://commons.erau.edu/db-theses/32>

This thesis is brought to you for free and open access by Embry-Riddle Aeronautical University – Daytona Beach at ERAU Scholarly Commons. It has been accepted for inclusion in the Theses - Daytona Beach collection by an authorized administrator of ERAU Scholarly Commons. For more information, please contact [commons@erau.edu](mailto:commons@erau.edu).

A THREE-YEAR STUDY OF THE MAGNETIC FIELD  
FLUCTUATIONS IN THE MAGNETOSPHERIC CUSP

By  
Christina Seiman Chu

A Thesis Submitted to the  
Physical Sciences Department  
In Partital Fulfillment of the Requirements for the Degree of  
Master of Science in Engineering Physics

Embry-Riddle Aeronautical University  
Daytona Beach, Florida  
Fall 2010



UMI Number: EP31912

### INFORMATION TO USERS

The quality of this reproduction is dependent upon the quality of the copy submitted. Broken or indistinct print, colored or poor quality illustrations and photographs, print bleed-through, substandard margins, and improper alignment can adversely affect reproduction.

In the unlikely event that the author did not send a complete manuscript and there are missing pages, these will be noted. Also, if unauthorized copyright material had to be removed, a note will indicate the deletion.



---

UMI Microform EP31912  
Copyright 2011 by ProQuest LLC  
All rights reserved. This microform edition is protected against  
unauthorized copying under Title 17, United States Code.

---

ProQuest LLC  
789 East Eisenhower Parkway  
P.O. Box 1346  
Ann Arbor, MI 48106-1346

© Copyright by Christina Seiman Chu 2010  
All Rights Reserved

# A THREE-YEAR STUDY OF THE MAGNETIC FIELD FLUCTUATIONS IN THE MAGNETOSPHERIC CUSP

by

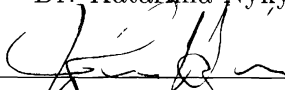
Christina Seiman Chu

This thesis was prepared under the direction of the candidate's thesis committee chair, Dr. Katariina Nykyri, Department of Physical Sciences, and has been approved by the members of the thesis committee. It was submitted to the Department of Physical Sciences and was accepted in partial fulfillment of the requirements of the Degree of Master of Science in Engineering Physics

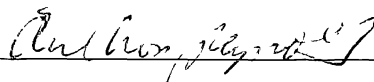
## THESIS COMMITTEE:




Dr. Katariina Nykyri, Chair



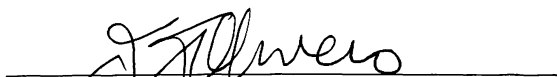
Dr. John Hughes, Member



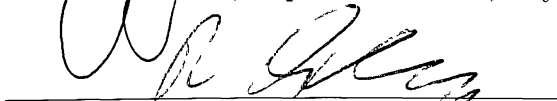
Dr. Anthony Reynolds, Member



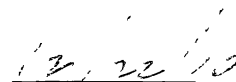
Dr. Peter Erdman, MSEP Graduate Program Coordinator



Dr. John Olivero, Department Chair, Physical Sciences



Dr. James Cunningham, Associate V.P. for Academics



Date

## ABSTRACT

Author: Christina Seiman Chu  
Title: A Three-Year Study of the Magnetic Field Fluctuations  
in the Magnetospheric Cusp  
Institution: Embry-Riddle Aeronautical University  
Degree: Master of Science in Engineering Physics  
Year: 2010

The high-altitude magnetospheric cusps are regions of significant magnetic field turbulence. There are also magnetic field fluctuations that cannot be called turbulence. Some of the low frequency fluctuations observed in the cusp have been shown to be motion of the cusp structure by the spacecraft (back and forth motion of the boundaries surrounding the cusp); others are transient reconnection signatures or flux transfer events (FTEs). Turbulence is important to understand because it has been proposed as a mechanism for particle energization in the cusps to MeV levels. High resolution magnetic field data from the Fluxgate Magnetometer instruments on the Cluster satellites were used to statistically map the power of the magnetic field fluctuations in the frequency ranges of 0.017-10 Hz, 0.017-0.1 Hz, and 0.1-10 Hz for the high-altitude cusp and surrounding boundaries for northward, southward, and all interplanetary magnetic field clock angle orientations by using three years of Cluster data, 118 northern hemisphere cusp crossings, from 2001-2003. The mean (compressive), total, and perpendicular (transverse) power were calculated. Analysis was done to check whether the locations of enhanced power were statistically consistent with the locations of crossing of cusp boundaries and diamagnetic cavities. Sources of power in all frequency ranges studied, 0.017-10 Hz, include reconnection, a gradient in the magnetic field strength when moving from the magnetosphere to the magnetosheath, and possibly the earthward propagation of magnetotail reconnection fluctuations. Sources of wave power from 0.017-0.1 Hz include mirror mode,

ion-cyclotron, and Alfvén waves. Sources of wave power from 0.1-10 Hz include ion-cyclotron and Alfvén waves.

## ACKNOWLEDGEMENT

The thesis writing process wraps up my time at Embry-Riddle and I have to say that I will miss roaming these halls. The people that have been a part of my life are truly cherished.

First and foremost, I would like to thank my thesis advisor Katariina Nykyri for her support in making this body of work possible. I am really lucky to have been able to work with her. Her guidance, helpful interpretation of the data, and many hours spent helping me prepare my thesis deserves more than just my thanks. I deeply appreciate her taking me to the GEM conference; I learned a lot about working in the field of space physics and I had a really amazing time. Her passion for space is catching and her profound understanding of science is something I aspire to one day obtain. She and her husband Mikko have been absolutely amazing to me. Thank you both for the delicious meals and good company. Katariina, your hard work and long days, even with your son Roni on the way, is an inspiration. You always come up with something hilarious when we talk, and I will miss that.

I appreciate my thesis committee members Dr. Hughes and Dr. Reynolds for their time in reading this document and for their suggestions.

I am grateful to Elena Budnik, Benoit Lavraud, and Andrei Federov for providing the Cluster orbital and solar wind condition files used in this study. Elena and Beniot's assessment of our conclusions were very beneficial. I also appreciate the Cluster FGM team for providing well calibrated magnetometer data.

To my many professors over the years, thank you for helping me get to where I am today.

To my father, Herbert Chu, and mother, Mei Hing Chu, thank you for always pushing me to do better. You have both worked extraordinarily hard to provide me with the opportunity to obtain a higher education and the assistance to live a comfortable lifestyle; I will always remember that. To my sister, Connie Chu, thank you for being there to help out when I needed it.

Jeff, Christy, Nhi, Chris, Gwen: thank you for being the random strangers I ran into during my first week at ERAU. I can truly say that my life wouldn't be the same without you all. Members of Dr. McKay's EP class (Lex, Rachel, Steve, Tyler,

Bill, Alex, Michaela, Marjory, Chau, Chris, Tom, Molly): you are all awesome and I will miss playing cards and going camping together. Alex, sorry I was the office mate with papers all over the place...all the time. Bunty, thanks for being outrageous and hilarious in D-Lab. Nick, Rachel, Jared, Chelsea, Byron, Jordan, Alecia, Tiffany, Adam, Nate, LeeAnn: I'm so glad that I met you. Thomas and Sanhan, aside from my family, I believe you two have kept me motivated to keep coming back to Georgia. Amber, Peebles, Dietz, Youn: GAMES was so much fun with our group; we haven't gotten together in forever and we should. To my fellow Housing and Residence Life staff members: thank you for giving me your respect and that break from science when I needed it.

To the many other unnamed individuals who inspired, encouraged, and supported me through the writing process, thank you!

*Christina Seiman Chu*  
*December 2010*

# Nomenclature

$\mu_0$  permeability of free space

$B_x$  x component of the magnetic field vector

$B_y$  y component of the magnetic field vector

$B_z$  z component of the magnetic field vector

$B_{tot}$  magnitude of the magnetic field vector

$D_{ST}$  disturbance storm time index

$P_{dynamic}$  dynamic pressure

$R_e$  Earth radius

AIMF all interplanetary magnetic field orientations

DFT Discrete Fourier Transform

DMC diamagnetic cavity [cusp]

FFT Fast Fourier Transform

FGM fluxgate magnetometer

GSM Geocentric Solar Magnetospheric coordinate system. (The X axis coincides with the direction from Earth to the Sun. The XZ plane contains Earth's dipole axis. Positive Z is in same sense as Earth's north magnetic pole [north



geographic hemisphere]. The Y axis supplements the other two, pointing toward dusk.) It rotates with both a yearly and daily period with respect to inertial coordinates.

IC ion-cyclotron

IMF interplanetary magnetic field

MHD magnetohydrodynamic

MSH magnetosheath

MSP magnetosphere

MVAE maximum variance analysis of the electric field

NIMF northward interplanetary magnetic field

SIMF southward interplanetary magnetic field

SM Solar Magnetic coordinate system. (The Z axis coincides with the north magnetic pole. The XZ plane contains Earth's dipole axis. The X axis does not always point directly at the Sun. The Y axis supplements the other two, pointing toward dusk.) It rotates with both a yearly and daily period with respect to inertial coordinates.

T96 Tsyganenko 1996 magnetic field line model

ULF ultralow frequency

UT universal time

# Contents

<b>Abstract</b>	<b>iv</b>
<b>Acknowledgement</b>	<b>vi</b>
<b>Nomenclature</b>	<b>viii</b>
<b>List of Figures</b>	<b>xii</b>
<b>1 Introduction</b>	<b>1</b>
1.1 The Magnetospheric Cusps . . . .	1
1.2 Cluster Spacecraft . . . . .	5
1.2.1 Background . . . . .	5
1.2.2 Flux Gate Magnetometer (FGM) . . . . .	6
1.3 The Cusp and Surrounding Regions from Cluster . . . . .	7
1.4 Magnetic Field Fluctuations in the Cusp: Turbulence or Structure?	12
<b>2 Data Preparation</b>	<b>16</b>
2.1 Fluxgate Magnetometer (FGM) Products . . . . .	16
2.2 Cusp Normalized Coordinates . . . . .	17
2.3 Magnetic Pressure Plots . . . . .	20
2.4 Calculating Power in the Magnetic Field Fluctuations	20
<b>3 Data Windowing, Artificially Induced Power, and Normalization</b>	<b>26</b>
3.1 Window Types . . . . .	26
3.2 Artificial Power . . . . .	28

---

3.3	Normalization	35
<b>4</b>	<b>Integrated Power</b>	<b>38</b>
4.1	Integrated Power . . . . .	38
4.2	Standard Deviation . . . . .	49
<b>5</b>	<b>Concluding Remarks</b>	<b>57</b>
<b>A</b>	<b>IDL Code</b>	<b>60</b>
A.1	Data Preparation Code . . . . .	60
A.2	Plotting Codes . . . . .	68
A.3	Supporting Functions . . . . .	88
<b>B</b>	<b>Unnormalized Integrated Power with Different Windowing</b>	<b>93</b>
<b>C</b>	<b>Unnormalized Integrated Power</b>	<b>100</b>
<b>D</b>	<b>Integrated Power Figures: Size Scaled by Number of Data Points</b>	
	Averaged	104
	<b>Bibliography</b>	<b>108</b>

# List of Figures

1.1	Earth's magnetosphere in the noon-midnight plane, artist representation. [ <i>NASA</i> ]	2
1.2	Chapman-Ferraro magnetosphere model. Earth is represented as a dipole and the solar wind as a conducting plane creating singular points $Q$ with zero magnetic field strength. [ <i>Chapman and Ferraro 1930</i> ]	3
1.3	3D high resolution MHD simulations of the cusp for northward (left) and southward (right) IMF. The sun is on the left in both simulations and the background color is total magnetic field strength. The region of depressed magnetic field (cavity) forms more sunward when the IMF is southward and more tailward when the IMF is northward. [ <i>Nykyri et al. 2010a</i> ]	5
1.4	Cluster II spacecraft prelaunch. [ <i>University of Sheffield Space Systems Team 2000</i> ]	6
1.5	Fluxgate magnetometer instrument used aboard Cluster spacecraft. [ <i>Imperial College 2000</i> ]	7
1.6	The magnetic field strength of a typical Cluster gradual and diamagnetic cavity cusp crossing.	8

- 1.7 Cluster plasma (left) and magnetic field (right) observations on 14 February 2003 from 18:30:00-20:30:00 UT for DMC intervals. Black, red, green, and blue correspond to spacecraft 1, 2, 3, and 4. The leftmost two boxes at the top right show Cluster separation relative to spacecraft 3 in the GSM xy-plane and xz-plane in units of thousands of kilometers. The rightmost two boxes at the top right show Cluster location in the GSM xy-plane and xz-plane in units of Earth radii. Approximate bowshock and magnetopause locations are drawn as parabolas. IMF components measured by the Advanced Composition Explorer (ACE) spacecraft are lagged by 44.0 minutes and plotted on the bottom right with black, red, and blue corresponding to IMF x, y, and z components. The solar wind pressure is plotted as the black line on the same plot with the greater number of variations. [*Nykyri et al.* 2010a] 10
- 1.8 Examples of mirror mode structures observed by Cluster spacecraft 3: peaks, dips, and quasi-sinusoidal waves. [*Soucek and Lucek* 2010] 11
- 1.9 Cluster constellation and trajectory on 14 February 2003 from 18:30:00-20:30:00 UT (spacecraft separation magnified by a factor of 3). On the left, they are plotted on top of the Tsyganenko 89 magnetic field line model (with Kp geomagnetic storm index of four) in GSM coordinates on the xz-plane. On the right, they are plotted on the xy-GSM plane. Cluster moves from the magnetosphere into the cusp. Black, red, green, and blue correspond to spacecraft 1, 2, 3, and 4. [*Nykyri et al.* 2010a] 14
- 1.10 Boundary normal components in x, y, and z GSM coordinates determined using maximum variance analysis of the electric field (MVAE) for a) 18:48:40-18:56:00 UT during the magnetosphere-diamagnetic cavity boundary (MSP-DMC) and b) 18:57:30-19:22:00 UT during the first cavity interval observed by spacecraft 1. The fourth row shows the maximum and intermediate eigenvalue ratio ( $\frac{\lambda_1}{\lambda_2}$ ) for MVAE. Below that is the magnetic field magnitude and  $\frac{\lambda_1}{\lambda_2} > 4$ . [*Nykyri et al.* 2010b] 15

- 2.1 Representation of data coordinate transformations to cusp normalized coordinates [Lavraud *et al.* 2005]. (a) Data points were rotated about the x solar magnetic axis to lie in the  $XZ_{SM}$  plane. (b) Data points were rotated about the  $Y_{SM}$  axis by the angle determined by the “current” separatrix and T96 magnetic field model separatrix (see text). (c) Data points were radially scaled relative to a reference magnetopause using the “current” solar wind conditions. Magnetopause model from Shue *et al.* [1997]. 19
- 2.2 Magnetic pressure from Cluster spacecraft 1 data.  $\log \frac{(MagneticField)^2}{(Tsyganenko96MagneticField)^2}$  is plotted over T96 field lines. **a)** the size of each data square is  $0.3 R_e$ . **b)** the size of each data square is scaled according to the number of data points averaged. The size reaches a maximum of  $0.3 R_e$  when 20 or more data samples are averaged. 21
- 2.3 Cluster data on 17 March 2001 from 5:00:00-6:00:00 UT for a gradual cusp interval. Black, red, green, and blue correspond to spacecraft 1, 2, 3, and 4. The bottom plot shows the total magnetic field data while  $B_x$ ,  $B_y$ , and  $B_z$  show the magnetic field components in x, y, and z respectively. The  $dB_T$  plot shows the total magnetic field after detrending (after subtracting the linear fit of the original data).  $dB_x$ ,  $dB_y$ , and  $dB_z$  plots show the detrended  $B_x$ ,  $B_y$ , and  $B_z$  magnetic field components respectively. The N plot shows the number of particles.  $V_T$  shows the total velocity while  $V_x$ ,  $V_y$ , and  $V_z$  plots show the x, y, and z plasma velocity components respectively. [Nykyri *et al.* 2004] 23
- 2.4 **a)** Example power spectrum showing two minutes of magnetic field data in the frequency domain; total power of the magnetic field fluctuations is plotted with respect to frequency. **b)** Artistic depiction of the middle Riemann sum used to calculate the integrated power (area under the black curve in **a)**) [Richards]. 24
- 3.1 Periodic and symmetric Hanning windows with different  $\alpha$  values and  $N = 100$ . 27

- 3.2 Plots investigating the effect on the total integrated power over a cusp crossing when leaving out the lowest frequencies. First row shows the integrated total power over an entire cusp crossing. The second row shows a sample total power spectrum of the cusp crossing. The area under the total power spectrum curve is the total integrated power for the windowed data. The data has been windowed with a Hanning window of  $\alpha = 0.5, 0.6, 0.7, 0.8, 0.9, 0.99$ , and  $1$ . 29
- 3.3 Total integrated power in the magnetic field fluctuations of the 0.008-10 Hz frequency range for NIMF, SIMF, and AIMF (rows) and Hanning window with  $\alpha = 0.5, 0.75$ , and  $1$  (columns). 31
- 3.4 Total integrated power in the magnetic field fluctuations of the 0.017-10 Hz frequency range for NIMF, SIMF, and AIMF (rows) and Hanning window with  $\alpha = 0.5, 0.75$ , and  $1$  (columns). 32
- 3.5 Total integrated power in the magnetic field fluctuations of the 0.025-10 Hz frequency range for NIMF, SIMF, and AIMF (rows) and Hanning window with  $\alpha = 0.5, 0.75$ , and  $1$  (columns). 33
- 3.6 Total integrated power of magnetic field fluctuations for Cluster spacecraft 1 from 0.017-10 Hz for NIMF and SIMF from Figure 3.3 using Hanning window with  $\alpha = 0.5$ . Regions of enhanced wave power are outlined. 34
- 3.7 Normalized (green) and unnormalized (red) integrated total power (Hanning windowed with  $\alpha = 0.5$ ) for Cluster cusp crossing on 14 February 2003. For the green curves, power is normalized to  $\alpha = 1$  (top) and  $\alpha = 0.95$  (bottom). For reference, the integrated total power calculated using a Hanning window with  $\alpha = 1$  and  $\alpha = 0.95$  is included in the top and bottom plots respectively (blue). Each data point is the integrated total power of a two minute data segment (points shown connected). 37

4.1	Normalized integrated mean, total, and perpendicular power in the magnetic field fluctuations of the 0.017-10 Hz frequency range for NIMF, SIMF, and AIMF	39
4.2	Normalized integrated mean, total, and perpendicular power in the magnetic field fluctuations of the 0.017-0.1 Hz frequency range for NIMF, SIMF, and AIMF	40
4.3	Normalized integrated mean, total, and perpendicular power in the magnetic field fluctuations of the 0.1-10 Hz frequency range for NIMF, SIMF, and AIMF	41
4.4	Locations of increased power in magnetic field fluctuations due to different reconnection sites during NIMF versus SIMF, 0.017-10 Hz.	43
4.5	Locations of increased power in magnetic field fluctuations due to spacecraft crossing from magnetotail into magnetosheath (gradient in the magnetic field strength) and/or mirror mode waves, 0.017-10 Hz.	44
4.6	Locations of increased power in magnetic field fluctuations due to different wave modes in the magnetosheath, 0.017-10 Hz.	45
4.7	Locations of increased power in magnetic field fluctuations possibly due to magnetotail reconnection, 0.017-10 Hz.	46
4.8	Normalized total integrated power of the magnetic field fluctuations from 0.017-10Hz for NIMF and SIMF from Figure 4.1. Regions of enhanced wave power are outlined.	47
4.9	Standard deviation for the mean, total, and perpendicular power in the magnetic field fluctuations of the 0.017-10 Hz frequency range for NIMF, SIMF, and AIMF.	51
4.10	Standard deviation for the mean, total, and perpendicular power in the magnetic field fluctuations of the 0.017-0.1 Hz frequency range for NIMF, SIMF, and AIMF.	52
4.11	Standard deviation for the mean, total, and perpendicular power in the magnetic field fluctuations of the 0.1-10 Hz frequency range for NIMF, SIMF, and AIMF	53



4.12	Normalized integrated mean, total, and perpendicular power in the magnetic field fluctuations of the 0.017-10 Hz frequency range for NIMF, SIMF, and AIMF. The data square is scaled smaller with higher standard deviation.	54
4.13	Normalized integrated mean, total, and perpendicular power in the magnetic field fluctuations of the 0.017-0.1 Hz frequency range for NIMF, SIMF, and AIMF. The data square is scaled smaller with higher standard deviation.	55
4.14	Normalized integrated mean, total, and perpendicular power in the magnetic field fluctuations of the 0.1-10 Hz frequency range for NIMF, SIMF, and AIMF. The data square is scaled smaller with higher standard deviation.	56
B.1	Mean integrated power for the magnetic field fluctuations of the 0.008-10 Hz frequency range for NIMF, SIMF, and AIMF (rows) and Hanning window with $\alpha = 0.5, 0.75$ , and 1 (columns).	94
B.2	Mean integrated power for the magnetic field fluctuations of the 0.017-10 Hz frequency range for NIMF, SIMF, and AIMF (rows) and Hanning window with $\alpha = 0.5, 0.75$ , and 1 (columns).	95
B.3	Mean integrated power for the magnetic field fluctuations of the 0.025-10 Hz frequency range for NIMF, SIMF, and AIMF (rows) and Hanning window with $\alpha = 0.5, 0.75$ , and 1 (columns).	96
B.4	Perpendicular integrated power for the magnetic field fluctuations of the 0.008-10 Hz frequency range for NIMF, SIMF, and AIMF (rows) and Hanning window with $\alpha = 0.5, 0.75$ , and 1 (columns).	97
B.5	Perpendicular integrated power for the magnetic field fluctuations of the 0.017-10 Hz frequency range for NIMF, SIMF, and AIMF (rows) and Hanning window with $\alpha = 0.5, 0.75$ , and 1 (columns).	98
B.6	Perpendicular integrated power for the magnetic field fluctuations of the 0.025-10 Hz frequency range for NIMF, SIMF, and AIMF (rows) and Hanning window with $\alpha = 0.5, 0.75$ , and 1 (columns).	99

C.1	Unnormalized integrated mean, total, and perpendicular power in the magnetic field fluctuations of the 0.017-10 Hz frequency range for NIMF, SIMF, and AIMF . . . . .	101
C.2	Unnormalized integrated mean, total, and perpendicular power in the magnetic field fluctuations of the 0.017-0.1 Hz frequency range for NIMF, SIMF, and AIMF . . . . .	102
C.3	Unnormalized integrated mean, total, and perpendicular power in the magnetic field fluctuations of the 0.1-10 Hz frequency range for NIMF, SIMF, and AIMF. . . . .	103
D.1	Normalized integrated power, with size scaled to the number of data points averaged, for the mean, total, and perpendicular power in the magnetic field fluctuations of the 0.017-10 Hz frequency range for NIMF, SIMF, and AIMF . . . . .	105
D.2	Normalized integrated power, with size scaled to the number of data points averaged, for the mean, total, and perpendicular power in the magnetic field fluctuations of the 0.017-0.1 Hz frequency range for NIMF, SIMF, and AIMF . . . . .	106
D.3	Normalized integrated power, with size scaled to the number of data points averaged, for the mean, total, and perpendicular power in the magnetic field fluctuations of the 0.1-10 Hz frequency range for NIMF, SIMF, and AIMF. . . . .	107

# Chapter 1

## Introduction

### 1.1 The Magnetospheric Cusps

The magnetospheric cusps are important structural elements in the magnetosphere because magnetosheath plasma has the most direct access to the ionosphere through the high altitude cusps [*Heikkila and Winningham 1971, Frank and Ackerson 1971*]

An artistic depiction of Earth's magnetosphere is shown in Figure 1.1. The sun ejects solar wind, consisting of mostly protons and electrons, radially outwards due to the large pressure difference between the hot solar corona and the interstellar medium. The solar wind carries with it a frozen-in interplanetary magnetic field (IMF). At Earth, the solar wind is traveling at a speed of  $\sim 400$  km/s with plasma density of  $\sim 5/\text{cm}^3$ . As the solar wind moves towards the planet, the Earth acts as an obstacle and pressure increases in front of it. The pressure will distribute itself as a compressional, fast mode wave [*Schwartz et al 1996*]. In the solar wind frame, the Earth is approaching faster than the speed of a fast mode wave, so a shock will form in front of the planet, similar to the shock formed in front of supersonic aircraft. This is called the bowshock and it is important because it slows, heats and deflects solar wind flow before it interacts with the Earth's magnetosphere. The magnetosheath is the region of turbulent plasma flow between the bowshock and magnetosphere, and it may play an important role in the structure of the bowshock and the magnetopause.

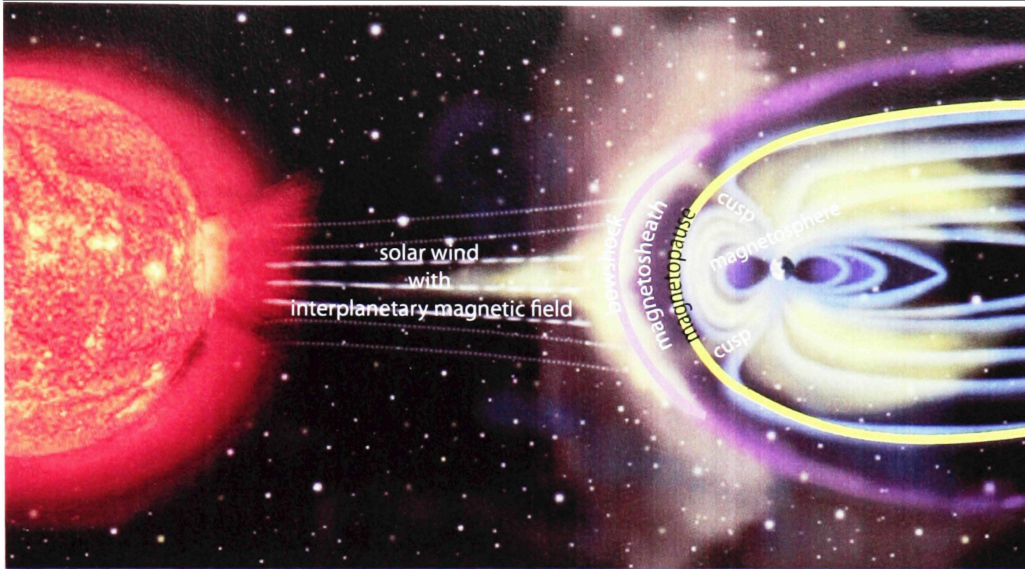


Figure 1.1: Earth's magnetosphere in the noon-midnight plane, artist representation. [NASA]

The magnetopause boundary is a current layer separating the Earth's magnetic environment from the solar wind. Its distance from the surface of the Earth is defined by the pressure balance between the dynamical pressure of the solar wind and the magnetic field pressure of the Earth. Magnetosheath material can enter the boundary layers of the magnetosphere through macroscopic processes such as magnetic reconnection and viscous interactions. Plasma does not get evenly distributed, but forms regions of different temperatures and densities. Earth's magnetic environment is the magnetosphere and is the region shown filled with magnetic field lines (blue). At the cusps, where Earth's field lines converge at the northern hemisphere and diverge at the southern hemisphere, solar wind particles can be coupled down into Earth's lower atmosphere. The cusps are regions of near zero magnetic field magnitude.

The magnetospheric cusps were first represented in Chapman and Ferraro's image dipole model of the magnetosphere [Chapman and Ferraro 1930]. In this model, the Earth has a dipole magnetic field and solar wind approaches Earth as an unmagnetized, infinite conducting plane. The mathematical effect on Earth's magnetic field is equivalent to placing an image dipole, equal in strength to Earth's dipole, at the

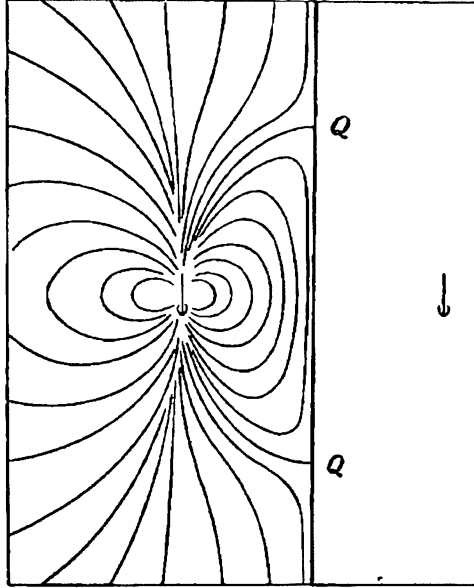


Figure 1.2: Chapman-Ferraro magnetosphere model. Earth is represented as a dipole and the solar wind as a conducting plane creating singular points  $Q$  with zero magnetic field strength. [*Chapman and Ferraro 1930*]

same distance away from the magnetopause as the Earth's dipole is (the conducting plane can be replaced with a copy of Earth's dipole at an equal distance on the other side of the plasma boundary). This distortion on Earth's dipole is shown in Figure 1.2. For a perfect dipole next to a perfect conductor, two singularities, points of zero magnetic field strength, are produced at the points labeled  $Q$ . The unmagnetized solar wind would then penetrate down into the ionosphere in a narrow funnel. Today, this funnel would be called the polar cusp.

In reality, the singular points  $Q$  do not exist, but field lines are closed through the dayside equatorward of the cusp, and through the nightside poleward of the cusp. Also, solar wind plasma does carry a magnetic field with it. In a collisionless plasma with normal plasma conditions, charged particles on a magnetic flux tube will stay with that flux tube. *Dungey* [1961] proposed that magnetic reconnection could change the field line topology so that solar wind charged particles could go to another flux tube, one connected to the Earth dipole, and be carried down into the cusp.

The total pressure, consisting of the plasma pressure and the magnetic pressure, must remain constant. The plasma pressure  $= nkT$  where  $n$  is the number density,  $k$  is Boltzmann's constant, and  $T$  is the temperature. The magnetic pressure  $= \frac{B^2}{2\mu_0}$  where  $B$  is the total magnetic field magnitude and  $\mu_0$  is the permeability of free space. When reconnection occurs, solar wind particles are injected along the field lines, increasing  $n$ . For pressure to remain constant, the magnetic pressure term must decrease meaning that  $B$  will decrease, forming an area of depressed magnetic field, a cusp diamagnetic cavity.

The interplanetary magnetic field has a variable northern or southern hemisphere pointing component which will be called  $z$ . For a northward IMF (NIMF), positive  $z$  component, magnetic reconnection is expected tailward of the cusp [Newell *et al.* 1989]. For a southward IMF (SIMF), negative  $z$  component, magnetic reconnection is expected sunward of the cusp. The location of the cusp will move tailward or sunward depending on the IMF condition. This is seen in the 3D high resolution magnetohydrodynamic (MHD) simulations for NIMF and SIMF shown in Figure 1.3 from Nykyri *et al.* [2010a]. If the IMF has a dawnward, negative  $B_y$ , component, the reconnection site will be shifted, and the location of the cusp shifts to earlier local times in the northern hemisphere [Russell 2000]. If the IMF has a duskward, positive  $B_y$ , component, the location of the cusp shifts to later local times in the northern hemisphere [Russell 2000]. High latitude reconnection was first predicted by Dungey [1963] and first observed by Kessel *et al.* [1996] with the Hawkeye spacecraft.

In-situ measurements of the polar cusps have been made by the Isis I [Heikkila and Winningham 1971], HEOS-2 [Paschmann *et al.* 1976; Dunlop *et al.* 2000], Hawkeye [Kessel *et al.* 1996], Polar [Chen and Fritz 1998; Zhou *et al.* 2000; Le *et al.* 2001], Interball [Sandahl *et al.* 2000], and Cluster [Lavraud *et al.* 2002; Nykyri *et al.* 2003; Cargill *et al.* 2004; Lavraud *et al.* 2005] satellite missions.

These missions have provided much information about the cusp. The location of the high-altitude cusp as a function of solar wind conditions was studied by Zhou *et al.* [2000] using Polar spacecraft data and by Dunlop *et al.* [2000] using HEOS-2. Zhou *et al.* [1999, 2000] investigated the spatial extent of the cusp. Savin *et al.* [1998]; Chen and Fritz [1998]; Le *et al.* [2001]; Savin *et al.* [2002, 2004]; Sundkvist *et al.*

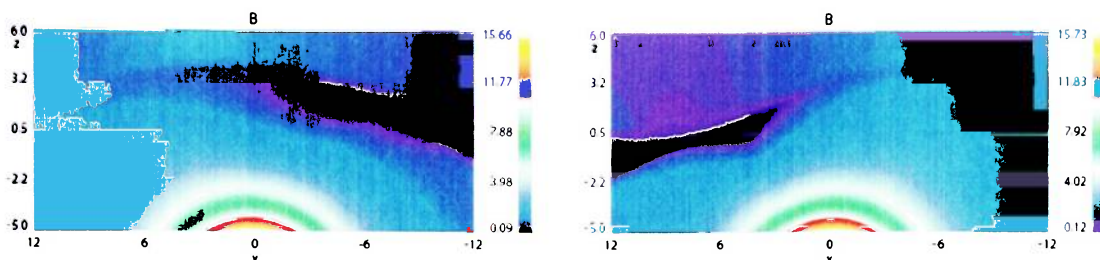


Figure 1.3: 3D high resolution MHD simulations of the cusp for northward (left) and southward (right) IMF. The sun is on the left in both simulations and the background color is total magnetic field strength. The region of depressed magnetic field (cavity) forms more sunward when the IMF is southward and more tailward when the IMF is northward. [Nykyri *et al.* 2010a]

[2005]; Nykyri *et al.* [2006] have studied in-situ cusp magnetic field fluctuations, wave activity, and turbulence. Cluster data has allowed for the identification of many cusp features. Lavraud *et al.* [2002] identified a stagnant exterior cusp with low magnetic field and flow for NIMF. Vontrat-Reberac *et al.* [2003] determined that for NIMF, lobe reconnection could play a large role in the origin of solar wind plasma inside the magnetopause and earthward plasma jets. For SIMF, Cargill *et al.* [2004] showed that the cusp is a dynamic region that could have sharp boundaries.

## 1.2 Cluster Spacecraft

### 1.2.1 Background

Cluster is a four satellite multi-instrument in-situ measurement mission of the magnetosphere, cusp, and magnetosheath. The satellites orbit Earth in a tetrahedral formation with separation distances ranging from 100 km up to 10,000 km. With four spacecraft taking measurements, spatial features can be distinguished from temporal ones. Each satellite carries an identical set of 11 instruments measuring charged particles, magnetic fields, and electric fields.

The original four Cluster satellites were launched aboard an Ariane 5 rocket on 4 June 1996. That rocket exploded shortly after liftoff, destroying the satellites. A



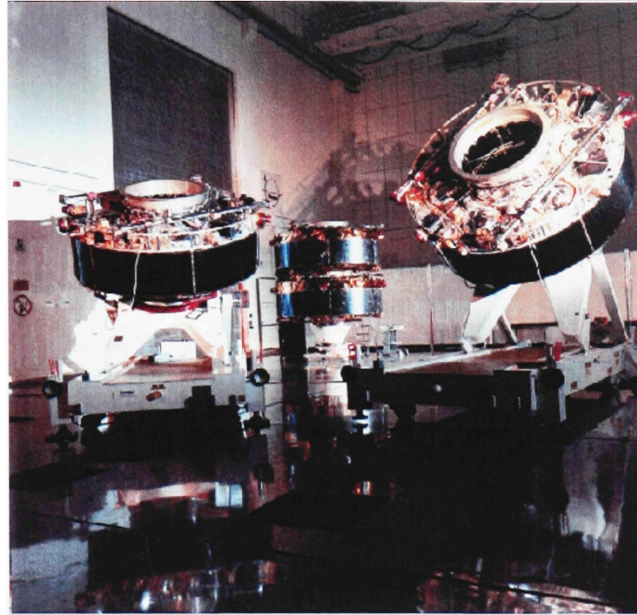


Figure 1.4: Cluster II spacecraft prelaunch. [*University of Sheffield Space Systems Team 2000*]

second set of Cluster spacecraft, with a few modifications to the instruments, were built and launched using two Soyuz rockets, with two satellites each, in the summer of 2000. Cluster II satellites are shown in Figure 1.4. The data used in this study comes from the second set of Cluster spacecraft.

### 1.2.2 Flux Gate Magnetometer (FGM)

The fluxgate magnetometer (FGM) instrument shown in Figure 1.5 samples the ambient magnetic along the spacecrafts' orbit. It can sample in the frequency range of 10 Hz in normal mode up to 32 Hz in burst mode in a field range of  $-65536$  nT to  $+65528$  nT. The instrument consists of two tri-axial fluxgate sensors and an electronics box. In order to minimize magnetic interference from the spacecraft, the magnetometer sensors were mounted at the tip of a 5.0 m radial boom. The control electronics are housed inside a box on the spacecraft Main Equipment Platform. [*Balogh et al. 2001*]



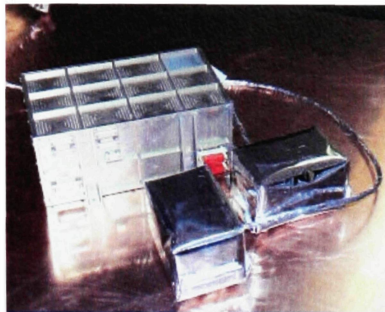


Figure 1.5: Fluxgate magnetometer instrument used aboard Cluster spacecraft. [*Imperial College* 2000]

The high resolution magnetic field data for this study is produced at a rate of 22.4 magnetic field vectors per second. The raw data of the FGM instrument is calibrated to correct for several factors including spacecraft and instrument clocks, sensor offsets, misalignments, sensitivities, and spacecraft attitude data.

A list of 118 Cluster northern hemisphere cusp crossings from 2001-2003 were provided by E. Budnik. Spacecraft orbital points were given in the geocentric solar magnetic (GSM) and solar magnetic (SM) coordinate systems. The low resolution magnetic field data was downloaded from the United Kingdom Cluster data center and the high resolution data was downloaded from the Imperial College Cluster server. Both these data sets are in the GSM coordinate system.

### 1.3 The Cusp and Surrounding Regions from Cluster

There are two different types of Cluster cusp crossings in terms of the magnetic field signature seen, “gradual” cusp and diamagnetic cavities (DMC). As shown in Figure 1.6, for a gradual cusp, the magnetic field drops off slowly as the spacecraft moves. For a DMC, the magnetic field drops off rapidly [Nykkyri *et al.* 2010b]. The times that Cluster was traveling through the magnetosphere (MSP), cusp, and magnetosheath (MSH) regions were identified by looking at the plasma parameters (number of particles, velocity components, and temperature).

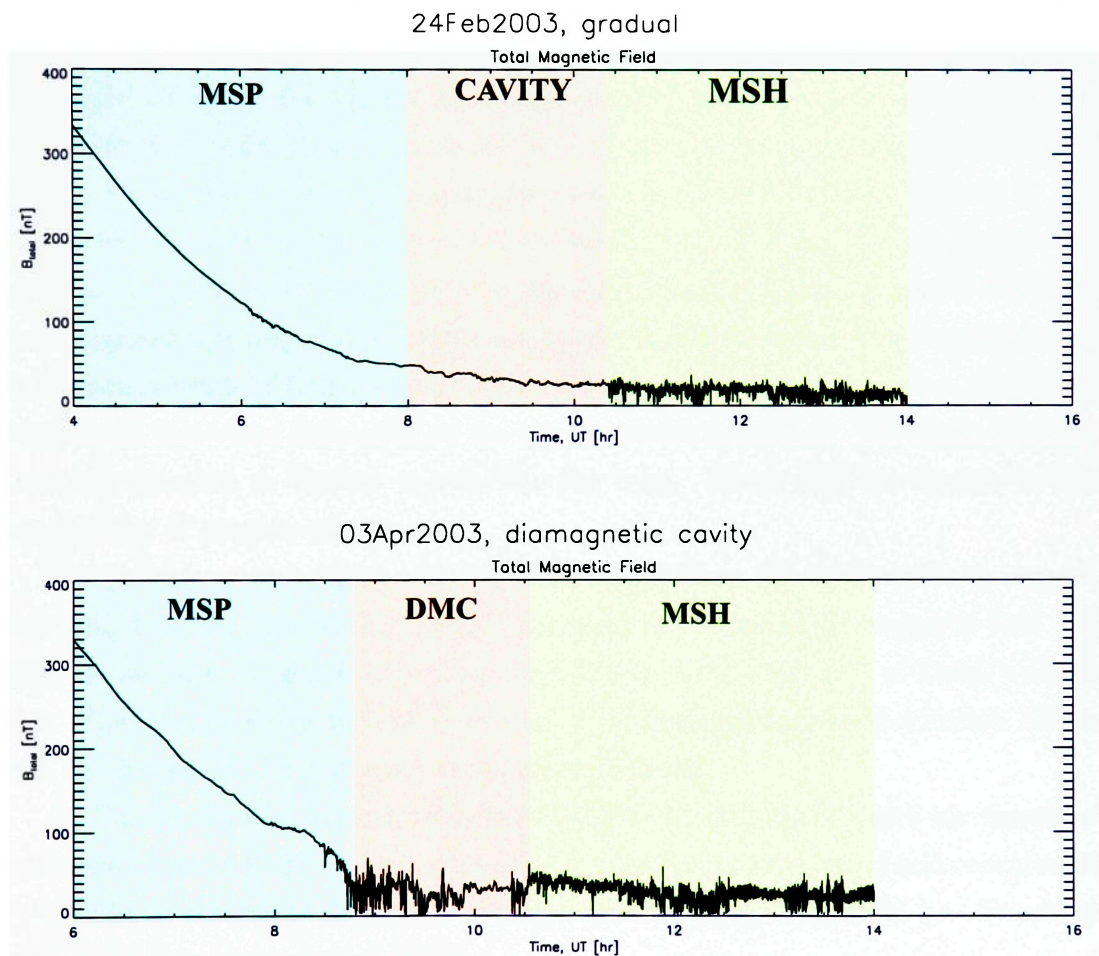


Figure 1.6: The magnetic field strength of a typical Cluster gradual and diamagnetic cavity cusp crossing.

Diamagnetic cavities are formed when reconnection at high latitudes open up the magnetic field lines. As high density solar wind plasma gets on the open field lines, the magnetic pressure is reduced, creating a cavity [Nykyri *et al.* 2010a,b]. Cluster only observes DMCs during intervals of enhanced dynamic pressure ( $\sim 2.6$  nPa) because of the nature of its orbit [Nykyri *et al.* 2010a]. In comparison, gradual cusp crossings observed by Cluster have an average dynamic pressure of  $\sim 1.8$  nPa.

Figure 1.7 shows the plasma and magnetic field observations in around a DMC on 14 February 2003 from 18:30:00-20:30:00 universal time (UT). In a typical DMC cusp crossing, the number of plasma particles (ions) observed will increase as the spacecraft moves from the magnetosphere into the cusp. Particle temperature will increase. In GSM coordinates, the x component of the measured magnetic field will go from positive to negative and the z component will go from negative to positive due to the components of Earth's dipole field. The y component may go from positive to negative or vice-versa depending on the spacecraft trajectory. The total magnetic field will decrease as Cluster travels into the cusp. There may be changes in the components of particle velocity.

The particle temperatures will drop when going from the cavity into the magnetosheath. In GSM coordinates, the x component of the measured magnetic field will decrease and the z component will increase due to the components of Earth's dipole field. The total magnetic field will increase. Particle temperature will decrease. There may be changes in the components of particle velocity.

As Cluster travels through areas surrounding the cusp, it can pick up signals of wave structures in those regions. As solar wind plasma is decelerated and compressed by bowshock traversal, conditions are favorable for large amplitude low frequency wave excitation [Soucek *et al.* 2008].

Figure 1.8 shows three distinct types of mirror mode activity in the magnetosheath magnetic field data: peaks, dips, and quasi-sinusoidal waves. The presence of mirror mode waves can induce higher power in the compressional magnetic field fluctuations.

Ion cyclotron (IC) waves in the high altitude cusp were shown by Le *et al.* [2001] to have been found both equatorward and poleward of the cusp, as well as in the cusp itself. Nykyri *et al.* [2004, 2003]; Sundkvist *et al.* [2005] have found evidence

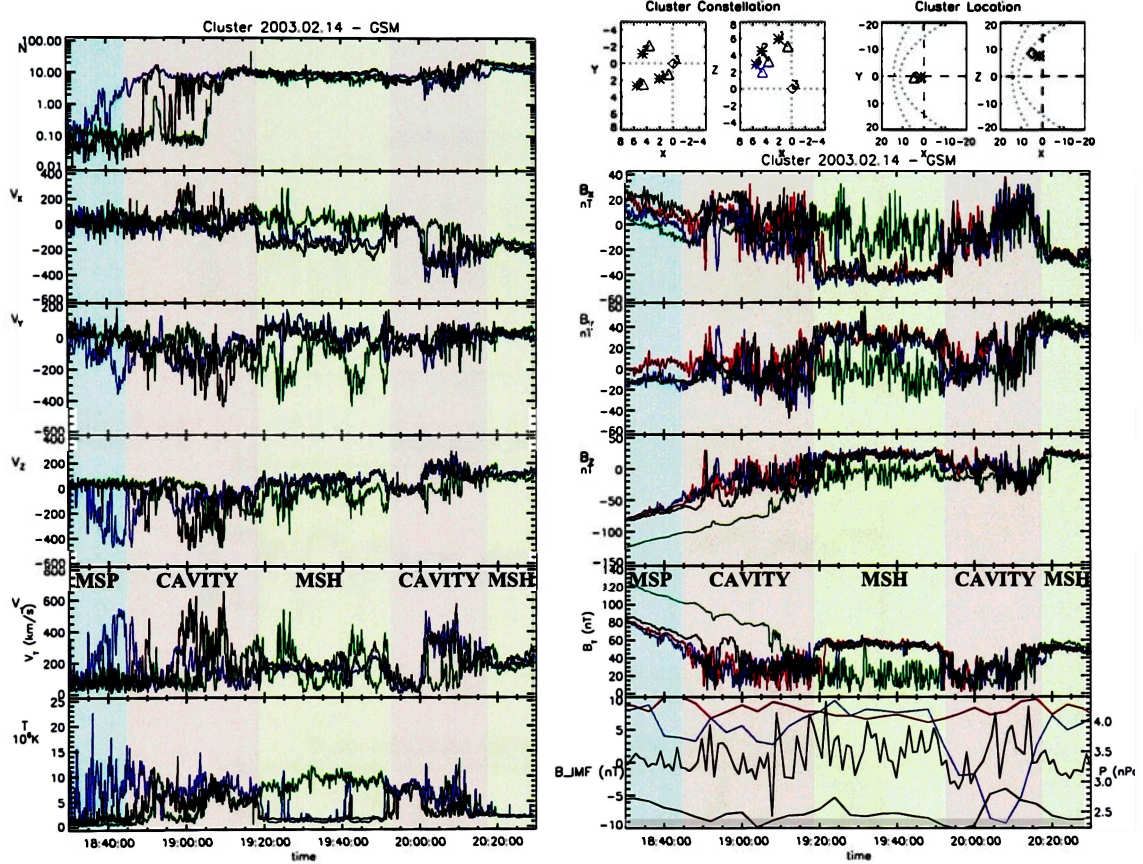


Figure 1.7: Cluster plasma (left) and magnetic field (right) observations on 14 February 2003 from 18:30:00-20:30:00 UT for DMC intervals. Black, red, green, and blue correspond to spacecraft 1, 2, 3, and 4. The leftmost two boxes at the top right show Cluster separation relative to spacecraft 3 in the GSM xy-plane and xz-plane in units of thousands of kilometers. The rightmost two boxes at the top right show Cluster location in the GSM xy-plane and xz-plane in units of Earth radii. Approximate bowshock and magnetopause locations are drawn as parabolas. IMF components measured by the Advanced Composition Explorer (ACE) spacecraft are lagged by 44.0 minutes and plotted on the bottom right with black, red, and blue corresponding to IMF x, y, and z components. The solar wind pressure is plotted as the black line on the same plot with the greater number of variations. [Nykyri *et al.* 2010a]

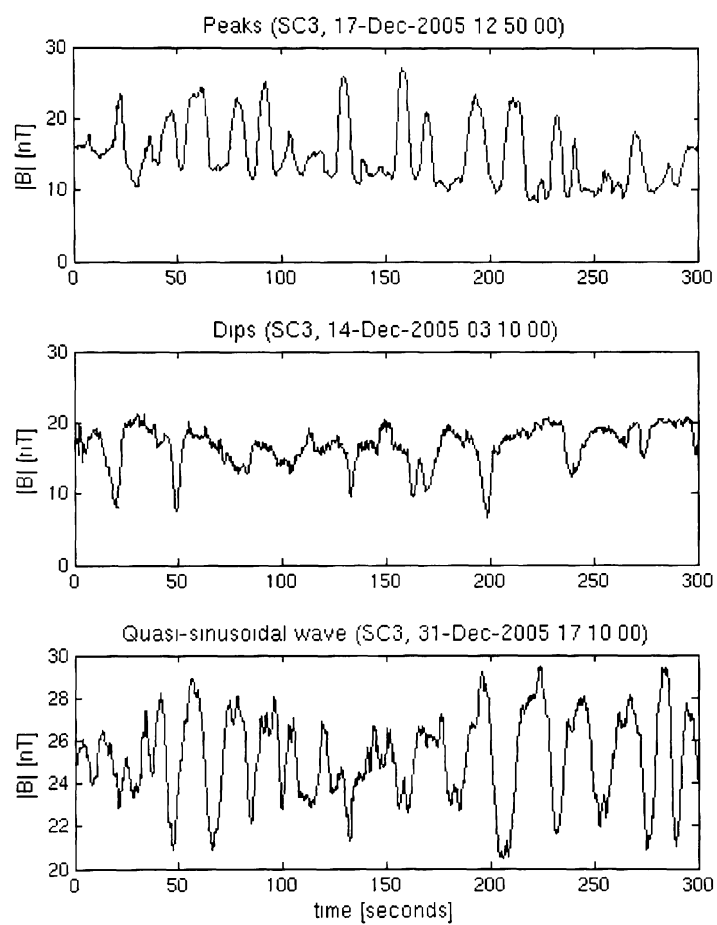


Figure 1.8: Examples of mirror mode structures observed by Cluster spacecraft 3: peaks, dips, and quasi-sinusoidal waves. [Soucek and Lucek 2010]

for left-hand polarized IC and Alfvén waves at the high altitude cusp. These wave types are characterized by a peak in the wave power at or near the local cyclotron frequency.

## 1.4 Magnetic Field Fluctuations in the Cusp: Turbulence or Structure?

Understanding the nature and origin of fluctuations in the cusp is important because turbulence in the cusp diamagnetic cavities has been suggested as a mechanism to heat and energize plasma up to MeV energies [Chen and Fritz 1998]. However, any period of fluctuation that is longer than the typical travel time through the cusp cannot be called turbulence in the traditional sense. It can take 0.1-1 second for a magnetosonic wave to travel through the cusp, setting the lowest frequency limit for turbulence to 0.1-1 Hz [Nykyri *et al.* 2010a,b]. In this study, several frequencies ranges from 0.017-10 Hz are examined.

There are currently three theories on the origin of high energy particles in the DMC: 1. Local acceleration from ultra-low frequency (ULF) “turbulence” [Chen and Fritz 1998; Chen 2008], 2. Bowshock source [Chang *et al.* 1998; Trattner *et al.* 2001], 3. Magnetospheric source [Sibeck *et al.* 1987; Fuseher *et al.* 1991; Asikainen and Mursula 2005, 2006].

Nykyri *et al.* [2010b] shows that many of the low frequency fluctuations in the DMC are actually a back-and-forth motion of the DMC boundary over the spacecraft. A case study was shown for 14 February 2003 (one of the dates used in this fluctuation power study). Figure 1.7 shows the plasma and magnetic field observations from 18:30:00-20:30:00 UT. Figure 1.9 shows the trajectory of the four Cluster spacecraft in formation in GSM coordinates during this time period. The magnetic field data in Figure 1.7 shows that the DMC has many magnetic field fluctuations. The normal direction to the boundary between the MSP-cusp and cusp-MSH were determined using maximum variance analysis of the electric field (MVAE). Figure 1.10 shows the boundary normal components for spacecraft 1 from a)

18 48 40-18 56 00 UT during the magnetosphere-diamagnetic cavity boundary crossing (MSP-DMC) and b) 18 57 30-19 22 00 UT during the first cavity interval observed by spacecraft 1. For the MSP-DMC boundary,  $N_x$ , the boundary normal in the x-GSM direction, is dominant and shows little variation. In the cavity  $N_x$  varies more. *Nykyri et al.* [2010b] says that at the MSP-cusp boundary, the dynamic pressure variation (see Figure 1.7) coinciding with the small  $N_x$  boundary normal variation suggests that the magnetic field variation at the inner boundary is mostly due to the back-and-forth motion of the MSP-DMC boundary over the spacecraft due to dynamic pressure variations in the solar wind. The large scale fluctuations in the cavity are due to both the back-and-forth motion of the cavity-magnetosheath (DMC-MSH) boundary over the spacecraft and transient reconnection signatures [*Nykyri et al.* 2010b]. These results strongly suggest that the low frequency fluctuations in the cavity are mostly structure, like moving boundaries, rather than wave turbulence.



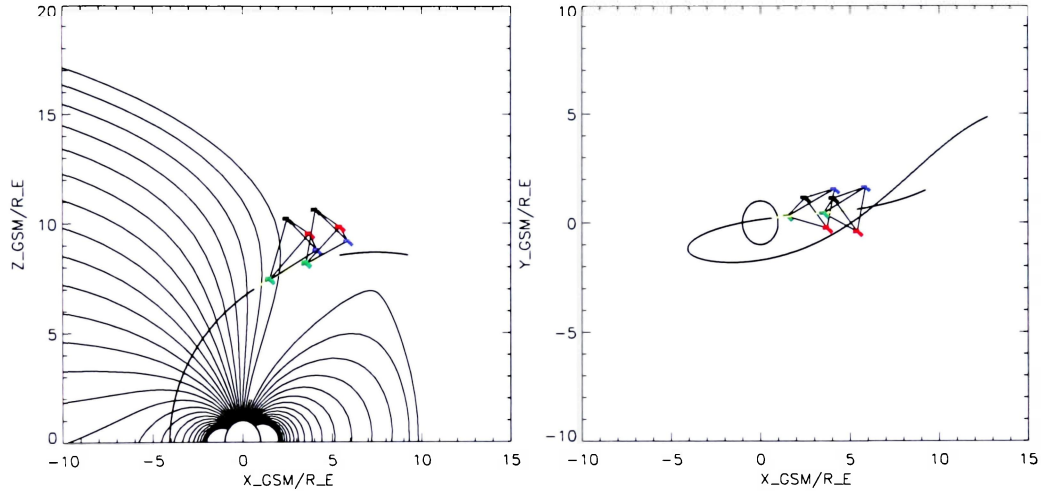


Figure 1.9: Cluster constellation and trajectory on 14 February 2003 from 18:30:00-20:30:00 UT (spacecraft separation magnified by a factor of 3). On the left, they are plotted on top of the Tsyganenko 89 magnetic field line model (with Kp geomagnetic storm index of four) in GSM coordinates on the xz-plane. On the right, they are plotted on the xy-GSM plane. Cluster moves from the magnetosphere into the cusp. Black, red, green, and blue correspond to spacecraft 1, 2, 3, and 4. [Nykyri *et al.* 2010a]



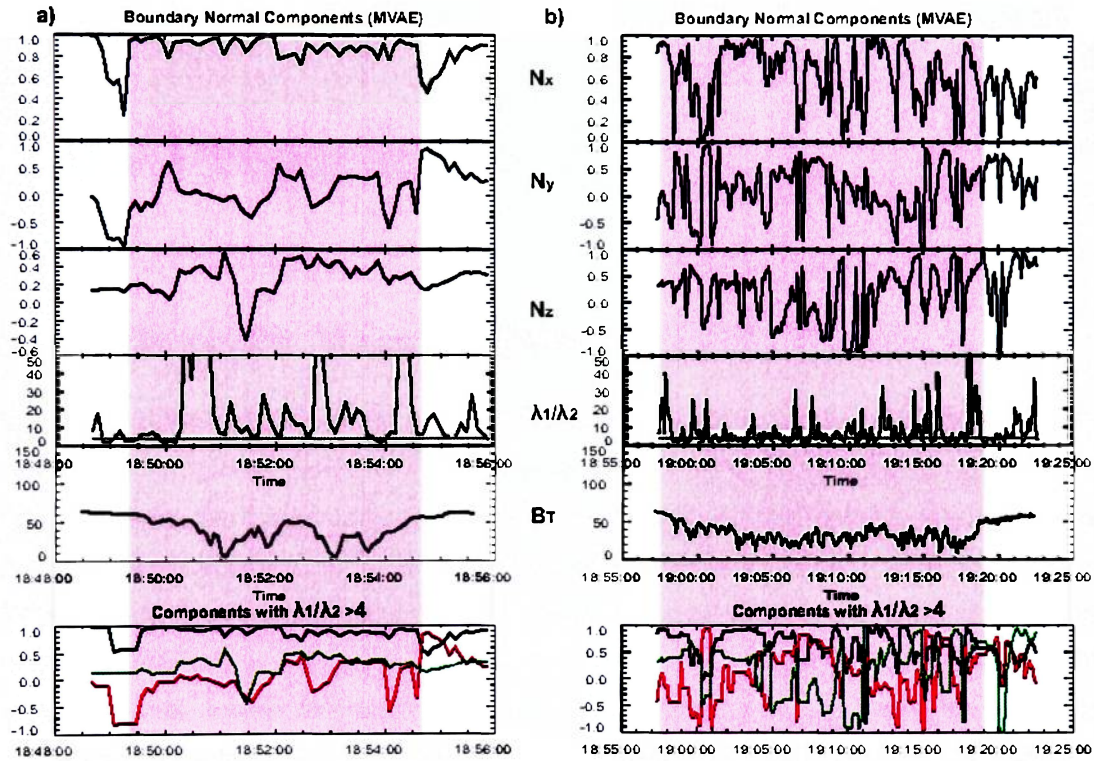


Figure 1.10: Boundary normal components in x, y, and z GSM coordinates determined using maximum variance analysis of the electric field (MVAE) for a) 18:48:40-18:56:00 UT during the magnetosphere-diamagnetic cavity boundary (MSP-DMC) and b) 18:57:30-19:22:00 UT during the first cavity interval observed by spacecraft 1. The fourth row shows the maximum and intermediate eigenvalue ratio ( $\frac{\lambda_1}{\lambda_2}$ ) for MVAE. Below that is the magnetic field magnitude and  $\frac{\lambda_1}{\lambda_2} > 4$ . [Nykyri *et al.* 2010b]

## Chapter 2

# Data Preparation

### 2.1 Fluxgate Magnetometer (FGM) Products

The low resolution data is the spacecraft spin-averaged magnetic field data. It has an average of one data point every four seconds. Initially, the integrated mean, total, and perpendicular power were calculated with the low resolution data. Because there are fewer data points than in the high resolution data set, it was quicker to use it to determine if the data processing and plotting routines were working correctly. The power calculation is defined in Section 2.4. The data was divided into two minute sections so the lowest frequency that could be resolved was  $\frac{1}{2 \text{ min}} \approx 0.008 \text{ Hz}$ . The data was interpolated so that there was a data point every four seconds. The highest frequency that could be resolved was twice that interval,  $\frac{1}{8 \text{ s}} \approx 0.125 \text{ Hz}$  (Nyquist frequency [Shannon 1949]). Using the low resolution data, power could be calculated from 0.008-0.125 Hz. Higher frequencies cannot be investigated because the sampling rate is too low.

The high resolution FGM data has an average of 22.4 data points every second. The data was divided into two minute sections so the lowest frequency that could be resolved was  $\frac{1}{2 \text{ min}} \approx 0.008 \text{ Hz}$ . The integrated mean, total, and perpendicular power was calculated with seven frequency ranges: 0.017-0.125 Hz (to compare with results using the low resolution data), 0.017-10 Hz, 0.017-0.1 Hz, 0.1-10 Hz, 0.017-1.0 Hz, 1.0-10 Hz, and 0.1-1.0 Hz. The reason the lowest frequency in these ranges is not

0.008 Hz is explained in Section 3.2. Spatial maps of the fluctuation power in the three frequency ranges 0.017-10 Hz, 0.017-0.1 Hz, and 0.1-10 Hz are shown in Chapter 4.

## 2.2 Cusp Normalized Coordinates

The cusp has traditionally been identified based on a plasma (ion) flux criteria [Heikkilä and Winningham 1971; Newell *et al.* 1989; Yamauchi *et al.* 1995] and/or magnetic field measurements. In this study, the cusp and surrounding regions will be presented in a cusp normalized coordinate system from Lavraud *et al.* [2004, 2005] that takes into account the lagged solar wind (IMF and dynamic pressure) and geomagnetic effects on cusp location and boundaries. The cusp location of the semi-empirical Tsyganenko 1996 (T96) magnetosphere magnetic field model [Tsyganenko 1995, 1996] and Shue *et al.* [1997] magnetopause model, created using inputs of the observed solar wind and geomagnetic activity level, is compared with the cusp location of a reference T96 and magnetopause model, created using reference solar wind and geomagnetic activity levels. The T96 model uses inputs of  $B_{IMF}$ , dynamic pressure ( $P_{dynamic}$ ), and the disturbance storm time index ( $D_{ST}$ , an index for monitoring worldwide geomagnetic storm levels).

Time lagged solar wind data and coordinate transformed Cluster orbital points were provided by E. Budnik. Solar wind conditions were provided by the ACE satellite which is located between the Earth and Sun. Time lagged solar wind condition files were used to determine the interplanetary magnetic field conditions and solar wind dynamic pressure at Cluster (time lagging is necessary because it takes time for solar wind conditions measured by ACE to reach the position of Cluster). These lagged parameters were updated every 10 minutes. The time lag was a ratio of the distance between the ACE and Cluster spacecraft and the solar wind velocity. The calculated lag time was also visually verified by comparing ACE IMF and Cluster magnetic field data in the magnetosheath (when available) [E. Budnik, *private communication*, 2010]. Spacecraft orbital parameter files contained Cluster spacecraft locations which were updated every two minutes. The coordinate transformation of orbit points into

cusp normalized coordinates followed the process shown in Figure 2.1 [Lavraud *et al.* 2004, 2005]:

- a. The orbit point, A, was rotated about the x solar magnetic axis so it lay in the xz solar magnetic plane. The orbit point was then called A'
- b. The T96 magnetic field model was used to create a reference frame with the conditions:  $B_{IMF} = [0.0, 2.0, 0.0]$  nT,  $P_{dynamic} = 2.5$  nPa, and  $D_{ST} = -10.0$  nT. The duskward IMF condition was chosen to avoid biasing the reference frame towards Earth's equator for southward IMF and towards the poles for northward IMF [Newell *et al.* 1989]. In the reference frame, the latitude angle of a reference separatrix was calculated between the last field line draped onto the dayside and the field line extending to the nightside. The observed lagged solar wind conditions and geomagnetic activity were used in the T96 model to calculate a "current" separatrix latitude angle between the dayside and nightside field lines. The A' point was rotated about the y solar magnetic axis ( $Y_{SM}$ ) so that its angular separation from the reference separatrix is the same as its angular separation was from the "current" separatrix. The new orbit point was called A''.
- c. Using the reference frame's solar and geomagnetic conditions, a reference magnetopause location was calculated using the Shue *et al.* [1997] magnetopause model. The Shue model was also used to calculate the actual magnetopause location relative to the orbit point A'' using the actual solar wind and geomagnetic conditions. The point A'' was radially scaled by the ratio of the reference magnetopause distance to the actual magnetopause to become point A'''

Only data points where the radial direction from the Earth to the spacecraft formed an angle less than  $25^\circ$  with the  $YZ_{SM}$  plane were used in this study. This avoids mixing cusp encounters with data from the low-latitude boundary layer and plasma sheet [Lavraud *et al.* 2004].

This study used 3D data transformed into the 2D xz plane to obtain distributions with large enough statistics for averaging purposes [Lavraud *et al.* 2004, 2005]. The

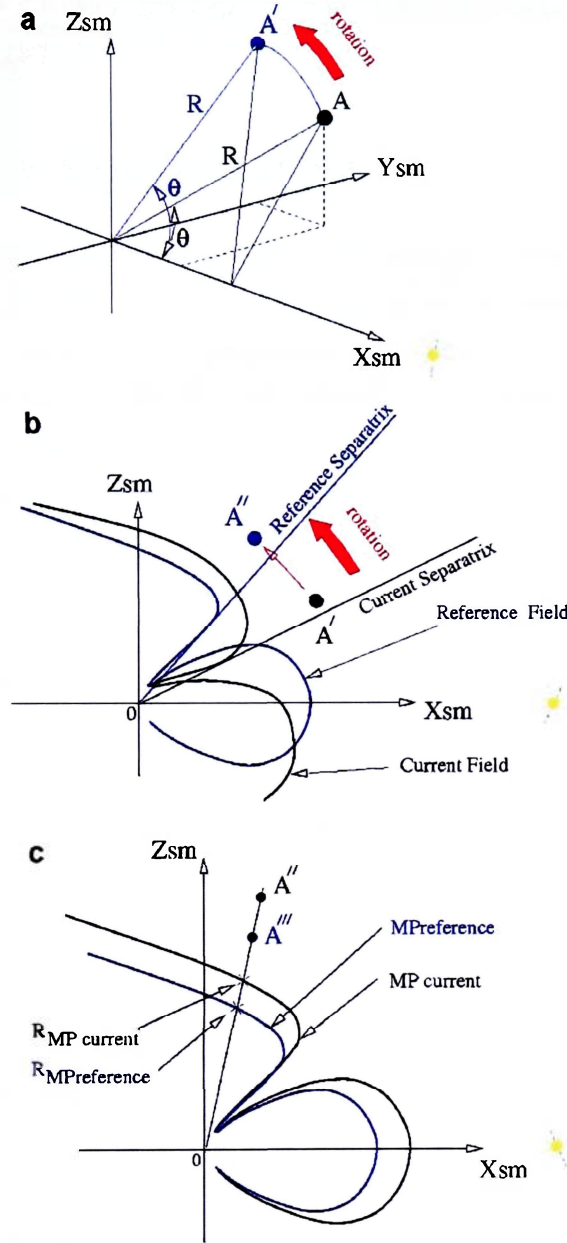


Figure 2.1: Representation of data coordinate transformations to cusp normalized coordinates [Lavraud *et al.* 2005]. (a) Data points were rotated about the  $x$  solar magnetic axis to lie in the  $XZ_{SM}$  plane. (b) Data points were rotated about the  $Y_{SM}$  axis by the angle determined by the “current” separatrix and T96 magnetic field model separatrix (see text). (c) Data points were radially scaled relative to a reference magnetopause using the “current” solar wind conditions. Magnetopause model from Shue *et al.* [1997].

high altitude cusp may have structure in the dawn-dusk directions which are not considered in this thesis.

## 2.3 Magnetic Pressure Plots

To ensure that the data processing and plotting software routines were working, the magnetic pressure,  $\frac{B^2}{2\mu_0}$ , was plotted for the low resolution magnetic field data from Cluster spacecraft 1 as a ratio to the magnetic pressure in the T96 model (Figure 2.2) and compared with a similar plot in *Lavraud et al.* [2004]. They both show that the highest magnetic pressure exists in the magnetosheath, that the cusp is a region of low magnetic pressure, and that the high-altitude magnetosphere has a magnetic pressure value between that of the magnetosheath and cusp.

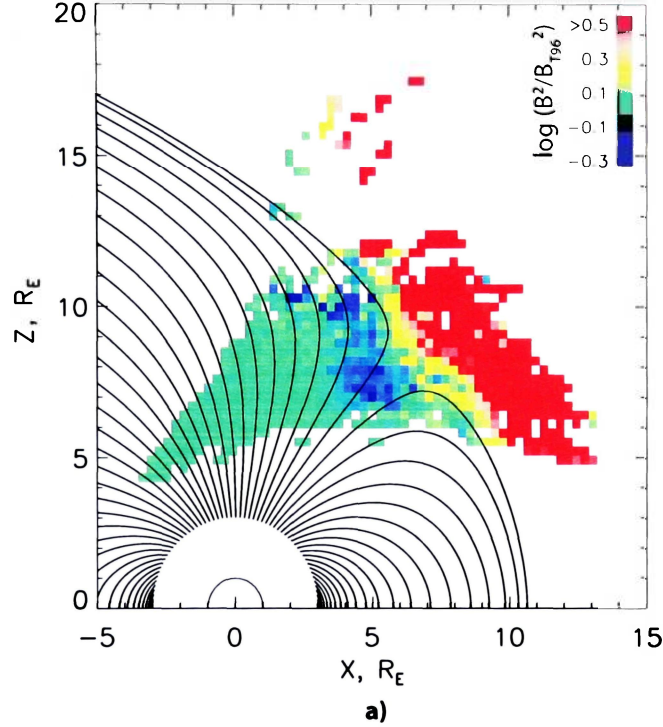
Each data square in Figure 2.2a represents  $0.3 R_e \times 0.3 R_e$ . In order to depict the number of data points averaged in this region of space, each square can be sized according to the number of data points averaged, with size saturation of  $0.3 R_e$  at 20 or more data points [*Lavraud et al.* 2005]. Figure 2.2b shows the data from Figure 2.2a where each data square has been sized according to the number of data points averaged in that  $0.3 R_e \times 0.3 R_e$  region of space.

The field lines in all such plots were generated with the T96 model using reference solar wind and geomagnetic conditions,  $B_{IMF} = [0.0, 2.0, 0.0]$  nT,  $P_{dynamic} = 2.5$  nPa, and  $D_{ST} = -10.0$  nT.

## 2.4 Calculating Power in the Magnetic Field Fluctuations

The fluxgate magnetometer data exists, and was used, in low and high resolution form. Data gaps in the magnetic field data were filled in with linear interpolation so the spacing between all data points was the same. The duration of each cusp crossing was broken into two minute sections, approximately the amount of time it would take Cluster to travel  $0.3 R_e$  at the cusp (and the amount of time between orbital parameter

Magnetic Pressure Ratio, All IMF clock angles



Magnetic Pressure Ratio, All IMF clock angles

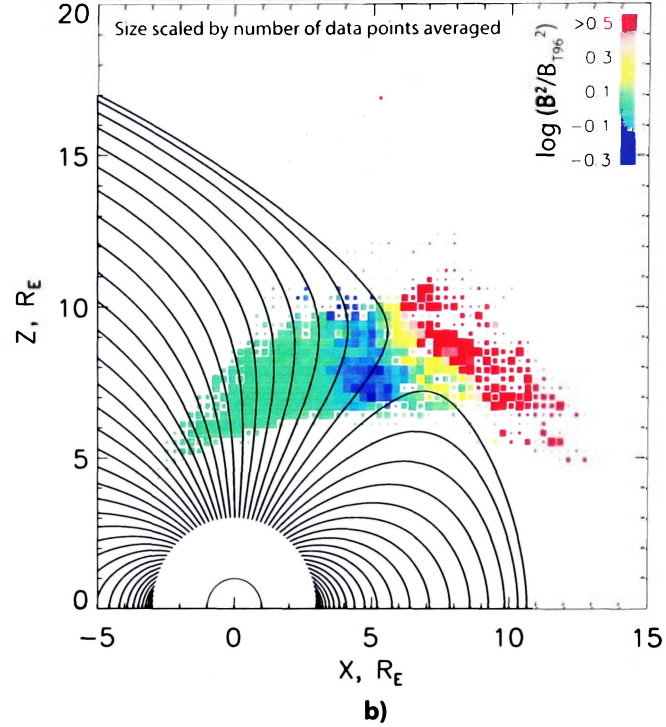


Figure 2.2: Magnetic pressure from Cluster spacecraft 1 data.  $\log \frac{(MagneticField)^2}{(Tsyganenko96MagneticField)^2}$  is plotted over T96 field lines. **a)** the size of each data square is  $0.3 R_E$ . **b)** the size of each data square is scaled according to the number of data points averaged. The size reaches a maximum of  $0.3 R_E$  when 20 or more data samples are averaged.

updates). For each two minute section, the data was first detrended. The detrending process subtracted a linear least squares fit from the magnetic field measurements. Without detrending, there would be an overestimation of the fluctuation power in the signal by the background magnetic field. The effect of detrending is seen in Figure 2.3 by comparing the bottom plot, which shows the total magnetic field data, and the  $dB_T$  plot, which shows the total magnetic field after detrending. Fluctuations in the undetrended data are small and look insignificant compared to the stronger [decreasing] background field, so to study them, detrending must be performed.

The detrended data was multiplied by a Hanning window to reduce spectral leakage when a Fourier transform was performed. A more in-depth discussion about windowing is provided in Chapter 3. A discrete Fourier transform (DFT) was performed on  $B_x$ ,  $B_y$ ,  $B_z$ , and  $B_{tot}$  so a study of the power in the fluctuations at different frequencies could be accomplished. Steps 1-3 below details how the mean, total, and perpendicular power were calculated for each measurement point of the data set. Figure 2.4a shows a two minute section of magnetic field data in frequency space after both a DFT and the total power calculation.

1. The mean (compressive) power was calculated by squaring the absolute value of the  $B_{tot}$  data in frequency space. It is the magnetic field power in fluctuations of the total magnetic field,  $B_{tot}$ .
2. The total power was calculated by taking the trace of the power spectral matrix: each data point for  $B_x$ ,  $B_y$ , and  $B_z$  in frequency space was squared; then the squared x, y, and z components were summed. It is the total power in the x, y, and z directions.
3. The perpendicular (transverse) power was calculated by subtracting the mean power from the total power (Power in  $B_x$  + Power in  $B_y$  + Power in  $B_z$  - Power in  $B_{tot}$ ). It is the magnetic field power in fluctuations perpendicular to the magnetic field.

Middle Riemann sums were used to calculate the integrated mean, total, and perpendicular power of the magnetic field fluctuations for each two minute segment.



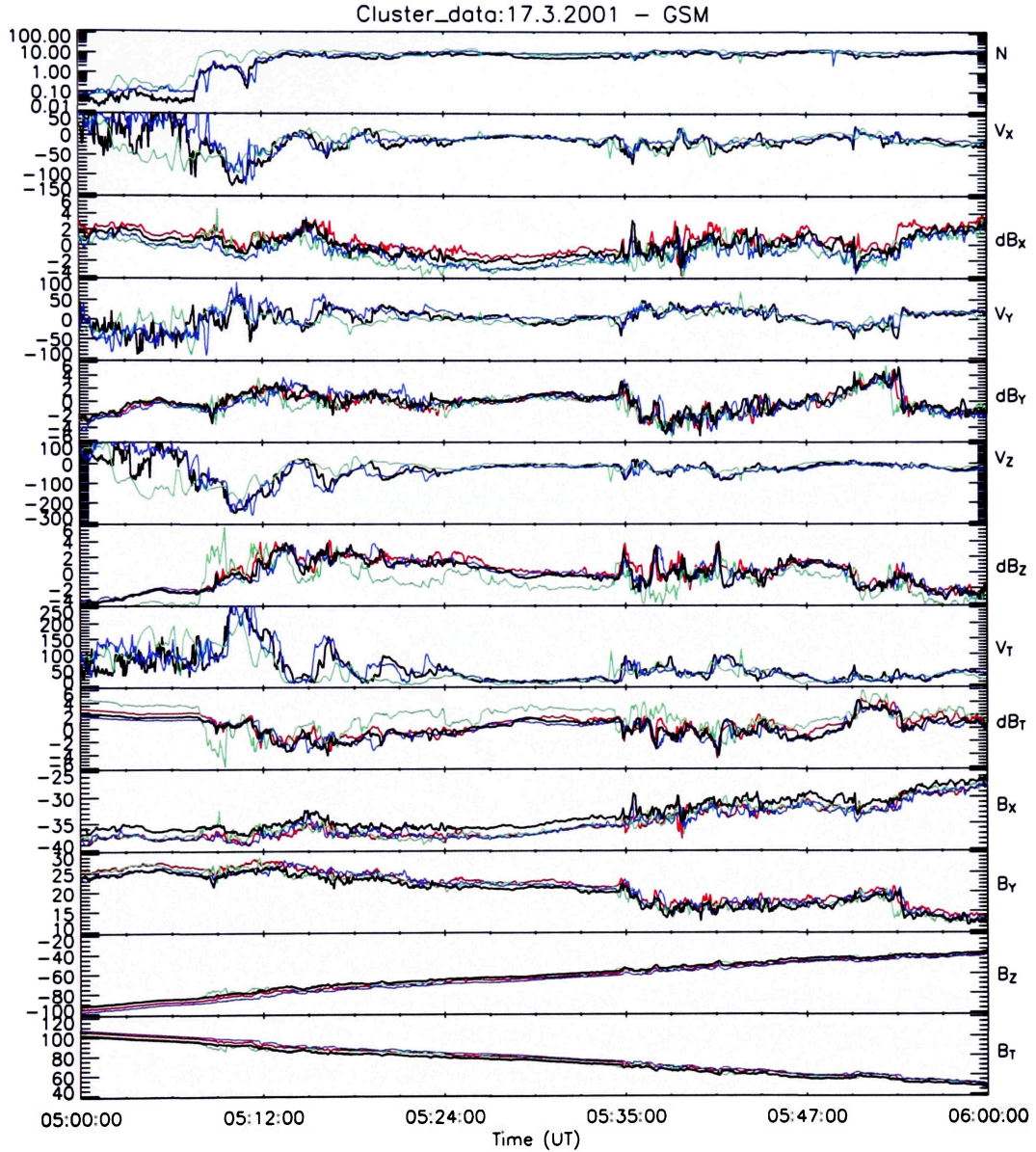


Figure 2.3: Cluster data on 17 March 2001 from 5:00:00-6:00:00 UT for a gradual cusp interval. Black, red, green, and blue correspond to spacecraft 1, 2, 3, and 4. The bottom plot shows the total magnetic field data while  $B_x$ ,  $B_y$ , and  $B_z$  show the magnetic field components in x, y, and z respectively. The  $dB_T$  plot shows the total magnetic field after detrending (after subtracting the linear fit of the original data).  $dB_x$ ,  $dB_y$ , and  $dB_z$  plots show the detrended  $B_x$ ,  $B_y$ , and  $B_z$  magnetic field components respectively. The N plot shows the number of particles.  $V_T$  shows the total velocity while  $V_x$ ,  $V_y$ , and  $V_z$  plots show the x, y, and z plasma velocity components respectively. [Nykyri et al. 2004]

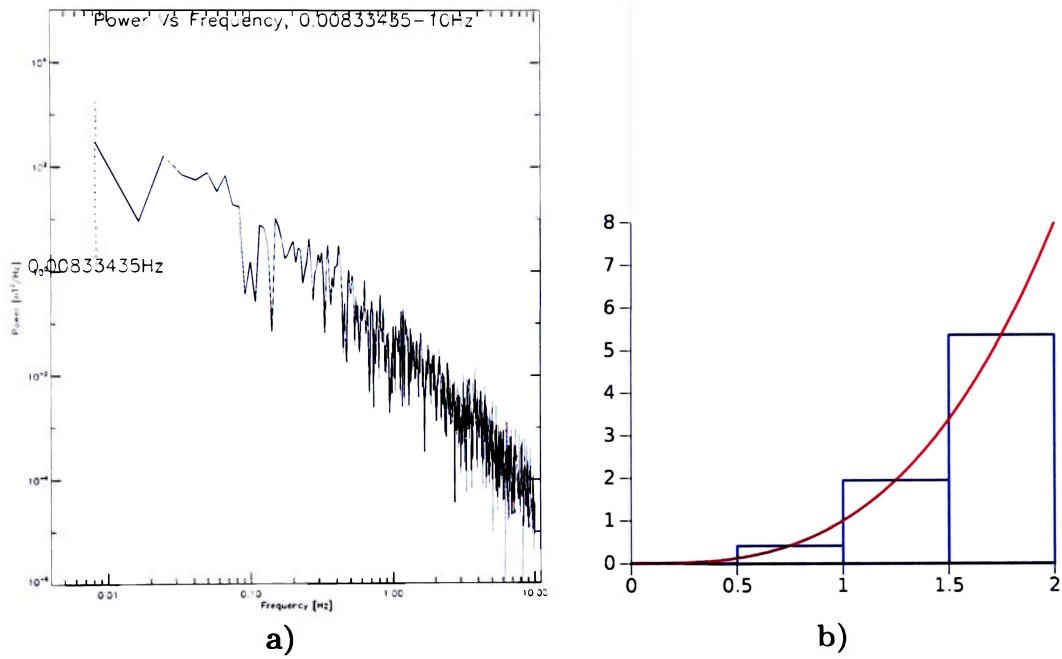


Figure 2.4: **a)** Example power spectrum showing two minutes of magnetic field data in the frequency domain; total power of the magnetic field fluctuations is plotted with respect to frequency. **b)** Artistic depiction of the middle Riemann sum used to calculate the integrated power (area under the black curve in **a**)) [Richards].

The start and stop points were changed to investigate different frequency ranges. An artistic representation of a middle Riemann sum is shown in Figure 2.4b. For this sketch, the power data would exist at points 0, 0.5, 1, 1.5, and 2 along the horizontal axis (frequency in this context). The vertical axis would be power (mean, total, or perpendicular). The red curve would be the theoretical curve connecting the data points. The middle Riemann sum is the sum of the area inside all the blue rectangles (the “area under the curve”).

Finally, the integrated power was normalized. Normalization is discussed in Chapter 3.

## Chapter 3

# Data Windowing, Artificially Induced Power, and Normalization

### 3.1 Window Types

The goal of this study was to analyze the power in the magnetic field fluctuations at different frequencies in the magnetospheric cusp and surrounding regions. To transform the magnetic field data into frequency space, a Discrete Fourier Transform (DFT) was performed. The DFT can be computed efficiently in practice using a Fast Fourier Transform algorithm (FFT). The use of “FFT” in this document will refer to the DFT. Because the start and end points of a data set are not necessarily equal and because of the mathematical properties of the DFT, an additional step was needed to reduce spectral leakage. Spectral leakage is when a wave’s frequency spectrum has energy in several frequency channels instead of just the exact frequency(ies) that correspond to that wave. It affects any frequency component of a signal which does not exactly coincide with the frequency channels defined by the DFT. Windowing reduces the effects of spectral leakage associated with finite observation intervals by multiplicatively weighting the data by a window function,  $w(k)$ , before a DFT is performed. The windowing process sets the endpoints of a signal at or near the same level. This allows the periodic extension of the data employed by the DFT to be continuous in many orders of derivative [Harris 1978].

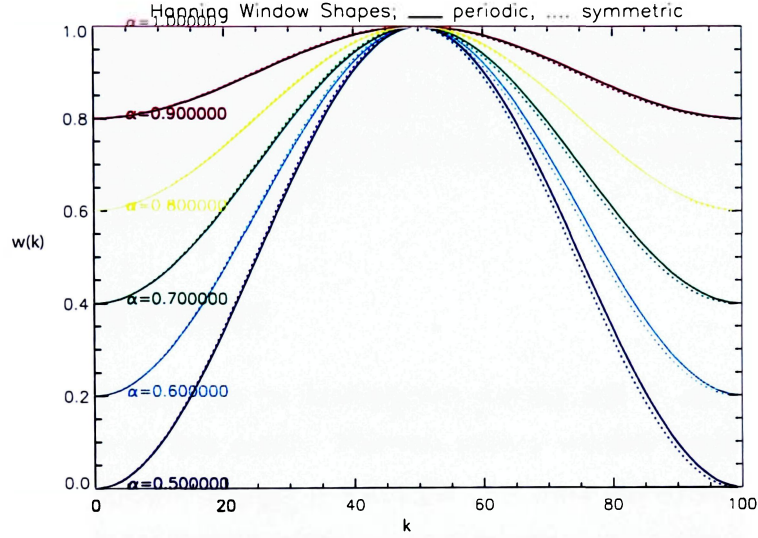


Figure 3.1: Periodic and symmetric Hanning windows with different  $\alpha$  values and  $N = 100$ .

A Hanning window was chosen because it is commonly used in power calculations. Hanning windows exist in a periodic and symmetric form. The periodic Hanning window is given by Equation 3.1 and the symmetric Hanning window is given by Equation 3.2.  $N$  is the number of points in the window and  $k$  is integer values from 0 to  $N$ .  $N$  equals the number of data points being analyzed.  $\alpha$  controls the shape of the window.

$$w(k) = \alpha - (1 - \alpha) \cos\left(\frac{2\pi k}{N}\right) \quad (3.1)$$

$$w(k) = \alpha - (1 - \alpha) \cos\left(\frac{2\pi k}{N-1}\right) \quad (3.2)$$

A plot of both types of Hanning windows for different  $\alpha$  values ( $\alpha = 0.5, 0.6, 0.7, 0.8, 0.9, 1.0$ ) is shown in Figure 3.1. When  $\alpha = 1$ , the window becomes equal to 1 at all  $k$ . This is called a rectangular window and is equivalent to not multiplying by a window at all. For  $\alpha = 0.5$ , the symmetric window equals zero at both endpoints  $k = 0 = N$  while the periodic window only equals zero at  $k = 0$  for  $k \leq N$ . The periodic Hanning window was chosen because the windowed data will have a FFT

performed on it [Harris 1978]. Because the DFT considers data sequences to be periodic, the window function at  $N+1$ ,  $w(k = N + 1)$ , must be equal to  $w(k = 0)$ , which describes a periodic window. All further references to  $\alpha$  values and windowing refers to a periodic Hanning window.

## 3.2 Artificial Power

The lowest frequency that can be investigated corresponds to the window width, which is two minutes in this study. The two minute window length chosen could artificially introduce power at  $\frac{1}{2 \text{ min}} = 0.008 \text{ Hz}$ . To avoid any extra artificial power when calculating the integrated power, it is good practice to drop the frequency corresponding to the window length. The effect of removing this and the next lowest frequency of the DFT is examined in this section (dropping no frequencies, dropping 0.008 Hz, dropping 0.008 Hz and 0.017 Hz). Figure 3.2 shows data from the cusp crossing of 14 February 2003. The top row shows the integrated total power over the entire the cusp crossing. The bottom row shows a two minute power spectrum from that cusp crossing. Each column shows the data with different frequency ranges integrated. The first column's frequency range is from the window length,  $\frac{1}{2 \text{ min}} = 0.008 \text{ Hz}$ , to 10 Hz. The second column does not include the window length (the first frequency from the FFT, 0.008 Hz) and runs from 0.017-10 Hz. The third column is from 0.025-10 Hz.

From the top row of Figure 3.2, it is seen that excluding the 1st, 2nd, 3rd, ... frequencies will lower the total integrated power calculated over a cusp crossing. As a convention, the lowest frequency of a DFT is not considered in calculating the integrated power so the first column of the figure is not considered. An examination of the top plot in the second column showed a difference in the total integrated power signal shape at the  $\sim 19.25 \text{ UT}$  peak between  $\alpha = 0.5, 0.7$ , and  $1.0$ . The signal for  $\alpha = 1$  peaks quickly with a sharp slope and falls off more slowly. Examining the signal for  $\alpha = 0.7$  and  $\alpha = 0.8$  indicates that  $\alpha \approx 0.75$  will most likely have a "flat" peak. The signal for  $\alpha = 0.5$  rises with a shallow slope and drops off quickly.

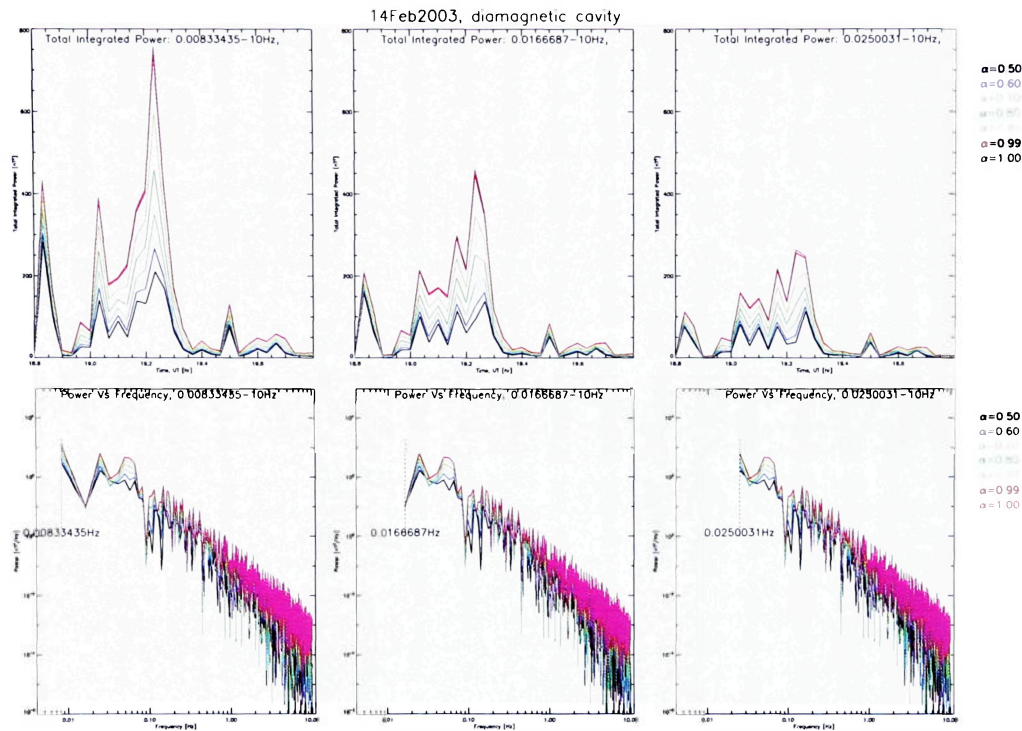


Figure 3.2: Plots investigating the effect on the total integrated power over a cusp crossing when leaving out the lowest frequencies. First row shows the integrated total power over an entire cusp crossing. The second row shows a sample total power spectrum of the cusp crossing. The area under the total power spectrum curve is the total integrated power for the windowed data. The data has been windowed with a Hanning window of  $\alpha = 0.5, 0.6, 0.7, 0.8, 0.9, 0.99, \text{ and } 1$ .



Magnetosphere, cusp, and magnetosheath plots of the integrated power for cusp crossings in cusp normalized coordinates (defined in Section 2.2), with and without the lowest two frequencies, 0.008 Hz and 0.017 Hz, were made for  $\alpha = 0.5, 0.75, 1.0$ . They are shown as Figures 3.3-3.5 in this section and Figures B.1-B.6 in Appendix B with individual figures for each type of power (mean, total, and perpendicular) and each frequency range (0.008-10 Hz, 0.017-10 Hz, and 0.025-10 Hz). Each column shows the integrated power for a different  $\alpha$  Hanning window value. Each figure's rows show the data with NIMF, SIMF, and all IMF orientations (AIMF) respectively. In this study, NIMF is considered to be IMF clock angles  $< 60^\circ$  and SIMF is IMF clock angles  $> 120^\circ$ . AIMF considers all clock angles. Clock angle is calculated as  $\arctan\left(\frac{B_y}{B_z}\right)$  for the IMF in GSM. Figures B.1-B.3 show mean power, Figures 3.3-3.5 show total power, and Figures B.4-B.6 show perpendicular power. Only the data from Cluster spacecraft 1 is used in these figures.

As  $\alpha$  increases, the overall integrated mean, total, and perpendicular power increases for all the figures, but the same main regions of enhanced power are present. When omitting the first and second frequencies, the overall integrated power is successively lowered, but the main regions of enhanced power are also still present. Figure 3.6 examines the different regions of enhanced total power between NIMF and SIMF shown in Figure 3.4 for 0.017-10 Hz and  $\alpha = 0.5$ . As mentioned above, the outlined regions of enhanced power in Figure 3.4 are visible in all the frequency ranges and  $\alpha$  values of Figures 3.3-3.5.

In Figures 3.3-3.5, for NIMF, there is a region of higher power tailward of the cusp proper. For SIMF, the region of higher power moves more towards the dayside lobe. These regions are labeled 1. in Figure 3.6. The location of enhanced power moves due to the movement of the reconnection site tailward or sunward due to NIMF or SIMF respectively. Additional examination of Figures 3.3-3.5 shows other repeated regions of enhanced power in the vicinity of the cusp for all three frequency ranges and  $\alpha$  values. These groups of enhanced power are labeled 2-4 in Figure 3.6. The points that have higher power due to the spacecraft crossing from the tail-lobe into the magnetosheath, where there is a gradient in the magnetic field strength, are labeled 2. Group 2 points may also include power due to mirror mode waves. The points labeled



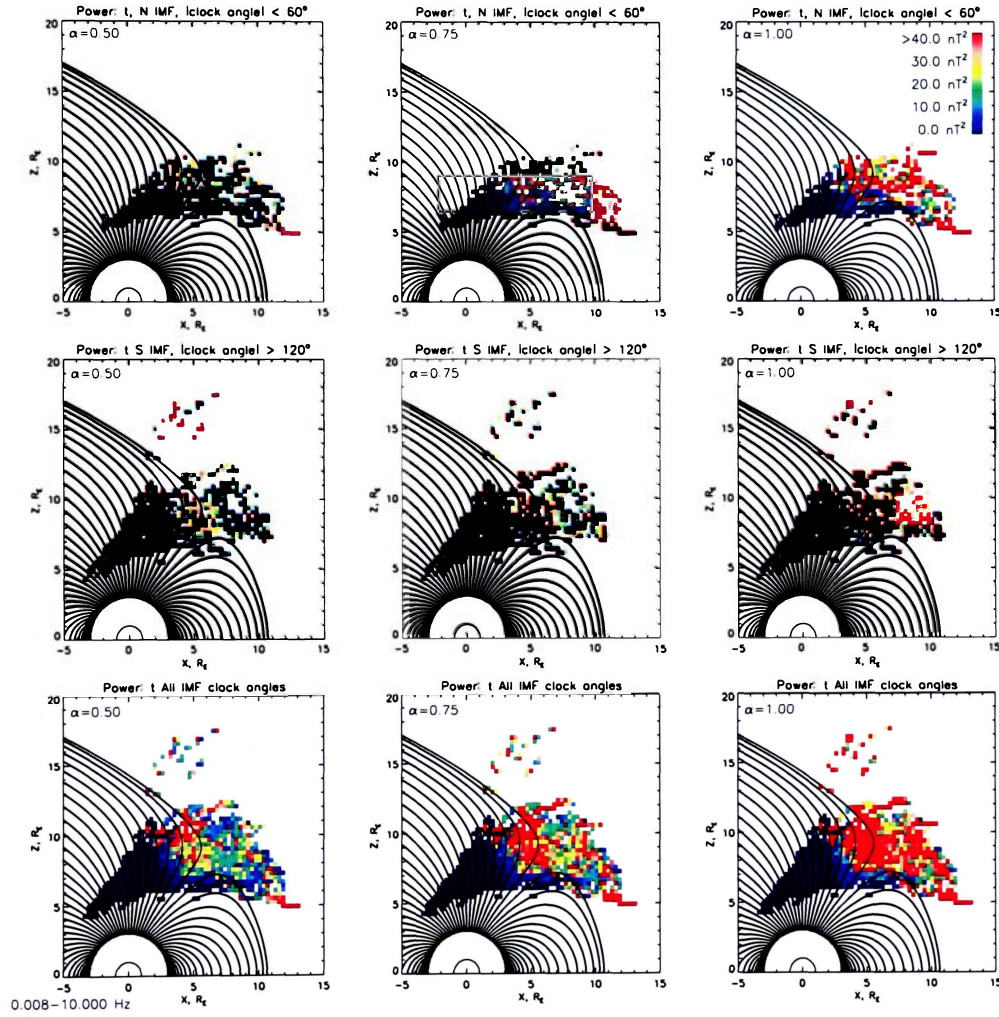


Figure 3.3: Total integrated power in the magnetic field fluctuations of the 0.008-10 Hz frequency range for NIMF, SIMF, and AIMF (rows) and Hanning window with  $\alpha = 0.5, 0.75, \text{ and } 1$  (columns).

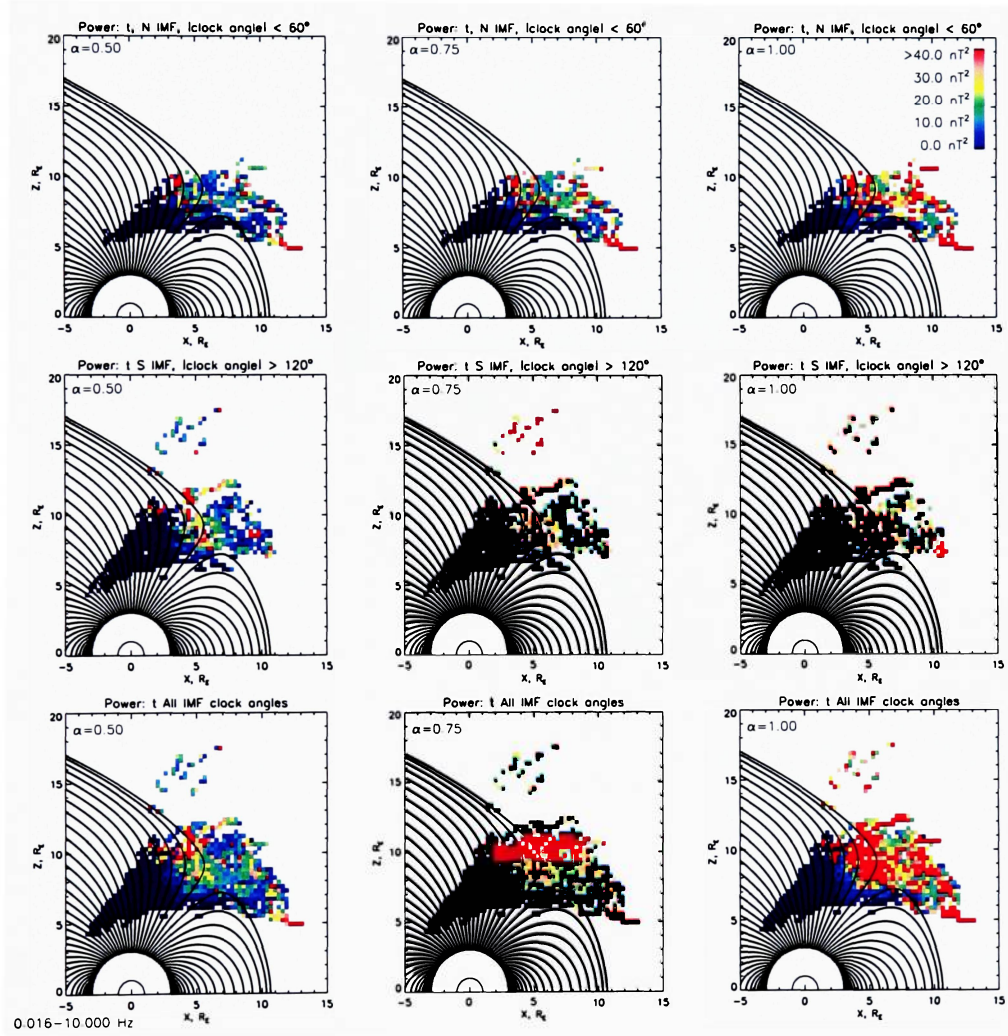


Figure 3.4: Total integrated power in the magnetic field fluctuations of the 0.017-10 Hz frequency range for NIMF, SIMF, and AIMF (rows) and Hanning window with  $\alpha = 0.5$ ,  $0.75$ , and  $1$  (columns).

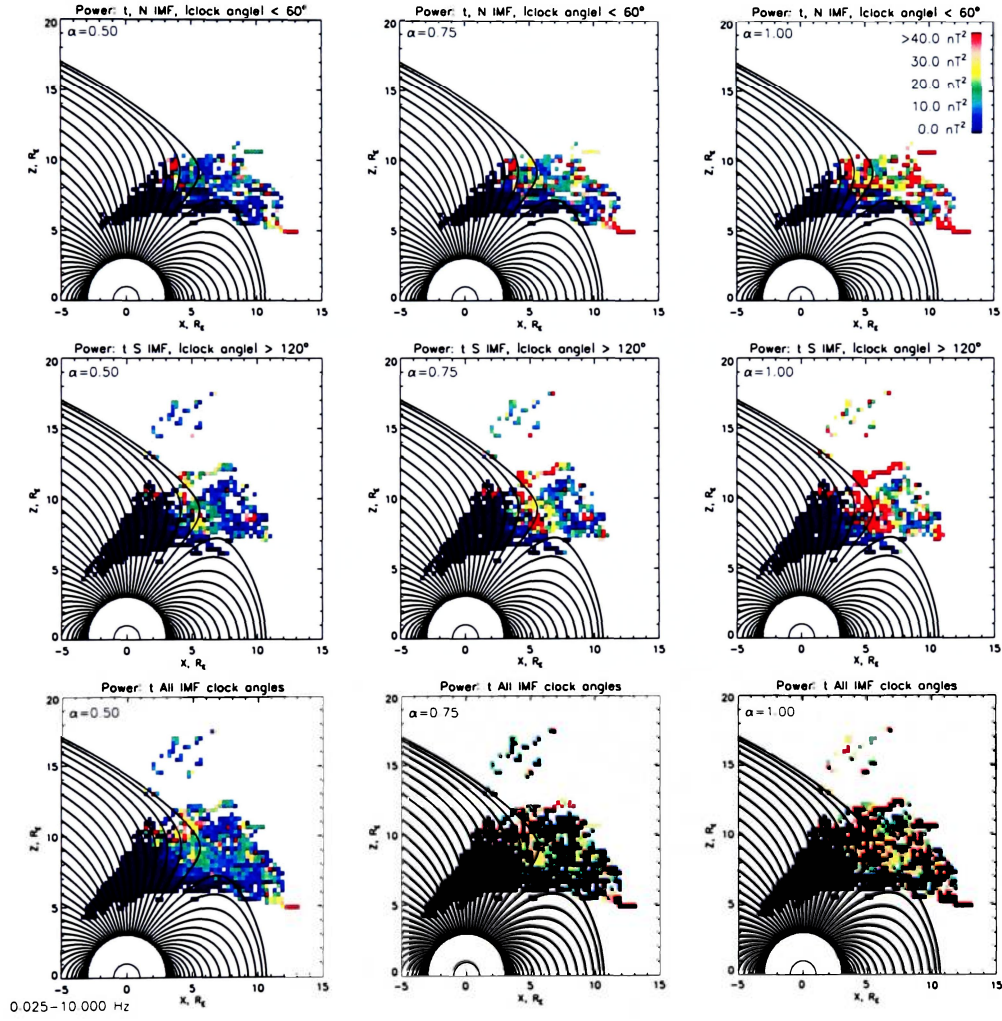


Figure 3.5: Total integrated power in the magnetic field fluctuations of the 0.025-10 Hz frequency range for NIMF, SIMF, and AIMF (rows) and Hanning window with  $\alpha = 0.5, 0.75$ , and 1 (columns).



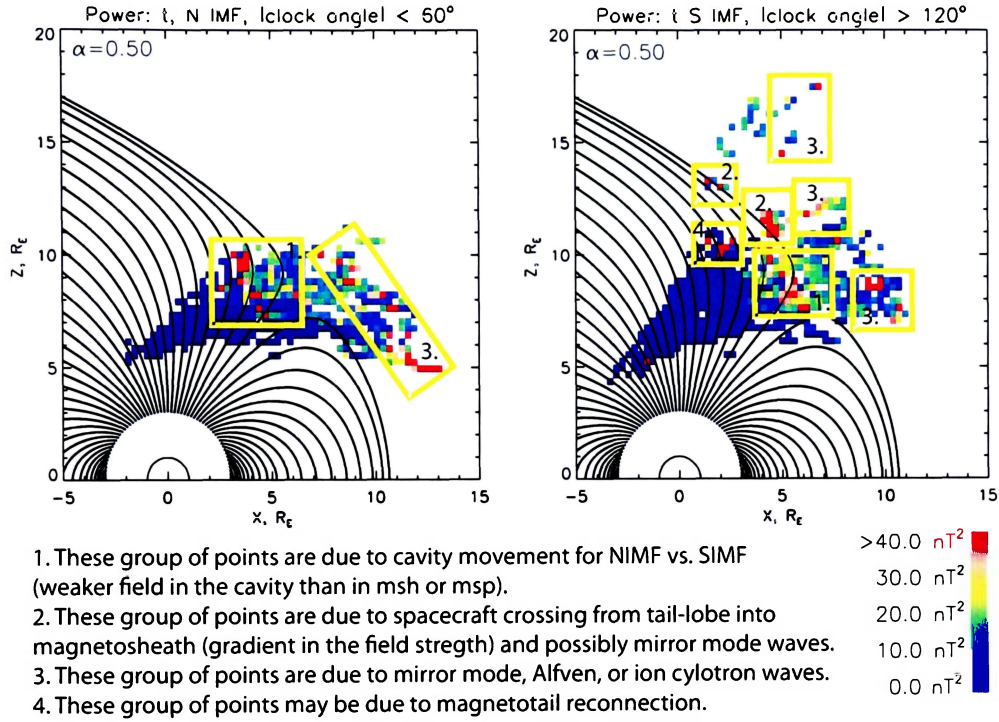


Figure 3.6: Total integrated power of magnetic field fluctuations for Cluster spacecraft 1 from 0.017-10 Hz for NIMF and SIMF from Figure 3.3 using Hanning window with  $\alpha = 0.5$ . Regions of enhanced wave power are outlined.

3. are in the magnetosheath and can be caused by mirror mode, Alfvén, and ion-cyclotron waves. The points labeled 4. could be caused by the effects of magnetotail reconnection propagating earthward. These groups are explained in more detail in Chapter 4.

Performing a similar analysis for the mean and perpendicular power, it was seen that most of the same enhanced power regions as Figure 3.6 were identifiable, with and without frequency exclusions, and for every  $\alpha$ .

The use of a Hanning window with  $\alpha \neq 0.5$  changes the frequency response of the DFT. For a  $\alpha = 0.5$  window, there is better rejection of unwanted frequency signals ( $> 10$  Hz) than with  $\alpha > 0.5$  [Martin 2007]. The analysis in this section showed that even with windowing, the main regions of enhanced power were not diminished. For

these reasons, and the fact that  $\alpha = 0.5$  has been used for power studies before, such as in *Nykyri et al.* [2003, 2004], a Hanning window with  $\alpha = 0.5$  was chosen.

It was decided to only exclude the power at  $\frac{1}{2_{\text{min}}} = 0.008$  Hz when calculating the integrated power to avoid any extra artificial power. No other frequencies were excluded.

### 3.3 Normalization

Any window besides a rectangular window will typically result in decreased power when a Fourier transform is performed, so the power with a Hanning window of  $\alpha = 1$  is higher than if  $\alpha = 0.5$ . In the event that windowing with  $\alpha = 0.5$  was underestimating the power because the windowed signal is increasingly decreased as you move away from the signal midpoint, a normalization process was used to correct the power level to what it would be without windowing (or  $\alpha = 1$ ), essentially multiplying the power by some factor. There is no spectral leakage reduction with  $\alpha = 1$  and there should be some level of spectral leakage reduction with  $\alpha = 0.95$ . To determine if there was significant difference in normalizing to  $\alpha \neq 1$ , the normalization to  $\alpha = 0.95$  was also performed.

In the normalization process, the data was first windowed with a Hanning window with  $\alpha = 0.5$  and a FFT was performed. Two normalization calculations were performed to correct integrated power levels to what it would be with 1.  $\alpha = 1$  and 2.  $\alpha = 0.95$ . The area under the Hanning window was calculated for  $\alpha = 0.5$ ,  $0.95$ , and  $1$ .

1. (Area under Hanning window  $\alpha = 1$ )\*(Integrated power of data using Hanning window  $\alpha = 0.5$ )/(Area under Hanning window  $\alpha = 0.5$ ) = integrated power normalized to the level it should be at if the integrated power was calculated with  $\alpha = 1$  Hanning window (rectangular window).
2. (Area under Hanning window  $\alpha = 0.95$ )\*(Integrated power of data using Hanning window  $\alpha = 0.5$ )/(Area under Hanning window  $\alpha = 0.5$ ) = integrated

power normalized to the level it should be at if the integrated power was calculated with  $\alpha = 0.95$  Hanning window.

Figure 3.7 shows the normalized (green) and unnormalized (red) total power for the cusp crossing of 14 February 2003. Blue shows the power level that the normalized power (green) is trying to obtain (but green is with reduced spectral leakage). From this figure, it can be seen that the normalized power is mostly below the reference level (blue), as expected. The normalization process only overshoots the reference level at 6 two-minute segments over the entire cusp crossing of about 1800 two-minute segments (an insignificant fraction of the total number of segments). Over all 118 cusp crossings the study considered, the integrated daily power of the normalized signal was never higher than the integrated daily power of the reference signal. It was also seen that there was no significant difference in normalizing to  $\alpha = 0.95$  versus  $\alpha = 1$ . A normalization to  $\alpha = 1$  was chosen because the  $\alpha = 1$  normalization has been used in other studies [Carozzi *et al.* 2001].

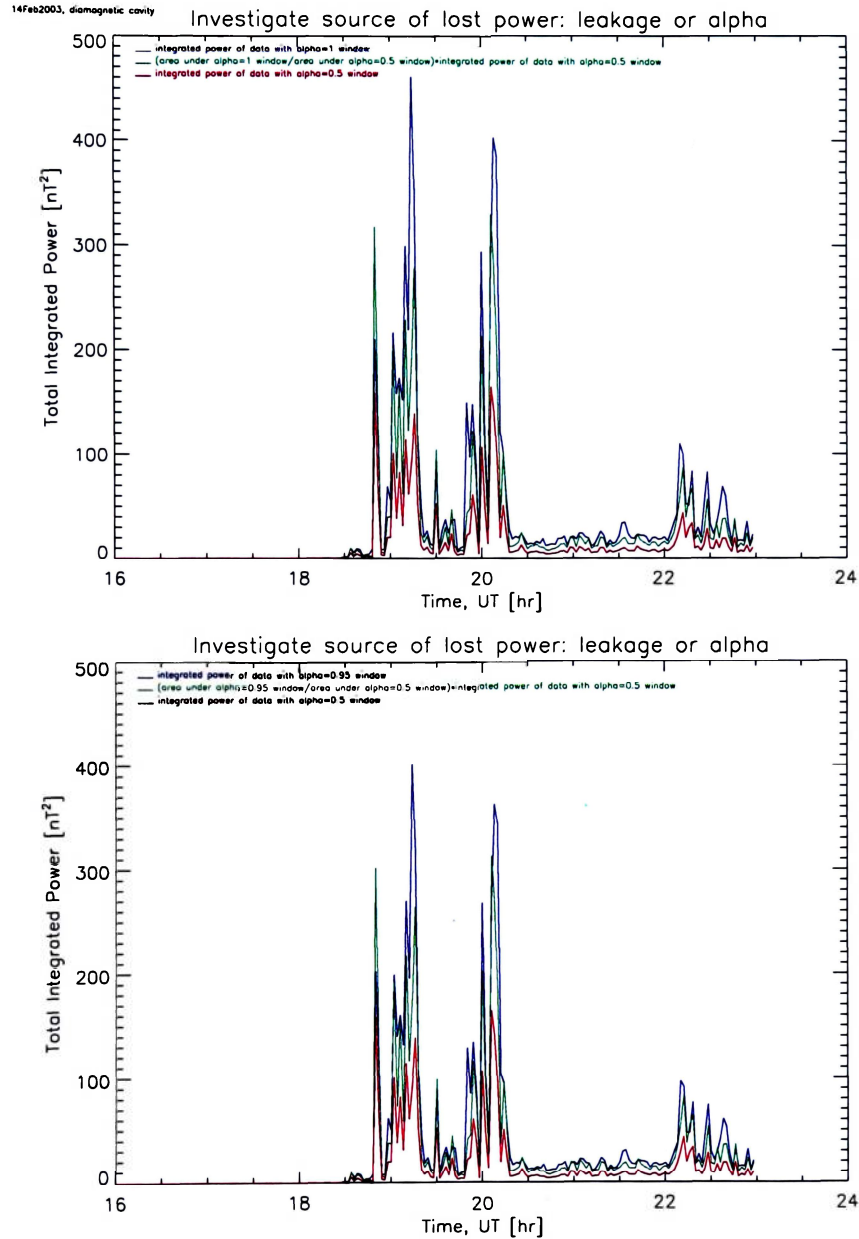


Figure 3.7: Normalized (green) and unnormalized (red) integrated total power (Hanning windowed with  $\alpha = 0.5$ ) for Cluster cusp crossing on 14 February 2003. For the green curves, power is normalized to  $\alpha = 1$  (top) and  $\alpha = 0.95$  (bottom). For reference, the integrated total power calculated using a Hanning window with  $\alpha = 1$  and  $\alpha = 0.95$  is included in the top and bottom plots respectively (blue). Each data point is the integrated total power of a two minute data segment (points shown connected).

# Chapter 4

## Integrated Power

### 4.1 Integrated Power

In this chapter, the normalized mean, total and perpendicular integrated power in the magnetic field fluctuations of the four Cluster spacecrafts' 2001-2003 cusp crossings are presented in cusp normalized coordinates for different frequency ranges. Mean, total, and perpendicular power were defined in Section 2.4. Figure 4.1 shows integrated power from 0.017-10 Hz. Figure 4.2 shows integrated power from 0.017-0.1 Hz. Figure 4.3 shows integrated power from 0.1-10 Hz. The rows present data for NIMF, SIMF, and AIMF. The first column is the mean power, the second column is the total power, and the third column is the perpendicular power. To see the unnormalized integrated power plots, see Appendix C. To see the data squares proportionally sized to the number of data points averaged (normalized integrated power), see Appendix D. For the standard deviation of the plots in Figure 4.1-4.3, see Section 4.2 below.

The notable regions of increased integrated power in the magnetic field fluctuations from 0.017-10 Hz in Figure 4.1 are outlined in Figures 4.4-4.7. Figure 4.4 outlines the shift of the increased power due to reconnection site changes for NIMF versus SIMF. Figure 4.5 outlines the points with increased magnetic field fluctuation power because of a gradient in the magnetic field strength as Cluster moves from the MSP into the MSH. Power in these points may also be caused by mirror mode waves. Figure 4.6 highlights the points with increased power due to different wave modes



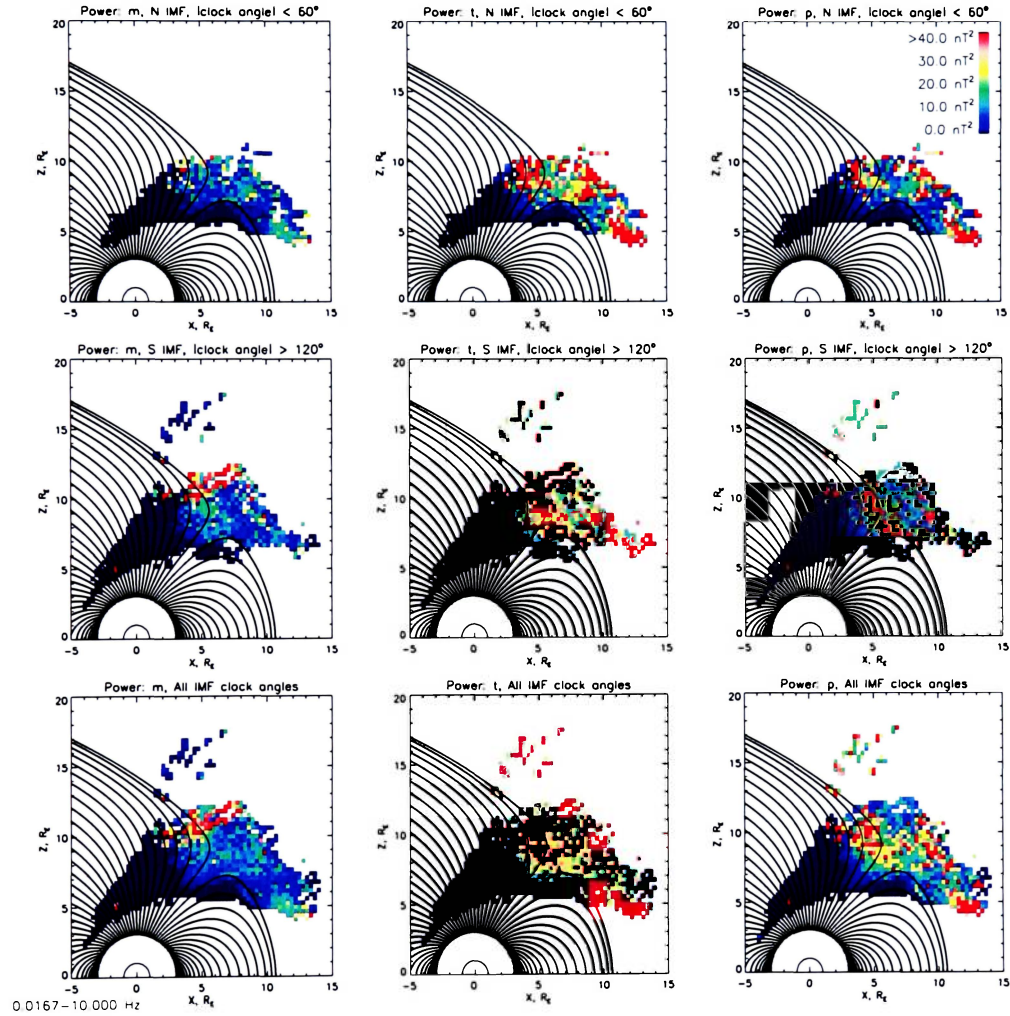


Figure 4.1: Normalized integrated mean, total, and perpendicular power in the magnetic field fluctuations of the 0.017-10 Hz frequency range for NIMF, SIMF, and AIMF.

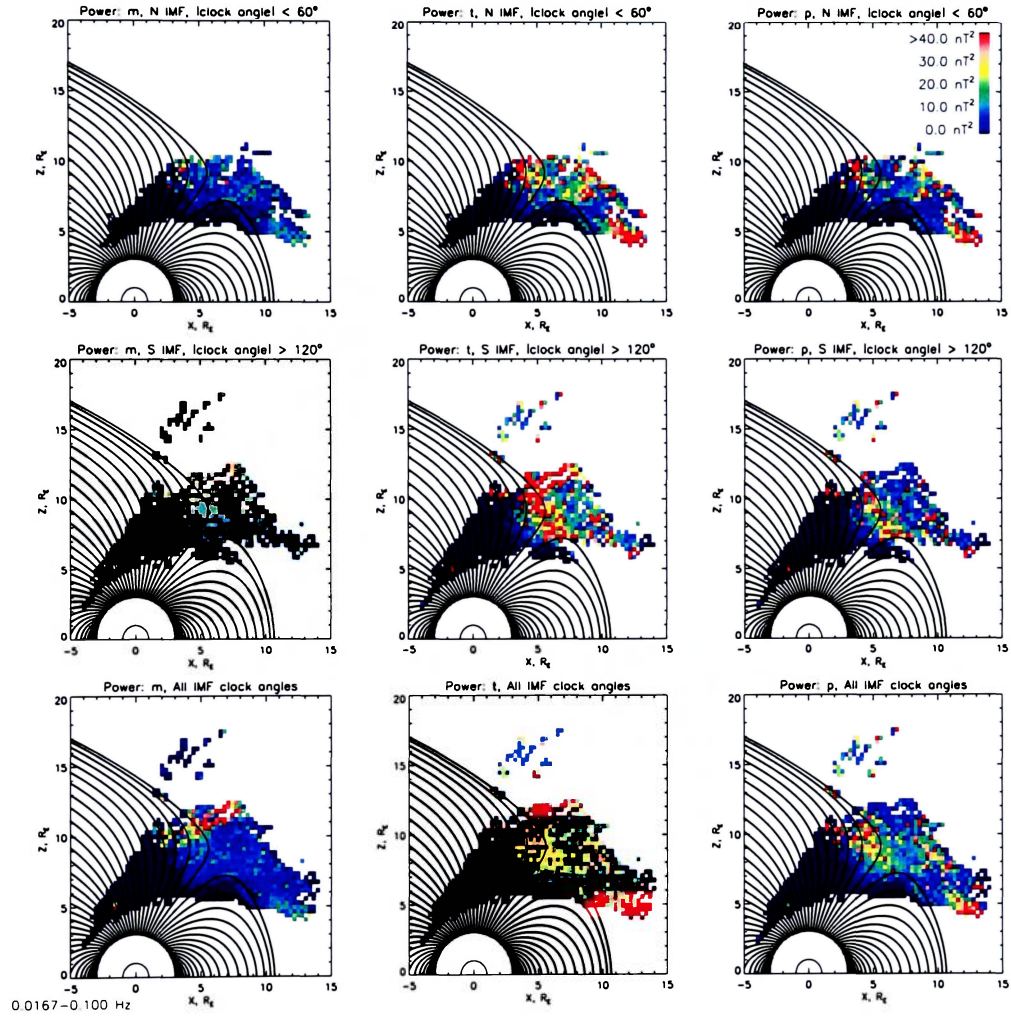


Figure 4.2: Normalized integrated mean, total, and perpendicular power in the magnetic field fluctuations of the 0.017-0.1 Hz frequency range for NIMF, SIMF, and AIMF.

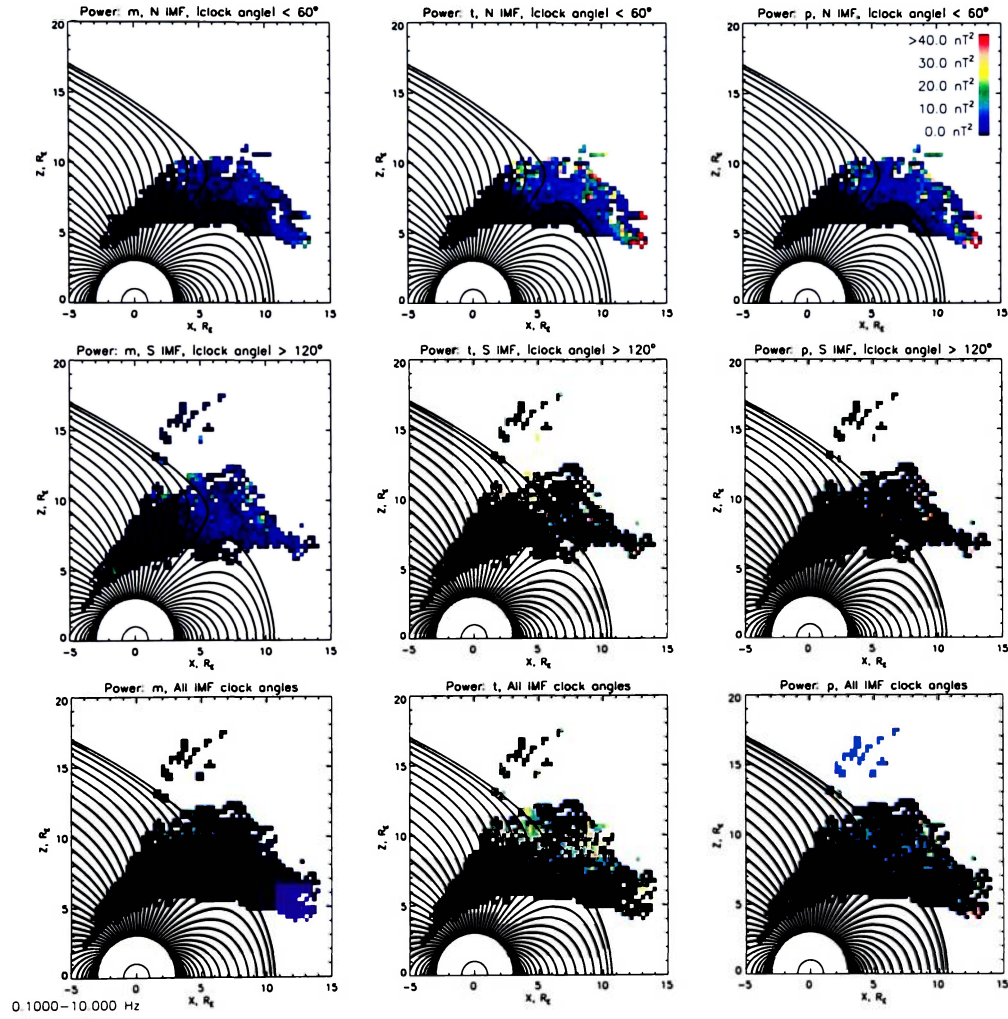


Figure 4.3: Normalized integrated mean, total, and perpendicular power in the magnetic field fluctuations of the 0.1-10 Hz frequency range for NIMF, SIMF, and AIMF.

present in the MSH. A justification for three specific wave modes (IC, Alfvén, and mirror) being present is provided later in this section. Figure 4.7 outlines the points that may have increased power due to effects of magnetotail reconnection propagating towards Earth. These points are at a location where the field lines could be open and about to reconnect, or closed and newly reconnected. *Lin et al.* [2000] showed that  $\sim 0.0006$ - $0.0022$  Hz compressional magnetic field fluctuations were seen by the WIND spacecraft in the magnetotail following dipolarization of the field lines. Although this is about an order of magnitude lower than the lowest frequency in this study, this does not rule out the possibility of some other type of magnetotail wave or fluctuation causing enhanced power near Earth. Simulations by *Ma et al.* [1995] have shown that magnetotail reconnection generates Alfvén waves that propagate parallel to the local magnetic field. This type of fluctuation could be causing this region of enhanced power. An analysis of the particle flux at these points could help support the magnetotail-reconnection-effect propagation hypothesis.

These four possible causes of enhanced power are summarized in Figure 4.8 for NIMF versus SIMF at 0.017-10 Hz. Most of these four regions of enhanced power also appear in the power plots of the frequency ranges 0.017-0.1 Hz and 0.1-10 Hz.

When examining the total and perpendicular power from 0.017-0.1 Hz, shown in Figure 4.2, there are regions of increased power that change location with NIMF and SIMF which can be attributed to the change in reconnection site location with NIMF versus SIMF (see similar points outlined in Figure 4.4). In Section 1.4, some of the magnetic field fluctuations were shown just to be the back and forth motion of the cusp structure over the spacecraft. Some of the enhanced power of the magnetic field fluctuations at the cusp boundaries for the 0.017-0.1 Hz frequency range will come from this source. Enhanced power points similar to those outlined in Figure 4.5, are seen at the total and perpendicular power from 0.017-0.1 Hz. For SIMF, these plots show enhanced power along the first field line poleward of the cusp. The cause is a gradient in the magnetic field strength as the spacecraft moves from the MSP into the MSH. The enhanced power possibly due to magnetotail reconnection in 0.017-0.1 Hz is seen for SIMF at all power types (see similar points outlined in Figure 4.7). NIMF



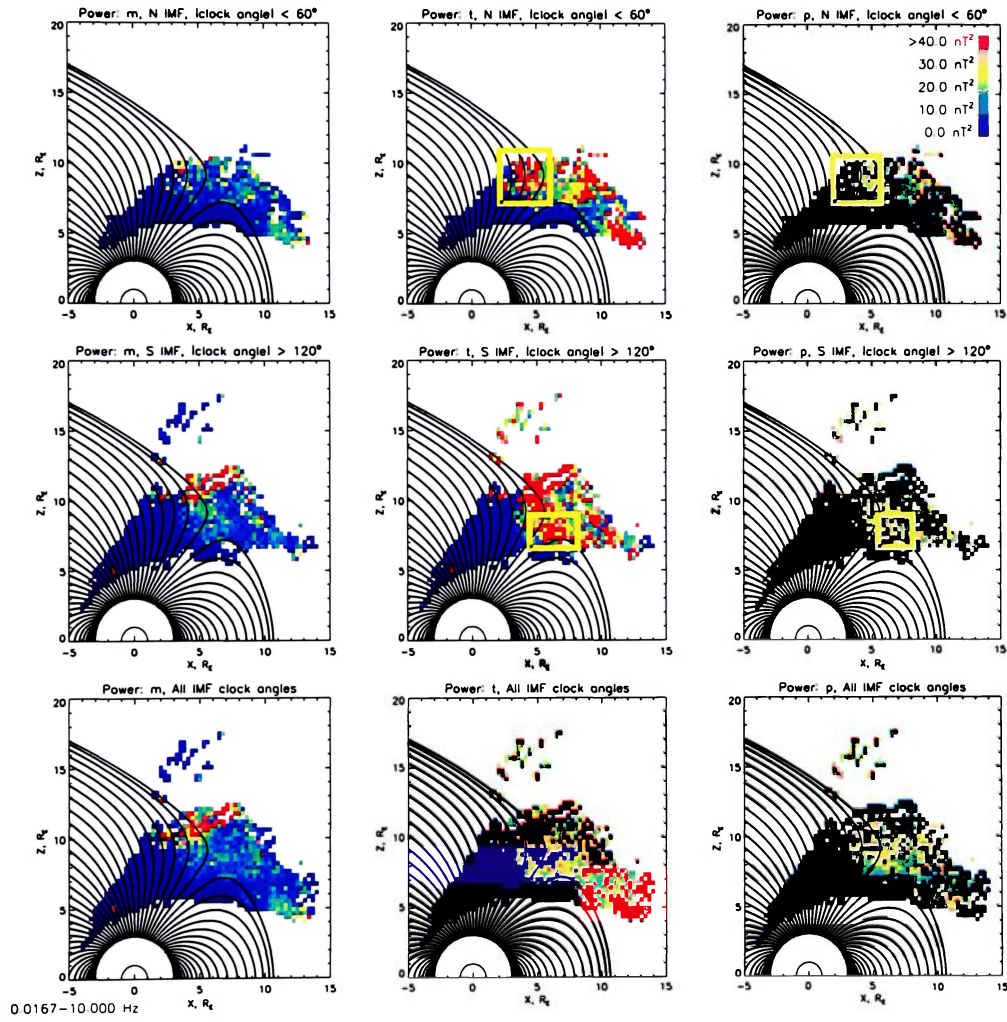


Figure 4.4: Locations of increased power in magnetic field fluctuations due to different reconnection sites during NIMF versus SIMF, 0.017-10 Hz.

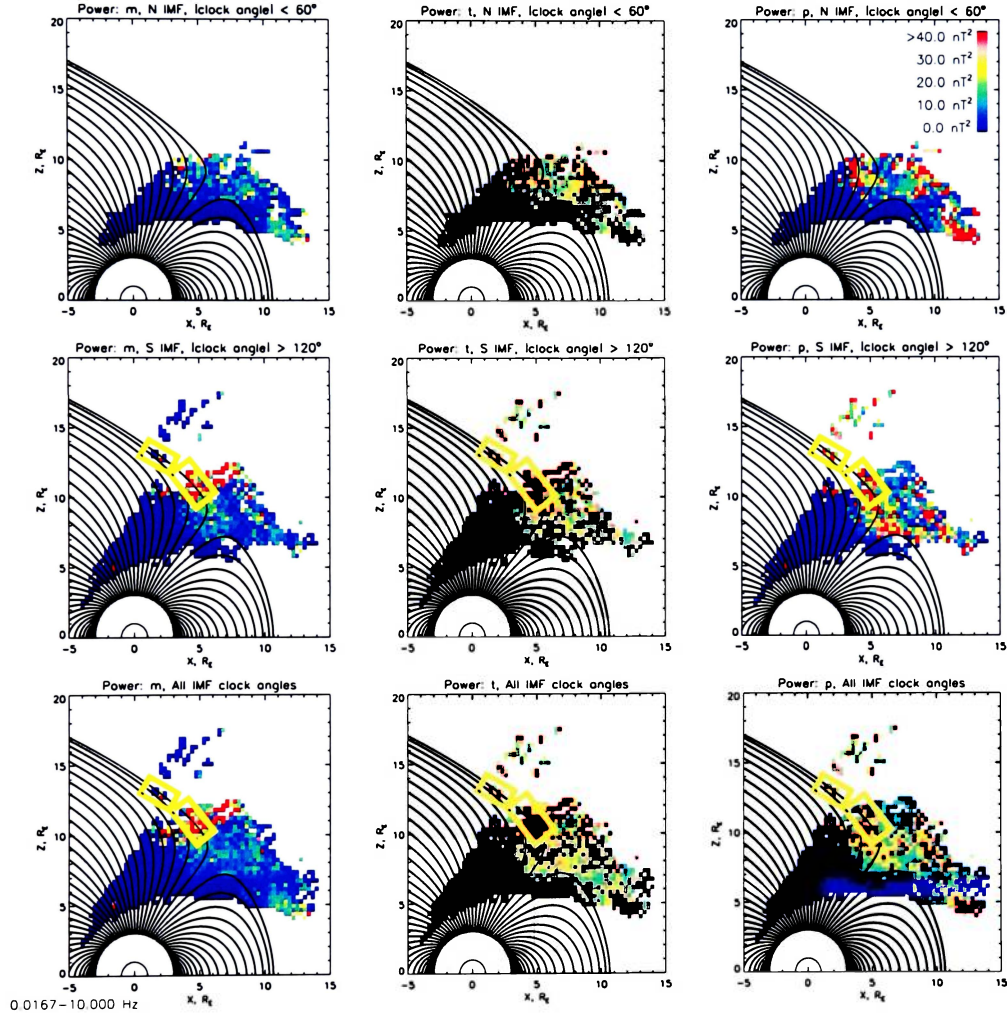


Figure 4.5: Locations of increased power in magnetic field fluctuations due to spacecraft crossing from magnetotail into magnetosheath (gradient in the magnetic field strength) and/or mirror mode waves, 0.017-10 Hz.

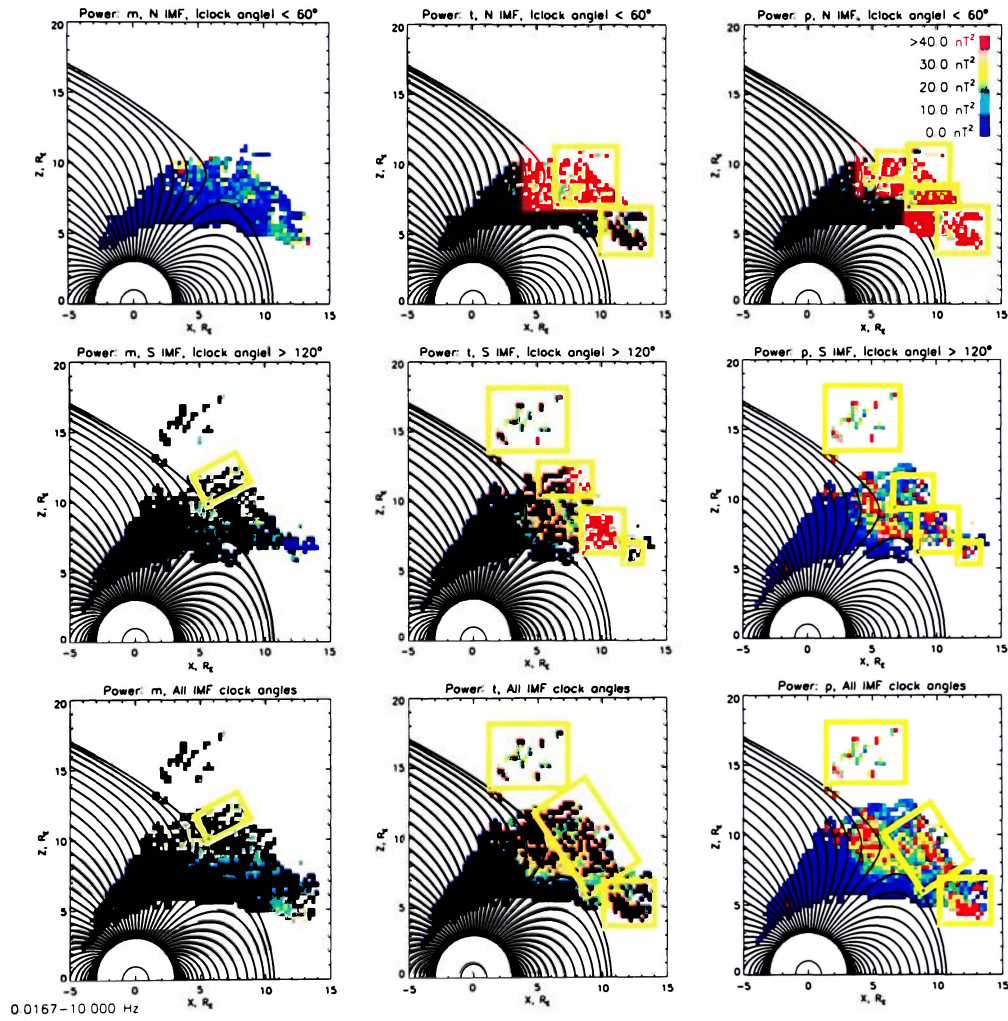


Figure 4.6: Locations of increased power in magnetic field fluctuations due to different wave modes in the magnetosheath, 0.017-10 Hz.



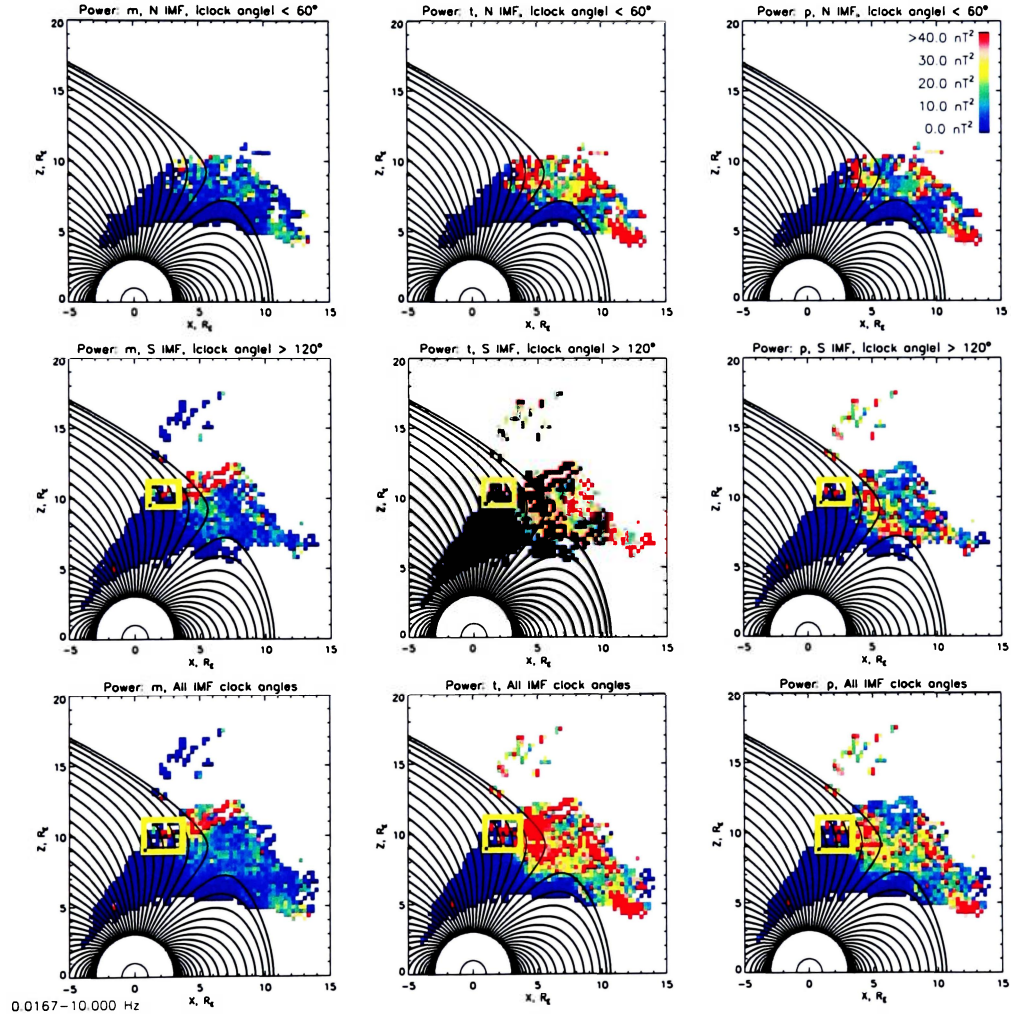


Figure 4.7: Locations of increased power in magnetic field fluctuations possibly due to magnetotail reconnection, 0.017-10 Hz.



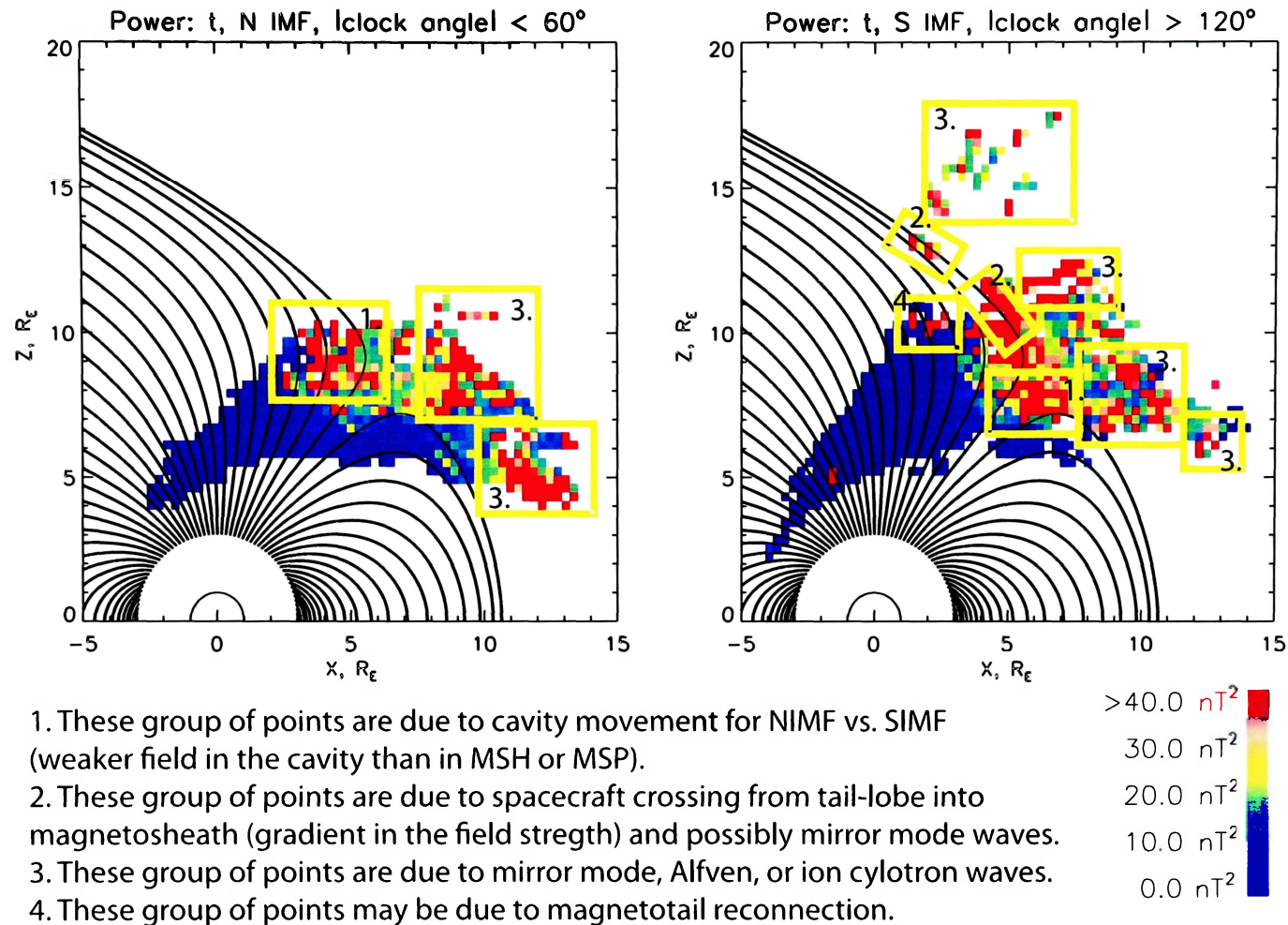


Figure 4.8: Normalized total integrated power of the magnetic field fluctuations from 0.017-10Hz for NIMF and SIMF from Figure 4.1. Regions of enhanced wave power are outlined.

does not have data at that location so no magnetotail reconnection conclusions are drawn for NIMF

As shown in *Denton et al.* [1995] and Figure 1.8, mirror mode waves can be expected to have frequencies less than 0.1 Hz. They contribute to the low frequency enhanced mean (compressional) integrated power outlined in Figure 4.6. The plasma parameters in the magnetosheath, such as the plasma  $\beta$  (ratio of the plasma pressure to the magnetic pressure) and ratio of the perpendicular to parallel plasma temperatures,  $\frac{T_{\perp}}{T_{\parallel}}$ , determine the amount of free energy available for fluctuations.  $\perp$  and  $\parallel$  respectively refer to the direction perpendicular and parallel to the magnetic field. The free energy available will determine if the dominant fluctuation type is mirror mode waves or cyclotron modes [Soucek et al. 2008]. For mirror mode waves,  $\frac{T_{\perp}}{T_{\parallel}} > 1 + \frac{1}{\beta_{\perp}}$  [Hasegawa 1969] and for proton cyclotron waves,  $T_{\perp} > T_{\parallel}$  [Soucek et al. 2008].

The cyclotron frequency of a charged particle of charge  $q$  and mass  $m$  in a magnetic field of magnitude  $B$  is given by  $f_{cyclotron} = \frac{qB}{2\pi m}$ . In the cusp and nearby surrounding regions, a magnetic field strength of 1-50 nT is normal, so the local proton cyclotron frequency would be about 0.01-1 Hz. The power plot from 0.017-0.1 Hz (Figure 4.2) and 0.1-10 Hz (Figure 4.3) includes power from proton cyclotron waves. For larger mass particles, the cyclotron frequency can be even lower than 0.1 Hz so enhanced power in 0.017-0.1 Hz (Figure 4.2) can have a contribution from IC waves. By analyzing the regions of enhanced magnetic field fluctuations for the IC frequency range, a source of particle energization may be found. It has been shown that the generation of IC waves in the cusp is related to reconnection flows and counterstreaming beams [Le et al. 2001; Nykyri et al. 2003] so these are some of the sources of increased fluctuation power.

From a minimum variance analysis [Sonnerup and Scheible 1998] of the Cluster cusp crossing on 17 March 2001 (one of the cusp crossings used in this study), left-hand polarized Alfvén/ion cyclotron waves were detected by Nykyri et al. [2004]. Alfvén waves are a MHD wave mode at a lower frequency than the IC frequency. Because the IC range can vary widely in the cusp and surrounding boundaries, the frequency

of Alfvén waves have a broad range too. Alfvén waves are a source of increased power in the power plots showing 0.017-0.1 Hz and 0.1-10 Hz.

When examining the total and perpendicular power from 0.1-10 Hz, shown in Figure 4.3, there are regions of increased power that change location with NIMF and SIMF which can be attributed to the change in reconnection site with NIMF versus SIMF (see similar points outlined in Figure 4.4). A slight enhancement in the total and perpendicular power along the first poleward field line from the cusp is seen for SIMF which can be attributed to a gradient in the magnetic field strength as the spacecraft move from the MSP to MSH (see similar points outlined in Figure 4.5). As shown earlier in this section, the local cyclotron frequency could be greater than 0.1 Hz, which means that cyclotron wave power could be present in the 0.1-10 Hz integrated power plots. Also, as shown above, Alfvén waves could also be present from 0.1-10 Hz (for IC and Alfvén induced power, see similar points outlined in Figure 4.6). The enhanced power possibly due to magnetotail reconnection in 0.1-10 Hz is seen for SIMF at all power types (see similar points outlined in Figure 4.7). In Section 1.4, the frequency range of actual wave turbulence was defined to be dependent on the dimension of the cusp cavity. Considering that it can take a fast mode wave 1-10 seconds to travel through the cavity, it is plausible that fluctuations in the 0.1-10 Hz range could be wave turbulence.

## 4.2 Standard Deviation

The standard deviation of each plot square was calculated using Equation 4.1.  $N$  is the number of data points averaged in the square and  $\bar{x}$  is the average of all data points in the square.

$$\sigma_x = \sqrt{\frac{1}{N} \sum_{i=1}^N (x_i - \bar{x})^2} \quad (4.1)$$

Figure 4.9 shows the standard deviation for the mean, total, and perpendicular power in the magnetic field fluctuations in the 0.017-10 Hz frequency range for NIMF,

SIMF, and AIMF. Figure 4.10 shows the standard deviation of the same plots in the 0.017-0.1 Hz frequency range, and Figure 4.11 shows 0.1-10 Hz.

A comparison of Figure 4.9 and Figure 4.11 shows that more points have a higher standard deviation when lower frequencies are included. As shown in Figure 2.3, a gradual cusp may have low frequency magnetic field fluctuations on the order of 0.5-5 nT after detrending. From Figure 1.7, a DMC may have low frequency fluctuations on the order of 20-50 nT after detrending. The relatively small fluctuations of a gradual cusp do not have a lot of power in them. Because of the relatively large magnetic field fluctuations seen with a DMC, DMC crossings will have higher integrated power. Because this study examines the power of both gradual and DMC crossings together, the standard deviation in this cusp is expected to be high at the lower frequencies analyzed. Power in the higher frequency fluctuations are of the same order for gradual cusps and DMCs so no increase in the standard deviation is expected nor seen for the higher frequencies analyzed.

The mean, total, and perpendicular integrated power for the frequency ranges 0.017-10 Hz, 0.017-0.1 Hz, and 0.1-10 Hz is shown in Figures 4.12-4.14 with the data squares scaled proportional to its standard deviation value. The largest square size corresponds to a standard deviation of 0 nT<sup>2</sup> and the smallest square corresponds to a standard deviation of 100 nT<sup>2</sup> or greater. These figures show that the regions of highest power tend to have the largest standard deviation. The analysis in the previous section relied on the precision of the enhanced integrated power values so it may seem that the conclusions obtained may not be completely accurate. Without accounting for the effect of a gradual cusp versus a DMC though, all standard deviation values should be looked at and used with care. Also, not all waves and sources of enhanced power may be present at all cusp crossings. For example, a certain data square may have a few crossings of similar and high power levels due to IC waves and have low (and similar) wave power all other days. The standard deviation of that data square could be relatively large and suggest that the precision is low when the data may in fact be very precise for two separate categories of the data, days with wave activity and days without wave activity. This is also the case if there is usually a lot of wave power (of similar level) but there are a few days with no wave power.

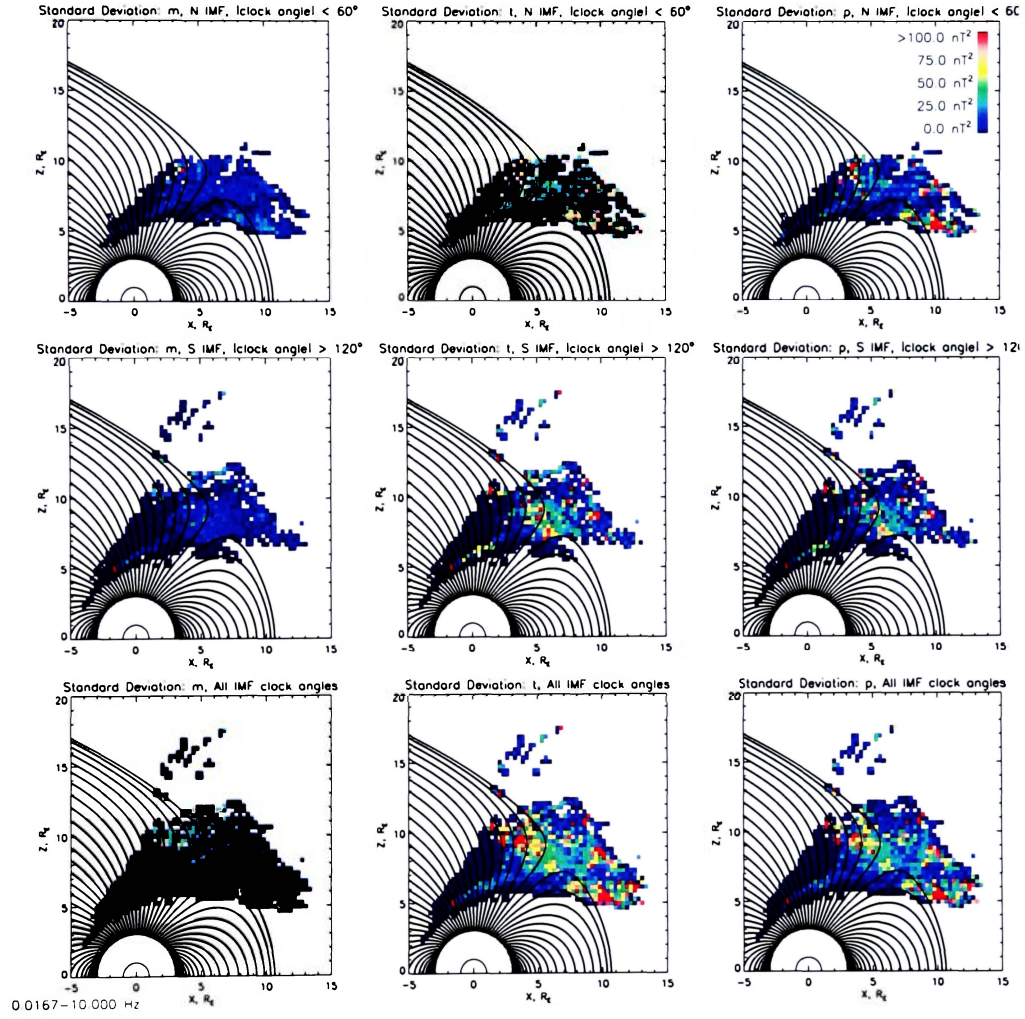


Figure 4.9: Standard deviation for the mean, total, and perpendicular power in the magnetic field fluctuations of the 0.017-10 Hz frequency range for NIMF, SIMF, and AIMF.



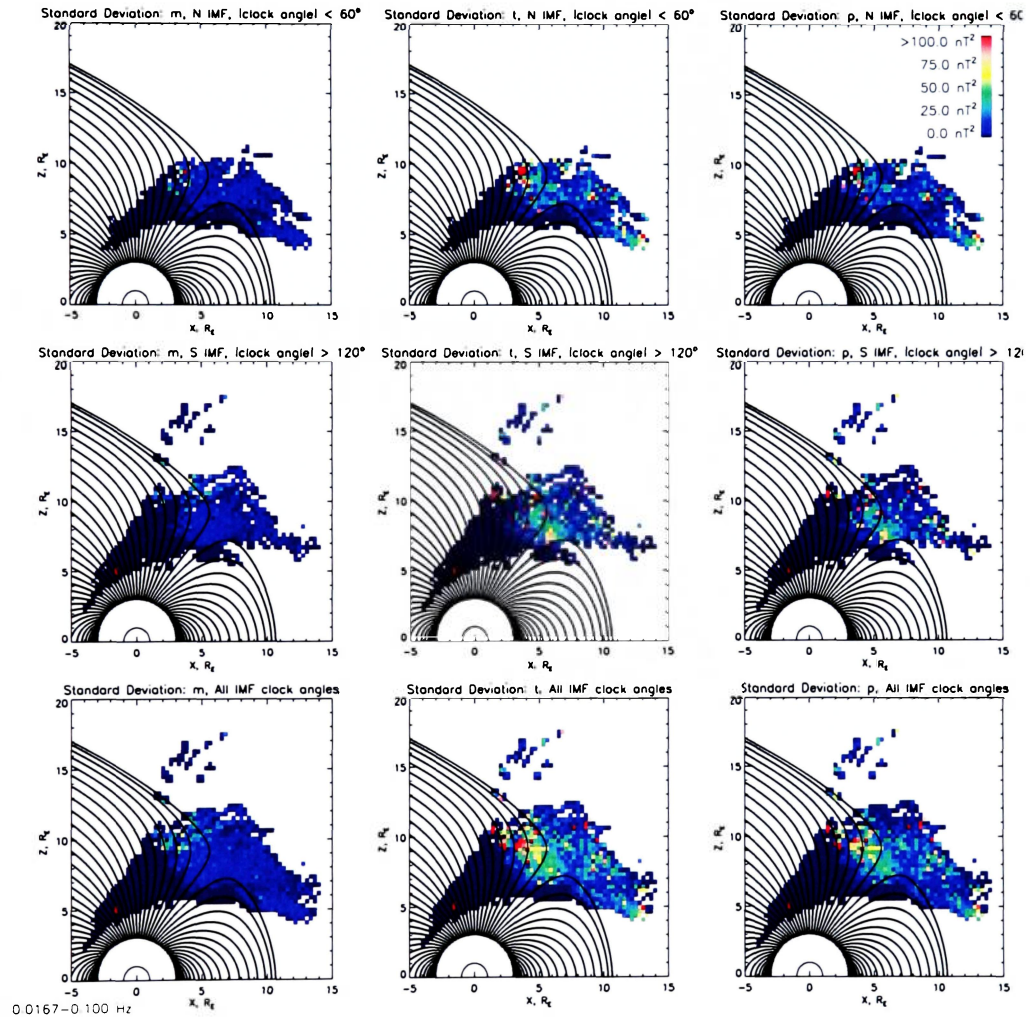


Figure 4.10: Standard deviation for the mean, total, and perpendicular power in the magnetic field fluctuations of the 0.017-0.1 Hz frequency range for NIMF, SIMF, and AIMF.

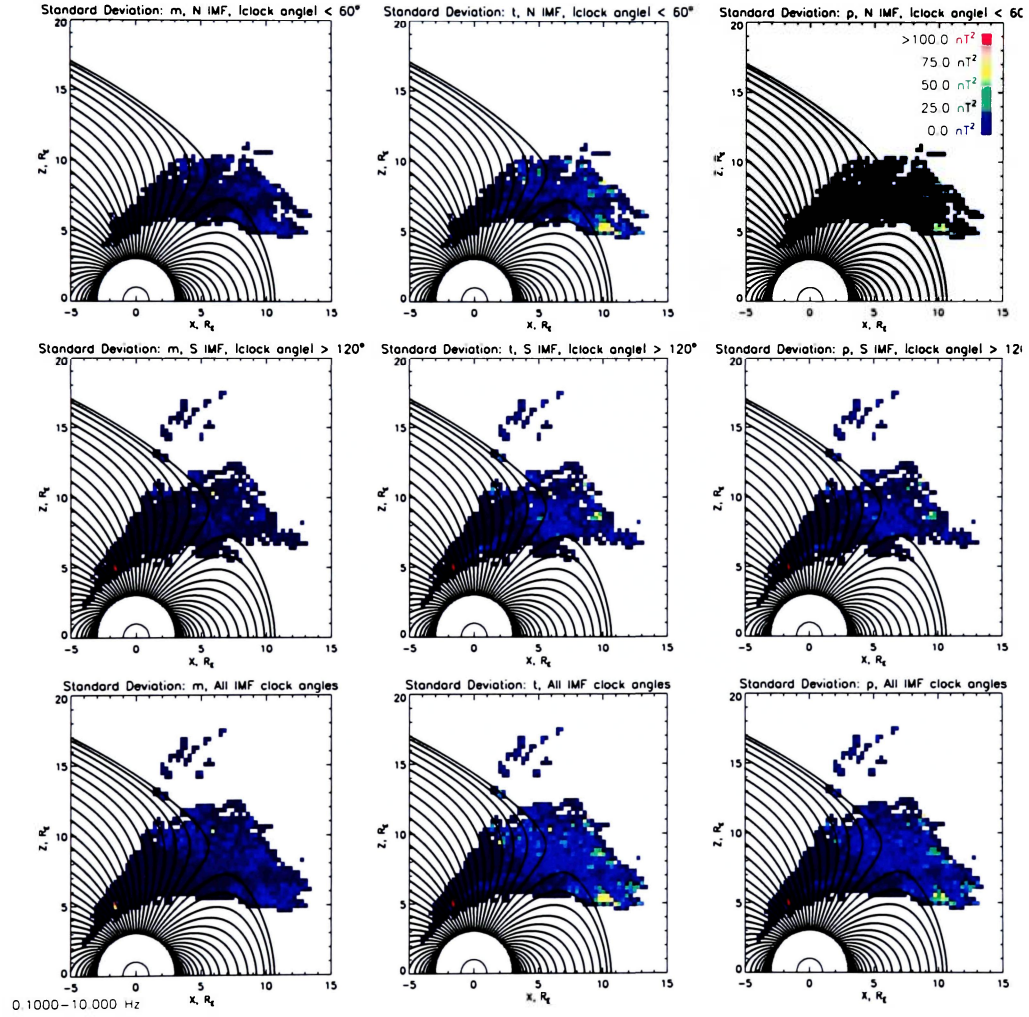


Figure 4.11: Standard deviation for the mean, total, and perpendicular power in the magnetic field fluctuations of the 0.1-10 Hz frequency range for NIMF, SIMF, and AIMF.

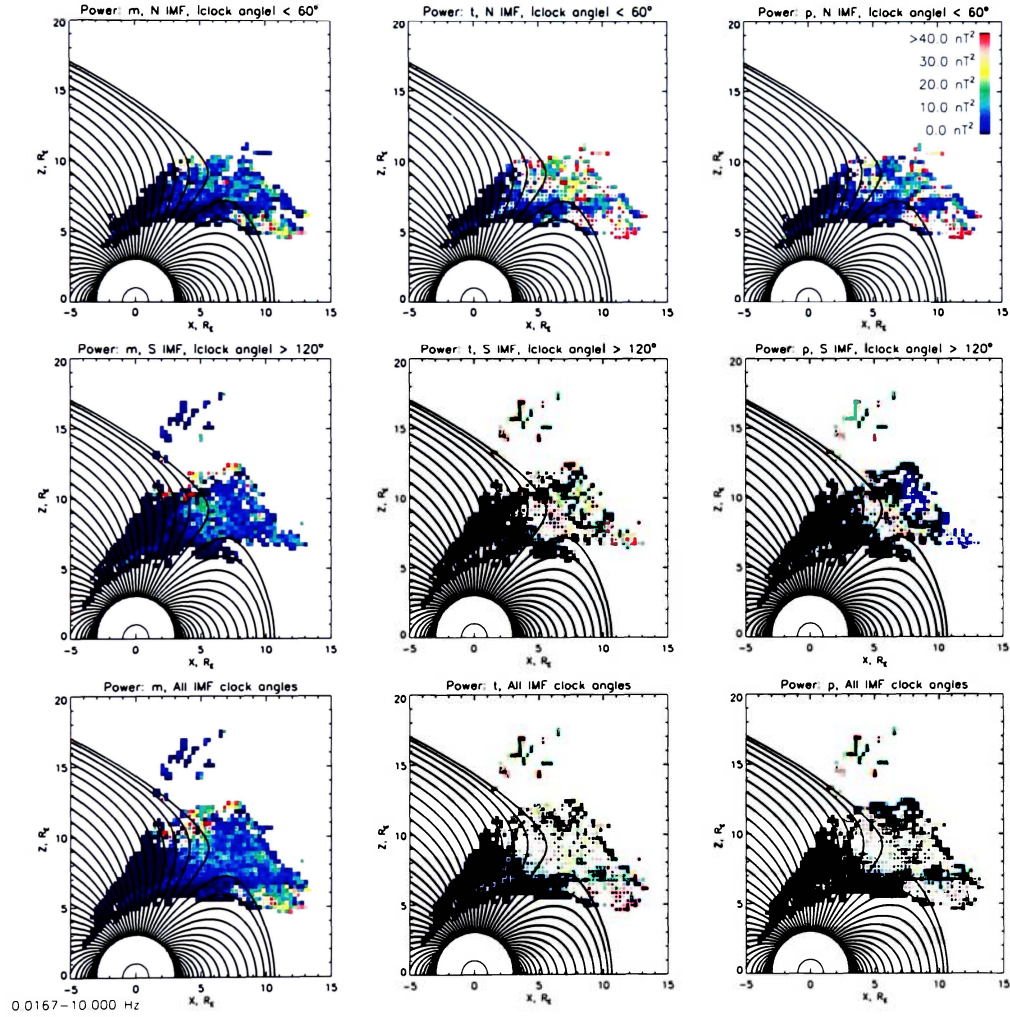


Figure 4.12: Normalized integrated mean, total, and perpendicular power in the magnetic field fluctuations of the 0.017-10 Hz frequency range for NIMF, SIMF, and AIMF. The data square is scaled smaller with higher standard deviation.



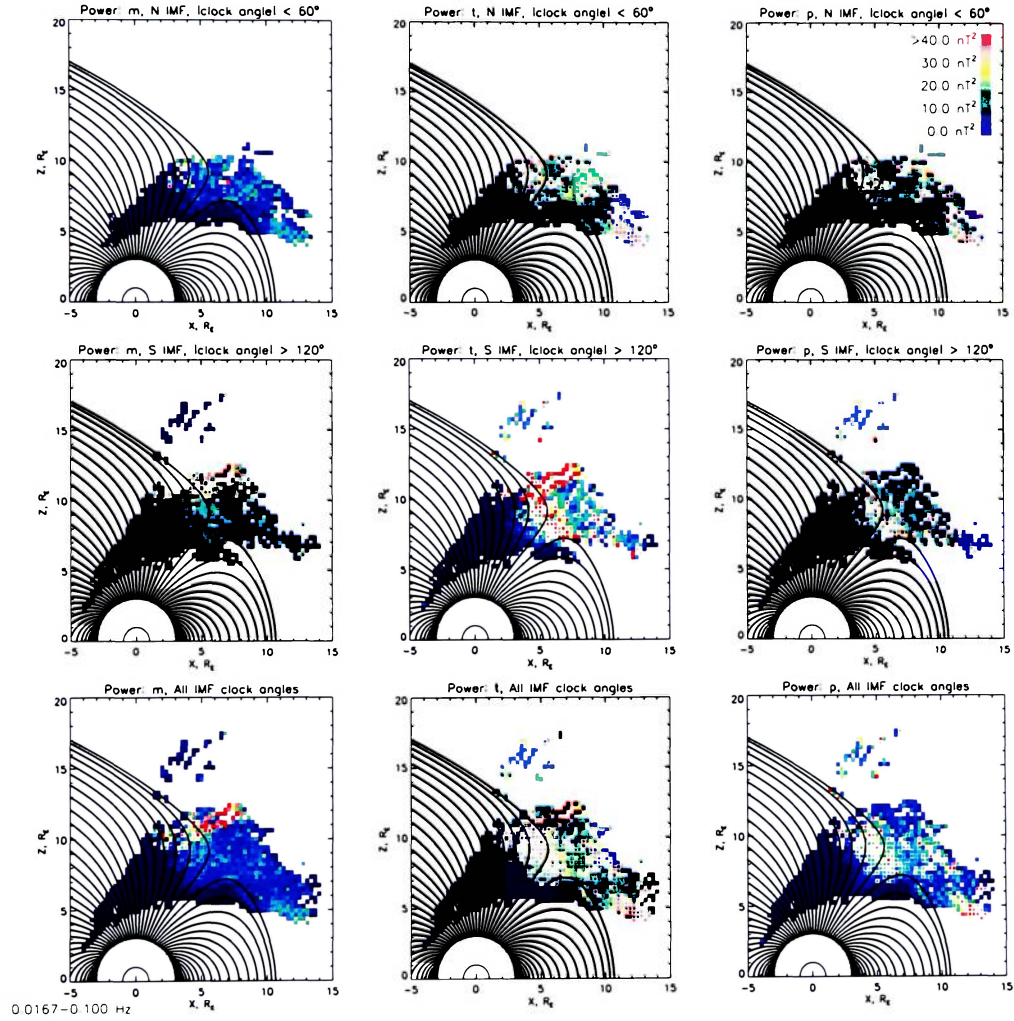


Figure 4.13: Normalized integrated mean, total, and perpendicular power in the magnetic field fluctuations of the 0.017-0.1 Hz frequency range for NIMF, SIMF, and AIMF. The data square is scaled smaller with higher standard deviation.

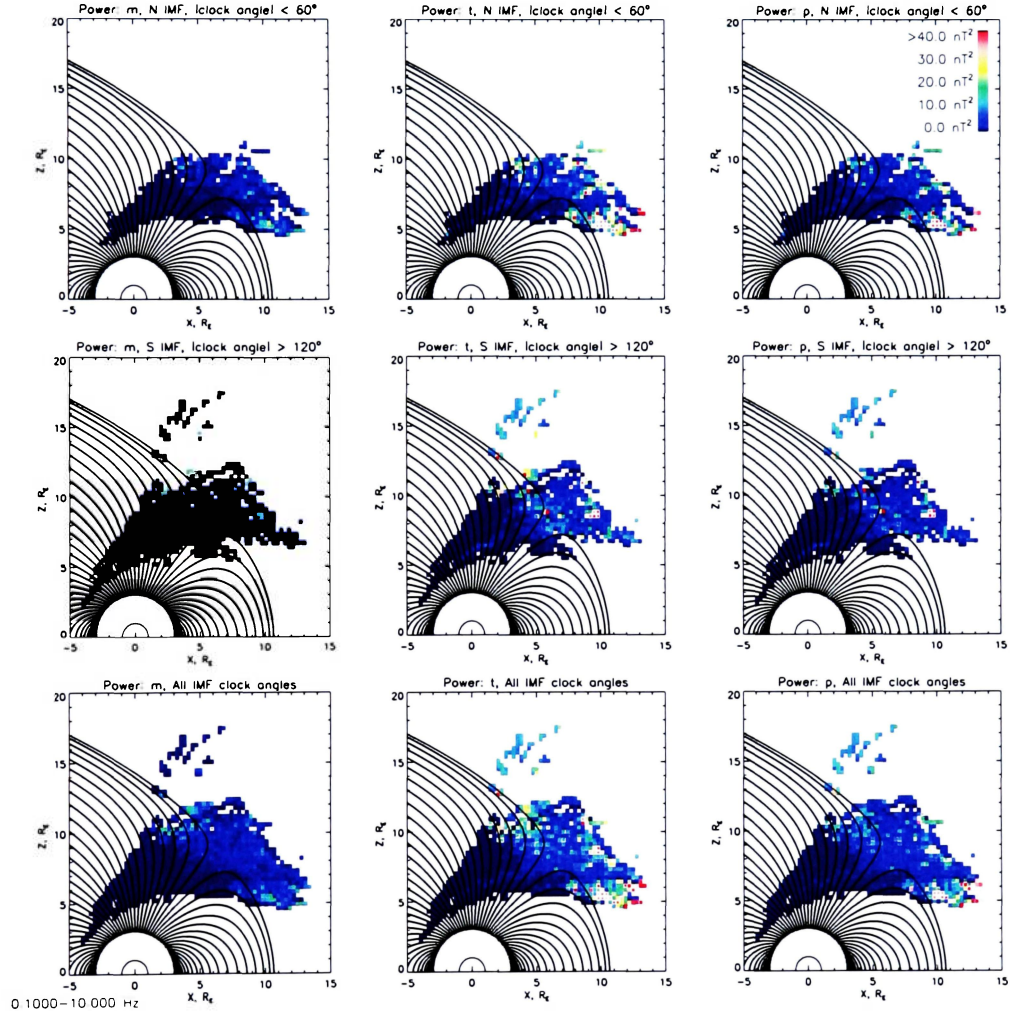


Figure 4.14: Normalized integrated mean, total, and perpendicular power in the magnetic field fluctuations of the 0.1-10 Hz frequency range for NIMF, SIMF, and AIMF. The data square is scaled smaller with higher standard deviation.

## Chapter 5

### Concluding Remarks

Understanding the origin and type of magnetic field fluctuations in the cusp is important for studying a possible correlation with high energy particle fluxes in the high altitude cusp. In summary, for this study, the solar wind and geomagnetic conditions of 118 Cluster cusp crossings from 2001-2003 were used to normalize the orbital data to cusp normalized coordinates. The FGM magnetic field data was detrended to remove the background magnetic field. The data segment was windowed with a periodic Hanning window of  $\alpha = 0.5$  to prevent spectral leakage in a DFT. In frequency space, the mean, total, and perpendicular integrated power was calculated and normalized to the level it would be at if a rectangular window were used. The three types of power were then analyzed for the frequency ranges 0.017-10 Hz, 0.017-0.1 Hz, and 0.1-10 Hz for NIMF, SIMF, and AIMF.

In all three frequency ranges, the integrated power plots show that a region of higher integrated power at the cusp is more tailward of the cusp for northward IMF and sunward for southward IMF. This movement of the location of higher power is consistent with the formation of diamagnetic cavity regions more tailward of the cusp for northward IMF and more sunward for southward IMF because the location of magnetic reconnection changes with northern versus southern IMF.

Possible sources of integrated power in the cusp proper or diamagnetic cavity also include reconnection flows, flux transfer events, and the back and forth motion of cusp boundaries. At cusp boundaries, sources of power include the back and forth

motion of the nightside MSP-cusp boundary passing by the spacecraft, the back and forth motion of the cusp-MSH boundary by the spacecraft, and the back and forth motion of the cusp-dayside MSP boundary by spacecraft.

There are regions of increased power where the spacecrafts cross from the tail lobe into the magnetopause and magnetosheath. The increased power could be caused by a gradient in the magnetic field strength as the spacecraft traverses this boundary. Points in this region could also be due to mirror mode waves. These regions of higher power were seen for SIMF at all frequency ranges considered. NIMF did not have any trajectories directly from the MSP into the MSH.

In the magnetosheath, sources of wave power include mirror mode, IC, and Alfvén waves at low frequencies and IC and Alfvén waves at high frequencies. IC waves also exist in the cusp. Analysis of individual cusp crossings can identify the specific wave type and corresponding location.

Enhanced power poleward of the cusp was observed. Because the power was on field lines that were open (about to reconnect) or closed (recently reconnected), it is plausible to hypothesize that magnetotail reconnection could be driving fluctuations earthward of the reconnection site. An examination of the power at similar field lines near the southern hemisphere polar cusp would be useful in further analysis.

Because of the nature of wave travel through the cusp, some of the fluctuation power in 0.1-10 Hz range could be wave turbulence. Some of the fluctuation power from 0.017-0.1 Hz could be due to the movement of the cusp structure.

Wavelet analysis could be used as an additional method of studying the power spectrum and integrated power instead of just the discrete Fourier transform. A different integration technique will yield different integrated power values and perhaps larger or smaller enhanced power regions in the cusp normalized maps.

This study showed high standard deviations for the larger integrated power values in the data squares. The use of other cusp crossings (other years) in addition to the crossings used this study will increase the number of data points averaged in the data squares, possibly reducing the standard deviations. The 118 crossings used were chosen so comparison with previously published work, *Lavraud et al.* [2004, 2005], could be done. Because it is known that a DMC will have more power in the magnetic

field fluctuations than a gradual cusp, performing a separate power analysis for each of the two cusp types separately may be beneficial. At the very least, it would lead to more precise standard deviation values in the cusp for each type of crossing.

The next step in this analysis is to use particle flux data from the Research with Adaptive Particle Imaging Detectors (RAPID) instruments on Cluster. Maps will be made of the amount of particle flux in and around the cusp (using the same cusp normalized coordinate system as in this study). By analyzing both the regions of enhanced flux and magnetic field fluctuations, a correlation could be found between the two. It may also provide evidence to support or deny the local wave acceleration theory of high energy cusp populations. As stated in *Niehof et al* [2010], “due to the cusp’s magnetic connection to many different regions of geospace, these particles may have significant effects when propagated out of the cusp or may be useful to remotely sense processes elsewhere in geospace.”

# Appendix A

## IDL Code

All computer code for this study was written in Interactive Data Language (IDL).

### A.1 Data Preparation Code

statcuspsavephr\_norm.pro Adapted from code courtesy of Elena Budnik, obtained through private communication. Produces .sav files with the normalized (C1\_P\*\_HR\_norm2.sav) and unnormalized (C1\_P\*\_HR\_2.sav) integrated mean, total and perpendicular power.

```
*****  
; Cusp Statistics  
;  
; statcuspsavephr_norm.pro ; saves normalized data  
;  
; Creates .sav File for Plotting ColorCoded turbulence on cusp-normalized field grid  
;  
; Input. "orb[S,T]YDDD.res" and "cond[S,T]YDDD.res" files  
;  
,  
,  
, September 2010  
,*****  
  
a=[0.5,1.0], alpha values for hanning window  
norm = 'n'  
for hrnum=1,2 do begin, 1:0.0083-0.25 /2.0.0083-1 /3.0.0083-10 /4:1-10 /5.0.1-10  
    /6:0.0028-10 Hz  
for scnum=2,4 do begin, chooses cluster spacecraft  
scnums=string(scnum,'(i1)'); spacecraft number. string  
  
seldate = 'n', choose specific date to read & plot?  
preent = 'y'; if seldate y, run specific date again and again for debugging?  
date='',  
if preent eq 'y' then date='20031*'  
  
;----- Main Definitions -----  
  
StartTime = ' ',  
TimeIntAll = ' ',  
TimeInt='0000000001000000',  
  
Start = ''
```

```

,-----
, for data from cond* asc files
,-----
  ParRet   fltarr(4) , RamPressure, IMF[3]
  SW_PAR   fltarr(4) , Np, Vp, alpha ratio, Tp[K]

  dst      0 0
  delay    0 0

,-----
, for data from orb* asc files
,-----

TimeOrb    dblarr(5) , UNIX time   secs from 1970-01-01
XYZ         fltarr(3,5) , orbit cusp-normalised frame
XYZ_GSM     fltarr(3,5) , orbit gsm
XYZ_SM      fltarr(3,5) , orbit sm
B_T96_gsm   fltarr(3,5) , model T96 field for real condition
,-----

B_IMF = fltarr(3)
,----- Start Reading Files -----
openw, gaps, 'DataGapsOver2min.txt', /GET_LUN
close, gaps
FREE_LUN, gaps
, *****
, RES_DIR => put name of directory where you keep
, cond* and orb* files
,
, *****
  RES_DIR = 'sc'+scnums+'hr/',
if seldate eq 'y' then begin
  if preent eq 'n' then READ, date, PROMPT='Enter Date to Process, format yyyyday
  FileNames = FindFile(RES_DIR+'cond_'+date+'.asc', count=NFiles)
endif else FileNames = FindFile(RES_DIR+'cond_* asc', count=NFiles)

powerarray PTRARR(1, NFiles, /ALLOCATE_HEAP)
powerarraya PTRARR(1, NFiles, /ALLOCATE_HEAP)
Bpsizep = PTRARR(1, NFiles, /ALLOCATE_HEAP)

  for FN 0, NFiles -1 do begin

    openr, COND, FileNames[FN], /GET_LUN
    openr, ORB, RES_DIR+'orbY_'+STRMID(FileNames[FN], STRLEN(RES_DIR)+5, 7)+'
      asc_with_sm', /GET_LUN

,-----

    readf, COND, StartTime
    print, StartTime

, *****
, GET HERE YOUR DATA ARRAY FOR
, Start Time StartTime, and Time Interval TimeIntAll
,
,
, *****
, the FGM data file name has the date in different format
, The StartTime string has the year, day of the year -1 and
, start time for the orbital and condition data We need to read these
, information and convert into form so that we can easily open the FGM
, data files of the type C1_PP_FGM_20011213_V01.cdf C1_PP_FGM-year-month-day_V01.cdf
, note that we have dayoy+1 because the original string has been saved
, as dayoy-1

year=Fix(StrMid(StrTrim(StartTime), 0, 4))
dayoy=Fix(StrMid(StrTrim(StartTime), 4, 3))

```

```

hour=Fix(StrMid(StrTrim(Starttime,2), 7, 2))
min=Fix(StrMid(StrTrim(Starttime,2), 9, 2))
sec=Fix(StrMid(StrTrim(Starttime,2), 11, 2))
msec=Fix(StrMid(StrTrim(Starttime,2), 13, 3))

ehour=Fix(StrMid(StrTrim(Starttime,2), 24, 2))
emin=Fix(StrMid(StrTrim(Starttime,2), 26, 2))
esec=Fix(StrMid(StrTrim(Starttime,2), 28, 2))
emsec=Fix(StrMid(StrTrim(Starttime,2), 30, 3))
CALDAT, JULDAY(1, dayoy+1, year), month, day

endin5 'n'
if (min eq 5) or (min eq 15) or (min eq 25) or (min eq 35) or (min eq 45) or (min eq
55) then begin
emin emin -1
endin5 'y'
endif
if (emin eq 5) or (emin eq 15) or (emin eq 25) or (emin eq 35) or (emin eq 45) or (emin
eq 55) then emin emin-1

tmin=hour+min/60.+sec/3600.
tmax=tmin+ehour+emin/60.+esec/3600.

secondfile='n'
if tmax gt 24. then begin
, some intervals continue into second day
dayoy2=dayoy+1
CALDAT, JULDAY(1, dayoy2+1, year), month2, day2
hour2=0.
tmin2=0.
ehour2=hour+ehour-24.
emin2=emin
esec2=esec
tmax2=tmin2+ehour2+min/60.+emin2/60.+esec2/3600.
secondfile='y'
tmax=24.
if endin5 eq 'y' then begin
tmax = 23+(59/60.)
endif
endif

, now let's open the FGM file corresponding to this year, month day
if month lt 10 and day ge 10 then begin
namefgm=FINDFILE(RES_DIR+'C_'+strmid(string(year,'(i4)'),2,2)+string(0,'(i1)')+
string(month,'(i1)')+string(day,'(i2)')+'.DAT'), magnetic data
if secondfile eq 'y' then begin
if day2 lt 10 then begin
namefgm2=FINDFILE(RES_DIR+'C_'+strmid(string(year,'(i4)'),2,2)+string(0,'(i1)')+
string(month2,'(i1)')+string(0,'(i1)')+string(day2,'(i1)')+'.DAT'), magnetic
data
endif else begin
namefgm2=FINDFILE(RES_DIR+'C_'+strmid(string(year,'(i4)'),2,2)+string(0,'(i1)')+
string(month2,'(i1)')+string(day2,'(i2)')+'.DAT'), magnetic data
endif
endif
endif

if month lt 10 and day lt 10 then begin
namefgm=FINDFILE(RES_DIR+'C_'+strmid(string(year,'(i4)'),2,2)+string(0,'(i1)')+
string(month,'(i1)')+string(0,'(i1)')+string(day,'(i1)')+'.DAT'), magnetic data
if secondfile eq 'y' then begin
if day2 lt 10 then begin
namefgm2=FINDFILE(RES_DIR+'C_'+strmid(string(year,'(i4)'),2,2)+string(0,'(i1)')+
string(month2,'(i1)')+string(0,'(i1)')+string(day2,'(i1)')+'.DAT'), magnetic
data
endif else begin

```



```

namefgm2=INDFILE(RES_DIR+'C*_'+strmid(string(year,'(14)'),2,2)+string(0,'(11)')+
    string(month2,'(11)')+string(day2,'(12)')+'_*.DAT'), magnetic data
endif
endif
endif

if month ge 10 and day ge 10 then begin
namefgm=INDFILE(RES_DIR+'C*_'+strmid(string(year,'(14)'),2,2)+string(month,'(12)')+
    string(day,'(12)')+'_*.DAT'), magnetic data
if secondfile eq 'y' then begin
namefgm2=INDFILE(RES_DIR+'C*_'+strmid(string(year,'(14)'),2,2)+string(month2,'(12)')+
    string(day2,'(12)')+'_*.DAT'), magnetic data
endif
endif

if month ge 10 and day lt 10 then begin
namefgm=INDFILE(RES_DIR+'C*_'+strmid(string(year,'(14)'),2,2)+string(month,'(12)')+
    string(0,'(11)')+string(day,'(11)')+'_*.DAT'), magnetic data
if secondfile eq 'y' then begin
if day2 lt 10 then begin
namefgm2=INDFILE(RES_DIR+'C*_'+strmid(string(year,'(14)'),2,2)+string(month2,'(12)')+
    string(0,'(11)')+string(day2,'(11)')+'_*.DAT'), magnetic data
endif else begin
namefgm2=INDFILE(RES_DIR+'C*_'+strmid(string(year,'(14)'),2,2)+string(month2,'(12)')+
    string(day2,'(12)')+'_*.DAT'), magnetic data
endif
endif
endif

    readfgmhr, namefgm,nfgm,timem,b,,tmin_t,tmax_t
tmin_t  tmin
tmax_t  tmax
    datagapfillhr, nfgm, timem, b, tmin_t, tmax_t, timemnew, bnew,nnew,Starttime ,do
        linear interpolation over data gaps
    timem  timemnew
    b      bnew
    nfgm   nnew

if secondfile eq 'y' then begin
readfgmhr, namefgm2, nfgm2,timem2,b2,,tmin2_t,tmax2_t
tmin2_t  tmin2
tmax2_t  tmax2
    datagapfillhr, nfgm2, timem2, b2, tmin2_t, tmax2_t, timemnew2, bnew2,nnew2,
        Starttime
    timem2  timemnew2
    b2      bnew2
    nfgm2   nnew2
endif

,now let's pull out the b-field data for tmin and tmax and
hindbd,60.*tmin,60.*tmax,nfgm,timem,ims,ime

nt  ceil((timem(ime)-timem(ims))/2) ,# of 2 min intervals in cusp crossing
Bp  make_array(3,nt,/FLOAT)
Bpa make_array(3,nt,/FLOAT)
j   ims
k   ims
cnt = tmin*60.
for i = 0,nt-2 do begin
    while (timem(k) lt cnt+2) do begin
        k  k+1
    endwhile
    if (timem(j) lt cnt) then j=j+1
    if (timem(k) gt cnt) then k=k-1
    m  k-j

```

```

        B_2min = fltarr(4,m+1)
        t_2min = fltarr(m+1)
        for i11 = 0, m do begin
            B_2min(0,i11) = b(0,j)
            B_2min(1,i11) = b(1,j)
            B_2min(2,i11) = b(2,j)
            B_2min(3,i11) = SQRT((b(0,j))^2+(b(1,j))^2+(b(2,j))^2)
            t_2min(i11) = timem(j)
            j = j + 1
        endfor
        powerhr_norm,B_2min,t_2min,Psig,Fsig,hrnum,a(0),norm
        Bp(*,1)=Psig(*)
        powerhr_norm,B_2min,t_2min,Psig,Fsig,hrnum,a(1),norm
        Bpa(*,1)=Psig(*)
        j = k
        cnt = cnt+2
    endfor
    k = ime
    if (timem(j) lt cnt) then j=j+1
    m = k-j
    B_2min = fltarr(4,m+1)
    t_2min = fltarr(m+1)
    for i11 = 0, m do begin
        B_2min(0,i11) = b(0,j)
        B_2min(1,i11) = b(1,j)
        B_2min(2,i11) = b(2,j)
        B_2min(3,i11) = SQRT((b(0,j))^2+(b(1,j))^2+(b(2,j))^2)
        t_2min(i11) = timem(j)
        j = j + 1
    endfor
    powerhr_norm,B_2min,t_2min,Psig,Fsig,hrnum,a(0),norm
    Bp(*,1)=Psig(*)
    powerhr_norm,B_2min,t_2min,Psig,Fsig,hrnum,a(1),norm
    Bpa(*,1)=Psig(*)

    nt2=0
    if secondfile eq 'y' then begin
        hindbd,60 *tmin2,60 *tmax2,nfgm2,timem2,ims2,ime2
        diff2 = ime2-ims2
        if diff2 ne 0 then begin
            nt2 = ceil((timem2(ime2)-timem2(ims2))/2) , # of 2 min intervals in cusp crossing
            Bp2 = make_array(3,nt2,/FLOAT)
            Bp2a = make_array(3,nt2,/FLOAT)
            j = ims2
            k = ime2
            cnt = tmin2*60
            for i1 = 0,nt2-2 do begin
                while (timem2(k) lt cnt+2) do begin
                    k = k+1
                endwhile
                if (timem2(j) lt cnt) then j=j+1
                if (timem2(k) gt cnt) then k=k-1
                m = k-j
                B_2min = fltarr(4,m+1)
                t_2min = fltarr(m+1)
                for i11 = 0, m do begin
                    B_2min(0,i11) = b2(0,j)
                    B_2min(1,i11) = b2(1,j)
                    B_2min(2,i11) = b2(2,j)
                    B_2min(3,i11) = SQRT((b2(0,j))^2+(b2(1,j))^2+(b2(2,j))^2)
                    t_2min(i11) = timem2(j)
                    j = j + 1
                endfor
                powerhr_norm,B_2min,t_2min,Psig,Fsig,hrnum,a(0),norm
                Bp2(*,i1)=Psig(*)
                powerhr_norm,B_2min,t_2min,Psig,Fsig,hrnum,a(1),norm
                Bp2a(*,i1)=Psig(*)
                j = k
            endfor
        end
    end

```

```

        cnt = cnt+2
    endfor
    k   ime2
    if (timem2(j) lt cnt) then j=j+1
    m   k-j
    B_2min   fltarr(4,m+1)
    t_2min   fltarr(m+1)
    for i=0, m do begin
        B_2min(0,i)   b2(0,j)
        B_2min(1,i)   b2(1,j)
        B_2min(2,i)   b2(2,j)
        B_2min(3,i)   Sqrt((b2(0,j))^2+(b2(1,j))^2+(b2(2,j))^2)
        t_2min(i)     timem2(j)
        j   j + 1
    endfor
    powerhr_norm,B_2min,t_2min,Psig,Fsig,hrnum,a(0),norm
    Bp2(*,11)=Psig(*)
    powerhr_norm,B_2min,t_2min,Psig,Fsig,hrnum,a(1),norm
    Bp2a(*,11)=Psig(*)
    Bp   [[Bp],[Bp2]]
    Bpa   [[Bpa],[Bp2a]]
    endif ,diff2 ne 0
    endif ,secondfile eq y
    Bpsize   nt+nt2

    *powerarray[FN] = Bp
    *powerarraya[FN]   Bpa
    *Bpsizep[FN]   Bpsize

    close,/file
    FREE_LUN, COND, ORB
    endfor , all files are processed

    if norm eq 'y' then begin
    SAVE,powerarray,powerarraya,Bpsizep,FILENAME='C'+scnums+'_P'+strtrim(string(hrnum),2)
    +'_HR_norm2 sav',$
    DESCRIPTION="integrated power does not include 0 0083Hz powerarray=(normalized
    integrated power) column0=mean/compressional| column1=trace/total| column2=
    perp-----powerarraya=integrated power with rectangular window, same columns as
    powerarray",/verbose
    endif else begin
    SAVE,powerarray,powerarraya,Bpsizep,FILENAME='C'+scnums+'_P'+strtrim(string(hrnum),2)
    +'_HR_2 sav',$
    DESCRIPTION="integrated power does not include 0 0083Hz powerarray=(not normalized
    integrated power) column0=mean/compressional| column1=trace/total| column2=
    perp-----powerarraya=integrated power with rectangular window, same columns as
    powerarray",/verbose
    endelse

    endfor ,scnum, data file for this spacecraft is done
    endfor ,frequency range of hrnum finished

end

```

**powerhr\_norm.pro** Adapted from code courtesy of Katariina Nykyri. Calculates the integrated mean, total, and perpendicular power. Also normalizes the power.

```

Pro powerhr_norm, signal_1, tsig, psignal, fsig, hrnum, a, norm

nsignal=N_ELEMENTS(signal_1(1,*))
psignal=FLTARR(3)
fsig=FLTARR(nsignal/2+1)
if nsignal ne 1 then detrendb2, tsig, signal_1, 0, nsignal-1, signal else signal=signal_1
, signal=signal_1, uncomment this line#comment line above for data without detrending
, =====
, calculate ratio of area under windows of different alphas
, =====
nsig = nsignal
indw=0
indw2=nsig-1
win1p=HANNING(nsig, alpha=1)
winp5=HANNING(nsig, alpha=0.5)
intwin1p=total( (win1p(indw indw2-1)+win1p(indw+1.indw2))/2.*1 )
intwinp5=total( (winp5(indw indw2-1)+winp5(indw+1.indw2))/2.*1 )
ratio = intwin1p/intwinp5
if (a eq 1) then ratio=1, if rectangular window is used, don't normalize
if N_ELEMENTS(norm) eq 0 then norm='y'
if (norm eq 'n') then ratio=1, if norm='n', don't normalize (ie multiply by 1)
, =====

hfsignalx=FFT(HANNING(nsignal, alpha=a)*signal(0,*))
hfsignaly=FFT(HANNING(nsignal, alpha=a)*signal(1,*))
hfsignalz=FFT(HANNING(nsignal, alpha=a)*signal(2,*))
hfsignaltot=FFT(HANNING(nsignal, alpha=a)*signal(3,*))

hpx=abs(hfsignalx(0:nsignal/2.))2
hpy=abs(hfsignaly(0:nsignal/2.))2
hpz=abs(hfsignalz(0:nsignal/2.))2
hpmean=abs(hfsignaltot(0:nsignal/2.))2
hptrace=hpx+hpy+hpz
hpperp=hptrace-hpmean
hpratio=hpperp/hpmean

delt=60.*(tsig(nsignal-1)-tsig(0))/(nsignal-1)
m2=FINDGEN(nsignal/2.+1)
freq2=m2/((nsignal-1)*delt)

CASE hrnum OF
0. indeces=where(freq2 ge 1./(2 *60 ))
1. indeces=where(freq2 ge 1./(2.*60.))
2. indeces=where(freq2 ge 1./(2.*60.))
3. indeces=where(freq2 ge 1./(2.*60 ))
4. indeces=where(freq2 ge 1.)
5. indeces=where(freq2 ge 0 1)
6. indeces=where(freq2 ge 1./(6.*60.))
7. indeces=where(freq2 ge 0.1)
endcase
CASE hrnum OF
0 indeces2=where(freq2 ge 0.1)
1. indeces2=where(freq2 ge 1./(2 *4 ))
2. indeces2=where(freq2 ge 1.)
3. indeces2=where(freq2 ge 10.)
4. indeces2=where(freq2 ge 10.)
5. indeces2=where(freq2 ge 10.)
6. indeces2=where(freq2 ge 10.)
7 indeces2=where(freq2 ge 1.)
endcase

ind=indec(0)
ind2=indec2(0)
ind3=N_ELEMENTS(freq2)-1
if ind2 eq -1 then ind2=ind3

```

---

```

if ind eq ind2 then ind = ind-1
if ind eq -1 then ind=0

if hrnum le 3 then ind=ind+1 , ind-start@0 008Hz, ind+1 start@0 016Hz, ind+2=start@0 025
factor=2*nsignal*delt

if ind eq 0 and ind2 eq 0 then begin
psignal(0)=factor*hpmean(ind)*freq2(ind)
psignal(1)=factor*hptrace(ind)*freq2(ind)
psignal(2)=factor*hpperp(ind)*freq2(ind)
endif else begin
fsig= freq2(0 nsignal/2)

psignal(0)=total( (factor*hpmean(ind ind2-1)+ factor*hpmean(ind+1 ind2))/2 *(freq2(
    ind+1 ind2)-freq2(ind ind2-1)) )*ratio
psignal(1)=total( (factor*hptrace(ind ind2-1)+ factor*hptrace(ind+1 ind2))/2 *(freq2(
    ind+1 ind2)-freq2(ind ind2-1)) )*ratio
psignal(2)=total( (factor*hpperp(ind ind2-1)+ factor*hpperp(ind+1 ind2))/2 *(freq2(
    ind+1 ind2)-freq2(ind ind2-1)) )*ratio
endelse

return
end

```

## A.2 Plotting Codes

**statcusp\_multifigure.pro** Adapted from code courtesy of Elena Budnik, obtained through private communication. Plots power figures in cusp normalized coordinates.

```
,*****
,   Cusp Statistics
,
,   statcusp_multifigure.pro      ,uses C1_P*_HR_norm2.sav and C1_P*_HR_2.sav, stddev.
,   sav files
,
,   Plots ColorCoded SOMETHING
,   on cusp-normalized field grid
,
,   Input. "orb[S,T]YDDD.res" and "cond[S,T]YDDD.res" files
,
,
,   June 2010
,*****

!p.multi=[0,3,3,0,1]
thisLetter="141B,"
alpha='!7'+String(thisLetter)+'!X'

for hrnum=0,7 do begin ,0.0.0083-0.1 /1.0.0083-0.25 /2.0 0083-1 /3.0.0083-10 /4.1-10
    /5.0.1-10/ 6 0 0028-10/ 7.0.1-1 Hz
for plotsnum=0,1 do begin
,*****
,   YOUR VALUES
,
,   norm          'y'          , use normalized data?
,   if plotsnum eq 0 then plotsc 'y' else plotsc 'n'          , scale bins
,   based on num of points?
,   stddevsc      'n'          , scale bins based on standard deviation value?
,   plotcol1 = 'n'          , max colorbar = max calculated value?
,   plotcol2 = 'y'          , min colorbar = min calculated value?
,   Value_Max = 40          , 40 for hrnum 1-3,5-6, 0.5 for hrnum4 to use, set
,   plotcol1=n
,   Value_Min = 0.0          , to use, set plotcol2=n
,*****

if (plotsc eq 'y' and norm eq 'y') then FILE 'power_norm2_hr'+string(hrnum,'(11)')+
'_scaled.eps'
if (plotsc eq 'y' and norm eq 'n') then FILE 'power2_hr'+string(hrnum,'(11)')+
'_scaled.eps'
if (plotsc eq 'n' and norm eq 'y') then FILE 'power_norm2_hr'+string(hrnum,'(11)')+
'.eps'
if (plotsc eq 'n' and norm eq 'n') then FILE 'power2_hr'+string(hrnum,'(11)')+'.eps'

if (hrnum eq 4 and Value_Max le 40.0 and plotsc eq 'y') then FILE='power_norm2_hr'+
string(hrnum,'(11)')+'_scaled_colorscaled.eps'
if (hrnum eq 4 and Value_Max lt 40.0 and plotsc eq 'n') then FILE='power_norm2_hr'+
string(hrnum,'(11)')+'_colorscaled.eps'
,   dev 'X'
,   dev 'PS'
if stddevsc eq 'y' then begin
RESTORE,filename='stddev.sav',/verbose
FILE 'power_norm2_hr'+string(hrnum,'(11)')+ '_stddevscaled_colorscaled.eps'
endif
,----- Device Setup -----
,   set_plot, DEV
,   !P POSITION [0.00,0.00,0.00,0.00]
,   if dev eq 'X' then begin
,       DEVICE, Decomposed=0
,       window, 0, xsize=500, ysize=500, retain 2
,       ch 1, thickness of words
,       th 1, outline of earth
```

```

        lth 1, thickness of field lines
    endif
    if dev eq 'PS' then begin
        device, /COLOR, BITS=8, XSIZE=27 94, YSIZE=27 94, file=FILE, $
        XOFFSET=0 84, YOFFSET =2 53, /BOLD, /ENCAPSULATED
        th = 2
        ch 3
        lth = 4
    endif
, -----
for p 0,2 do begin , 0 mean, 1 trace, 2 perp
if p eq 0 then ptype 'm'
if p eq 1 then ptype 't'
if p eq 2 then ptype 'p'
, -----
for plotn 1,3 do begin , which IMF condition?

seldate 'n', choose specific date to read@plot? CANNOT USE THIS YET WITH SAV FILES
preent 'n', if seldate y, run specific date again and again for debugging?
date='',
if preent eq 'y' then date='2001*'

, ----- Plot Range -----
XTitle=['X, R'DE', ' ', ' ', ' ']
YTitle=['Z, R'DE', ' ', ' ', ' ']
CASE plotn OF
1 begin
    , MainTitle 'N IMF, |clock angle| < 20'Uo'N'
    MainTitle 'Power '+ptype+', N IMF, |clock angle| < 60'Uo'N'
    ang1=60
    ang2=-1 *ang1
    plotnh=0 965
end
2 begin
    MainTitle 'Power '+ptype+', S IMF, |clock angle| > 120'Uo'N'
    ang1=120
    plotnh=0 63
end
3 begin
    MainTitle = 'Power '+ptype+', All IMF clock angles'
    ang1=360
    ang2=-360
    plotnh=0 294
end
4 begin
    MainTitle 'Horizontal IMF, 60'Uo'N < |clock angle| < 120'Uo'N'
    FILE = 'IMFH eps'
end
5 begin
    MainTitle '-90'Uo'N < clock angle < -60'Uo'N', (1)
    FILE = 'IMFH1 eps'
    ang1=-60
    ang2=-90
end
6 begin
    MainTitle '-120'Uo'N < clock angle < -90'Uo'N', (2)
    FILE 'IMFH2 eps'
    ang1=-90
    ang2=-120
end
7 begin
    MainTitle '60'Uo'N < clock angle < 90'Uo'N', (3)
    FILE 'IMFH3 eps'
    ang1=90
    ang2=60
end
8 begin

```

```

MainTitle = '90!Uo!N < clock angle < 120!Uo!N' , (4)
FILE      'IMFH4.eps'
ang1=120.
ang2=90.
end
9. begin
MainTitle      'Duskward IMF, 45!Uo!N < clock angle < 135!Uo!N'
FILE = 'IMFDusk.eps'
ang1=135.
ang2=45.
end
10. begin
MainTitle = 'Dawnward IMF, -135!Uo!N < clock angle < -45!Uo!N'
FILE      'IMFDawn.eps'
ang1=-45.
ang2=-135.
end
11. begin
MainTitle      '-120!Uo!N < clock angle < -60!Uo!N'
FILE = 'IMFH5.eps'
ang1=-60.
ang2=-120.
end
12. begin
MainTitle      '60!Uo!N < clock angle < 120!Uo!N'
FILE = 'IMFH6.eps'
ang1=120.
ang2=60.
end
endcase
, ----- Settings for Averaging. Grid Preparation -----
XRange  [-5.0, 15.0] , [-5 ,15 ]
YRange  [0.0,15.0]
ZRange  [0.0, 20.0] , [0.0,20 0]

YZangle  25.

stepx   .3 , 0.3 Re
stepz   .3

Nx = fix((XRange(1)-XRange(0))/stepx+0.5)
Nz = fix((ZRange(1)-ZRange(0))/stepz+0.5)

stepx =(XRange(1)-XRange(0))/Nx
stepz =(ZRange(1)-ZRange(0))/Nz

Value = fltarr(Nx,Nz)
N_value = intarr(Nx,Nz)

, *****
; LOAD HERE YOUR COLOR TABLE
,
loadct, 38, FILE=getenv("DDLIB")+"DDcolors.tbl"
, *****
dnc = !D.N_COLORS < 256

, ----- Earth, Field and Plot SetUp -----

plot,cos(findgen(40.)*!PI/40.),sin(findgen(40.)*!PI/40.),xrange=XRange, $
yrange=ZRange, xtitle=XTitle(0),ytitle=YTitle(0),title=MainTitle, $
xthick=2, ythick=2, thick th, charsize 15, color= dnc-1, xstyle 1,
ystyle 1, $
charthick ch

, ----- Plot Reference Frame and precalculated T96 field lines
; All orbital data have been converted into this frame
; Conditions.
, DATE. 2001-07-01 10.34 00

```



```

,                                     RamPressure 1 5 nPa
,                                     IMF 0 0, 2 0, -0 1 nT
,                                     Dst -10nT
,-----
    plotnormallines, 'XZ'. dnc-1, lth

for scnum=1,4 do begin, chooses cluster spacecraft
scnums=string(scnum, '(i1)'), spacecraft number, string
if norm eq 'n' then RESTORE, 'C1_P'+strtrim(string(hrnum),2)+'_HR_2 sav', /VERBOSE
    else RESTORE, 'C'+scnums+'_P'+strtrim(string(hrnum),2)+'_HR_norm2 sav', /VERBOSE,
        not normalized vs normalized data
,----- Main Definitions -----

StartTime      ' '
TimeIntAll     - ' '
TimeInt='0000000001000000'

Start          ''

,-----
, for data from cond* asc files
,-----
    ParRet      fltarr(4) , RamPressure, IMF[3]
    SW_PAR      fltarr(4) , Np, Vp, alpha ratio, Tp[K]

    dst      0 0
    delay = 0 0

,-----
, for data from orb* asc files
,-----

TimeOrb      dblarr(5) , UNIX time      secs from 1970-01-01
XYZ = fltarr(3,5) , orbit cusp-normalised frame
XYZ_GSM      fltarr(3,5) , orbit gsm
XYZ_SM       fltarr(3,5) , orbit sm
B_T96_gsm     fltarr(3,5) , model T96 field for real condition
,-----

B_IMF      fltarr(3)
,----- Start Reading Files -----
, *****
, RES_DIR => put name of directory where you keep cond* and orb* files
, *****
    RES_DIR      'sc'+scnums+'hr/',
if seldate eq 'y' then begin
    if preent eq 'n' then READ, date, PROMPT-'Enter Date to Process, format   yyyydoy
        FileNames      FindFile(RES_DIR+'cond_'+date+' asc', count=NFiles)
endif else FileNames = FindFile(RES_DIR+'cond_* asc', count=NFiles)

,-----
    for FN = 0, NFiles -1 do begin

        openr, COND, FileNames[FN], /GET_LUN
        openr, ORB, RES_DIR+'orbY_'+STRMID(FileNames[FN], STRLEN(RES_DIR)+5, 7)+'
            asc_with_sm', /GET_LUN

        readf, COND, StartTime
        print, StartTime

,-----
pwrarr      *powerarray[FN]
Bp      pwrarr(p,*)
Bp_size=*Bp_sizep[FN]
,----- Read Files 10 min portions -----
cnt      -1
if (plotn eq 4) then begin

```

```

while (not EOF(COND)) do begin
    readf, COND, Start
    readf, ORB, Start
    readf, COND, dst
    readf, COND, delay
    readf, COND, SW_PAR
    readf, COND, ParRet
    readf, COND, Delta_Theta

    B_IMF = ParRet[1 3]

    for jj = 0, 4 do begin
        readf, ORB, TTime, XX, YY, ZZ
        readf, ORB, Xgsm, Ygsm, Zgsm
        readf, ORB, Xsm, Ysm, Zsm
        readf, ORB, BT96x, BT96y, BT96z

        TimeOrb[jj] = TTime
        XYZ[0,jj] = XX
        XYZ[1,jj] = YY
        XYZ[2,jj] = ZZ
        XYZ_GSM[0,jj] = Xgsm
        XYZ_GSM[1,jj] = Ygsm
        XYZ_GSM[2,jj] = Zgsm
        XYZ_SM[0,jj] = Xsm
        XYZ_SM[1,jj] = Ysm
        XYZ_SM[2,jj] = Zsm
    endfor

,=====
,                               IMF Conditions
,
, YOU MAY PUT HERE SOME FILTER  PROCESS DATA ONLY FOR HORIZONTALWARD IMF, f1
,=====

    if (abs(atan(B_IMF[1],B_IMF[2])) lt 120 *'pi/180  and abs(atan(B_IMF[1],B_IMF
[2])) gt 60 *'pi/180 ) then begin

,-----

        for jj = 0, 4 do begin ,   orbital points   every 2 min => so 5 points for 10
            min interval

            if(abs(atan(XYZ_SM[1,jj],XYZ_SM[2,jj]))*180 /'pi le YZangle) then begin

,----- Making Averaging -----

                ix = fix((XYZ(0,jj)-XRange(0))/stepx)
                iz = fix((sqrt(total(XYZ(1 2,jj)^2))-ZRange(0))/stepz)

                if ((ix ge 0) and (ix le Nx-1) and (iz ge 0) and (iz le Nz-1)) then
                    begin
                        cnt = cnt +1
                    if cnt ge Bpsize then break
                        if Bp(cnt) ne -1e31 then begin
                            N_value(ix,iz) = N_value(ix,iz)+1
                            Value(ix,iz) = Value(ix,iz) + Bp(cnt)
                        endif
                        endif else begin
                            cnt = cnt + 1 ,data not within plot region
                    if cnt ge Bpsize then break
                        endelse
                            endif else begin, If YZ angle not too large
                                cnt = cnt+1
                    if cnt ge Bpsize then break
                        endelse
                            endfor , for jj 0, 4
                    endif else begin, IMF conditions
                        cnt = cnt + 5

```

```

if cnt ge Bpsize then break
endelse, IMF Conditions
endwhile , EOF COND FILE

endif else begin

if (plotn eq 2) then begin , plotn NOT EQ 4
while (not EOF(COND)) do begin
  readf, COND, Start
  readf, ORB, Start
  readf, COND, dst
  readf, COND, delay
  readf, COND, SW_PAR
  readf, COND, ParRet
  readf, COND, Delta_Theta

  B_IMF = ParRet[1 3]

  for jj = 0, 4 do begin
    readf, ORB, TTime, XX, YY, ZZ
    readf, ORB, Xgsm, Ygsm, Zgsm
    readf, ORB, Xsm, Ysm, Zsm
    readf, ORB, BT96x, BT96y, BT96z

    TimeOrb[jj] = TTime
    XYZ[0,jj] = XX
    XYZ[1,jj] = YY
    XYZ[2,jj] = ZZ
    XYZ_GSM[0,jj] = Xgsm
    XYZ_GSM[1,jj] = Ygsm
    XYZ_GSM[2,jj] = Zgsm
    XYZ_SM[0,jj] = Xsm
    XYZ_SM[1,jj] = Ysm
    XYZ_SM[2,jj] = Zsm
  endfor

,=====
,
, IMF Conditions
,
, YOU MAY PUT HERE SOME FILTER PROCESS DATA ONLY FOR SOUTHWARD IMF, f1
,=====
  if (abs(atan(B_IMF[1],B_IMF[2])) gt ang1*p1/180 ) then begin

,-----

  for jj = 0, 4 do begin , orbital points every 2 min => so 5 points for 10
    min interval

    if(abs(atan(XYZ_SM[1,jj],XYZ_SM[2,jj]))*180 /'p1 le YZangle) then begin

,----- Making Averaging -----

    ix = fix((XYZ[0,jj]-XRange(0))/stepx)
    iz = fix((sqrt(total(XYZ[1 2,jj]^2))-ZRange(0))/stepz)

    if ((ix ge 0) and (ix le Nx-1) and (iz ge 0) and (iz le Nz-1)) then
      begin
        cnt = cnt +1
      end
    if cnt ge Bpsize then break
    if Bp(cnt) ne -1e31 then begin
      N_value(ix,iz) = N_value(ix,iz)+1
      Value(ix,iz) = Value(ix,iz) + Bp(cnt)
    endif
  endif else begin
    cnt = cnt + 1 ,data not within plot region
  end
if cnt ge Bpsize then break
endelse
endif else begin, If YZ angle not too large
  cnt = cnt+1

```

```

if cnt ge Bpsize then break
    endelse
    endfor , for jj 0, 4
    endif else begin, IMF conditions
        cnt cnt + 5
    if cnt ge Bpsize then break
    endelse, IMF Conditions
    endwhile , EOF COND FILE

    endif else begin , plotn NOT EQ 2 or 4
    while (not EOF(COND)) do begin
        readf, COND, Start
        readf, ORB, Start
        readf, COND, dst
        readf, COND, delay
        readf, COND, SW_PAR
        readf, COND, ParRet
        readf, COND, Delta_Theta

        B_IMF ParRet[1 3]

        for jj 0, 4 do begin
            readf, ORB, TTime, XX, YY, ZZ
            readf, ORB, Xgsm, Ygsm, Zgsm
            readf, ORB, Xsm, Ysm, Zsm
            readf, ORB, BT96x, BT96y, BT96z

            TimeOrb[jj] TTime
            XYZ[0,jj] = XX
            XYZ[1,jj] = YY
            XYZ[2,jj] = ZZ
            XYZ_GSM[0,jj] Xgsm
            XYZ_GSM[1,jj] Ygsm
            XYZ_GSM[2,jj] Zgsm
            XYZ_SM[0,jj] Xsm
            XYZ_SM[1,jj] Ysm
            XYZ_SM[2,jj] Zsm
        endfor
    ,=====
    ,
    , IMF Conditions
    ,
    , YOU MAY PUT HERE SOME FILTER PROCESS DATA ONLY FOR NORTHWARD IMF, f1
    ,=====

    if((atan(B_IMF[1],B_IMF[2])) lt ang1*'pi/180 and (atan(B_IMF[1],B_IMF[2])) gt ang2*'
        pi/180 ) then begin
    ,-----

        for jj 0, 4 do begin , orbital points every 2 min => so 5 points for 10
            min interval

            if(abs(atan(XYZ_SM[1,jj],XYZ_SM[2,jj]))*180 /'pi le YZangle) then begin
    ,----- Making Averaging -----

                ix fix((XYZ[0,jj]-XRange(0))/stepx)
                iz fix((sqrt(total(XYZ[1 2,jj]^2))-ZRange(0))/stepz)

                if ((ix ge 0) and (ix le Nx-1) and (iz ge 0) and (iz le Nz-1)) then
                    begin
                        cnt cnt +1
                    end
            if cnt ge Bpsize then break
            if Bp(cnt) ne -1e31 then begin
                N_value(ix,iz) N_value(ix,iz)+1
                Value(ix,iz) = Value(ix,iz) + Bp(cnt)
            endif
        endfor
    ,=====

```

```

                                endif else begin
                                    cnt      cnt + 1 ,data not within plot region
if cnt ge Bpsize then break
                                endelse
                                    endif else begin, If YZ angle not too large
                                        cnt      cnt+1
if cnt ge Bpsize then break
                                endelse
                                    endfor , for jj      0, 4
                                endif else begin, IMF conditions
                                    cnt      cnt + 5
if cnt ge Bpsize then break
endelse, IMF Conditions
endwhile , EOF COND FILE
endelse
endelse

close,/file
FREE_LUN, COND, ORB

endfor , all files are processed, FN
endifor , end of the data for this spacecraft, see scnum

,----- Drawing -----
,----- Weighting a Result-----
Value_Min_1=Value_Max ,Setup for finding min value

for i      0, Nx-1 do for j = 0, Nz-1 do if (N_value[i,j] ne 0) then begin
    Value[i,j]      Value[i,j]/N_value[i,j]
    if (Value[i,j] lt Value_Min_1) then Value_Min_1      Value[i,j]
endif
if (plotcol2 eq 'y') then Value_Min      Value_Min_1

Value_Max_1 = MAX(Value)
if (plotcol1 eq 'y') then if (Value_Max_1 ne Value_Min) then Value_Max      Value_Max_1

XGRID      XRange[0] + indgen(Nx)*stepx + stepx
ZGRID      ZRange[0] + indgen(Nz)*stepz + stepz

KF = float(dnc      2)/(Value_Max-Value_Min)
,----- Linear Scale
,-----Cell Size is independent on N_value[i,j]
if stddevsc eq 'y' then begin
    stddev=*stddevarr[p,plotn-1,hrnum]
    pfillstx      stepx/199
    pfillstz      stepz/199
    for i      1, Nx-1 do for j      1, Nz-1 do if (N_value[i,j] ne 0) then begin
        col      (Value[i,j]-Value_Min)*KF < (dnc-2) , > Max in RED
        col      col > 1
if stddev[i,j] gt 0 then begin
    if stddev[i,j] ge 100 then begin
        POLYFILL, $
[XGRID[i-1]+100*pfillstx,XGRID[i-1]+100*pfillstx,XGRID[i]-100*pfillstx,XGRID[i]-100*
    pfillstx,XGRID[i-1]+100*pfillstx], $
[ZGRID[j-1]+100*pfillstz,ZGRID[j]-100*pfillstz,ZGRID[j]-100*pfillstz,ZGRID[j-1]+100*
    pfillstz,ZGRID[j-1]+100*pfillstz], $
color      col
    endif else begin
POLYFILL, $
[XGRID[i-1]+(stddev[i,j])*pfillstx, XGRID[i-1]+(stddev[i,j])*pfillstx, XGRID[i]-(
    stddev[i,j])*pfillstx, XGRID[i]-(stddev[i,j])*pfillstx, XGRID[i-1]+(stddev[i,j])*
    pfillstx], $
[ZGRID[j-1]+(stddev[i,j])*pfillstz,ZGRID[j]-(stddev[i,j])*pfillstz,ZGRID[j]-(stddev[i
    ,j])*pfillstz,ZGRID[j-1]+(stddev[i,j])*pfillstz,ZGRID[j-1]+(stddev[i,j])*pfillstz
    ], $
color      col

```

```

endelse
endif else begin
POLYFILL, [XGRID[1-1],XGRID[1-1],XGRID[1],XGRID[1],XGRID[1-1]], $
          [ZGRID[j-1],ZGRID[j],ZGRID[j],ZGRID[j-1],ZGRID[j-1]], $
          color = col

endelse
endif ,STDDEV EQ 0
endif else begin
pfillstx stepx/39.
pfillstz stepz/39.
if plots eq 'y' then begin , Make plot square proportional to # samples
  for i = 1, Nx-1 do for j = 1, Nz-1 do if (N_value[i,j] ne 0) then begin
    col (Value[i,j]-Value_Min)*KF < (dnc-2) , > Max in RED
    col col > 1
  if N_value[i,j] lt 20 then begin
POLYFILL, $
[XGRID[1-1]+(20.-N_value[i,j])*pfillstx,XGRID[1-1]+(20.-N_value[i,j])*pfillstx,XGRID[1-1]+(20.-N_value[i,j])*pfillstx,XGRID[1-1]+(20.-N_value[i,j])*pfillstx,XGRID[1-1]+(20.-N_value[i,j])*pfillstx], $
[ZGRID[j-1]+(20.-N_value[i,j])*pfillstz,ZGRID[j-1]+(20.-N_value[i,j])*pfillstz,ZGRID[j-1]+(20.-N_value[i,j])*pfillstz,ZGRID[j-1]+(20.-N_value[i,j])*pfillstz,ZGRID[j-1]+(20.-N_value[i,j])*pfillstz], $
color col
endif else begin
POLYFILL, [XGRID[1-1],XGRID[1-1],XGRID[1],XGRID[1],XGRID[1-1]], $
          [ZGRID[j-1],ZGRID[j],ZGRID[j],ZGRID[j-1],ZGRID[j-1]], $
          color = col

    endelse
    endif ,N_value ne 0
endif else begin, begin plots eq n below, Do NOT make plot square proportional to #
samples
for i = 1, Nx-1 do begin
  for j = 1, Nz-1 do begin
    if (N_value[i,j] ne 0) then begin
      col (Value[i,j]-Value_Min)*KF < (dnc-2) , > Max in RED
      col col > 1
      POLYFILL, [XGRID[1-1],XGRID[1-1],XGRID[1],XGRID[1],XGRID[1-1]], $
                [ZGRID[j-1],ZGRID[j],ZGRID[j],ZGRID[j-1],ZGRID[j-1]], $
                color = col
    endif
  endfor
endif
stop ; include this stop to plot column by column
endfor
endelse, plots eq n

,-----
, Overplotting reference frame
,-----
plotnormallines, 'XZ', dnc-1

endifor,IMF condition loop, plotn
,----- Color Scale -----
, COLOR SCALE HERE
if plotcol eq 'y' then pci = ' ' else if Value_Max lt 1 then pci = ' >' else pci = ' >'
loc [0.96, 0.87, 0.97, 0.97]
bar REPLICATE(1B, 10) # BINDGEN(256)
xsize (loc(2) loc(0)) * !D.X_VSIZE
ysize (loc(3) loc(1)) * !D.Y_VSIZE
xstart loc(0) * !D.X_VSIZE
ystart loc(1) * !D.Y_VSIZE
bar = BYTSC1(bar, TOP=dnc-1)
IF !D.NAME EQ 'PS' THEN $
TV, bar, xstart, ystart, XSIZE=xsize, YSIZE=ysize ELSE $
TV, CONGRID(bar, xsize, ysize), xstart, ystart
xtext = (loc(0)-0.1) * !D.X_VSIZE
XYOUTS,xtext,ystart,string(Value_Min,FORMAT='(F10.1)')+ ' nT!U2!N',/DEVICE,COLOR=255

```

```

XYOUTS,xtext,ystart+ysize*0.225,string(Value_Max*0.25+Value_Min*0.75,FORMAT='(F10.1)'
)+ ' nT'U2'N',/DEVICE,COLOR=255
XYOUTS,xtext,ystart+ysize*0.450,string((Value_Max+Value_Min)*0.50,FORMAT='(F10.1)')+
nT'U2'N',/DEVICE,COLOR=255
XYOUTS,xtext,ystart+ysize*0.675,string(Value_Max*0.75+Value_Min*0.25,FORMAT='(F10.1)'
)+ ' nT'U2'N',/DEVICE,COLOR=255
XYOUTS,(loc(0)-0.07)*'D X_VSIZE',ystart+ysize*0.900,pc1+STRTRIM(string(Value_Max,
FORMAT='(F10.1)'),1)+' nT'U2'N',/DEVICE,COLOR=255

CASE hrnum OF
'0' freq1=1/(2*60*0.5)
'1' freq1=1/(2*60*0.5)
'2' freq1=1/(2*60*0.5)
'3' freq1=1/(2*60*0.5)
'4' freq1=1/0
'5' freq1=0/1
'6' freq1=1/(6*60)
'7' freq1=0/1
endcase
CASE hrnum OF
'0' freq2=0/1
'1' freq2=1/(2*4)
'2' freq2=1
'3' freq2=10
'4' freq2=10
'5' freq2=10
'6' freq2=10
'7' freq2=1
endcase

XYOUTS,-0.025,0.007,string(freq1,'(F10.4)')+ '-' +strtrim(string(freq2,'(F10.3)'),1)+'
Hz',/normal,COLOR=255
,-----
endfor,power type loop (m,t,p)
if (dev eq 'PS') then DEVICE, /close_file
endfor,see plotscnum
endfor,see hrnum above, loop through different frequency ranges
end

```

**statcusp\_multifigure\_variance.pro** Adapted from code courtesy of Elena Budnik, obtained through private communication. Plots standard deviation of power figures in cusp normalized coordinates.

```
,*****
,   Cusp Statistics
,
;   statcusp_multifigure_variance.pro           ,uses C1_P*_HR_norm2.sav, C1_P*_HR_2
;   .sav, and averagepower.sav files (set saveorigval='y' if using for the 1st time to
;   create averagepower.sav files)
;   Plots ColorCoded SOMETHING
;   on cusp-normalized field grid
,
,   Input. "orb[S,T]YDDD.res" and "cond[S,T]YDDD.res" files
,
,   June 2010
,*****
,
saveorigval 'n' , create sav file of the original integrated power values?
if saveorigval eq 'y' then valuearr PTRARR(3,3,8,/ALLOCATE_HEAP) else restore,
  FILENAME='averagepower.sav'
savestddev 'n' , create sav file of the standard deviation values?
if savestddev eq 'y' then stddevarr = PTRARR(3,3,8,/ALLOCATE_HEAP)
!p.multi=[0,3,3,0,1]
thisLetter="I41B,"
alpha='!7'+String(thisLetter)+'!X'

for hrnum=0,7 do begin ;0 0.0083-0 1 /1.0.0083-0 25 /2 0 0083-1 /3.0.0083-10 /4.1-10
  /5 0.1-10/ 6.0.0028-10/ 7 0 1-1 Hz
for plotscnum=0,1 do begin,plots scaled (0) and not scaled (1) box images
,*****
,   YOUR VALUES
,
,   norm 'y' , use normalized data?
if plotscnum eq 0 then plotsc 'y' else plotsc 'n' , scale bins based on
  num of points?
multicolorbar = 'n' , each plot has its own colorscale?
plotcol1 'y' , max colorbar max calculated value?
plotcol2 'y' , min colorbar min calculated value?
if multicolorbar eq 'n' then plotcol1 'n'
Value_Max 100.0 , to use, set plotcol1=n
Value_Min 0.0 ; to use, set plotcol2=n
,*****

if (plotsc eq 'y') then FILE 'stddev_hr'+string(hrnum,'(i1)')+ '_scaled eps'
if (plotsc eq 'n') then FILE 'stddev_hr'+string(hrnum,'(i1)')+ '.eps'
if (hrnum eq 5 and Value_Max le 40.0 and plotsc eq 'y') then FILE='stddev_norm2_hr'+
  string(hrnum,'(i1)')+ '_scaled_colorscaled eps'
if (hrnum eq 5 and Value_Max lt 40.0 and plotsc eq 'n') then FILE='stddev_norm2_hr'+
  string(hrnum,'(i1)')+ '_colorscaled.eps'
,   dev 'X'
,   dev 'PS'
,FILE 'stddev_hr'+string(hrnum,'(i1)')+ '_multicolorbar.eps'
FILE 'test.eps'
;----- Device Setup -----
set_plot, DEV
!P.POSITION [0.00,0.00,0.00,0.00]
if dev eq 'X' then begin
  DEVICE, Decomposed=0
  window, 0, xsize=500, ysize=500, retain = 2
  ch = 1, thickness of words
  th = 1, outline of earth
  lth = 1, thickness of field lines
endif
if dev eq 'PS' then begin
  device, /COLOR, BITS=8, XSIZE=27.94, YSIZE=27.94, file=FILE, $
```



```

        XOFFSET=0.84, YOFFSET =2.53, /BOLD, /ENCAPSULATED
        th      2
        ch      3
        lth     4
    endif
,-----
for p = 0,2 do begin      , 0.mean, 1.trace, 2.perp
if p eq 0 then ptype      'm'
if p eq 1 then ptype      't'
if p eq 2 then ptype      'p'
,-----
for plotn 1,3 do begin , which IMF condition?

seldate - 'n', choose specific date to read&plot? CANNOT USE THIS YET WITH SAV FILES
preent   'n', if seldate y, run specific date again and again for debugging?
date=''
if preent eq 'y' then date='2001*'

;----- Plot Range -----
XTitle=['X, R'DE', ' ', ' ']
YTitle=['Z, R'DE ', ' ', ' ']
CASE plotn OF
1: begin
    ,MainTitle      'N IMF, |clock angle| < 20!Uo!N'
    MainTitle = 'Standard Deviation '+ptype+', N IMF, |clock angle| < 60!Uo!N'
    ang1=60.
    ang2=-1.*ang1
    plotnh=0.965
end
2: begin
    MainTitle = 'Standard Deviation '+ptype+', S IMF, |clock angle| > 120!Uo!N'
    ,
    ang1=120
    plotnh=0.63
end
3: begin
    MainTitle      'Standard Deviation. '+ptype+', All IMF clock angles'
    ang1=360.
    ang2=-360.
    plotnh=0.294
end
4: begin
    MainTitle      'Horizontal IMF, 60!Uo!N < |clock angle| < 120!Uo!N'
    FILE = 'IMFH.eps'
end
5: begin
    MainTitle      '-90!Uo!N < clock angle < -60!Uo!N', (1)
    FILE = 'IMFH1.eps'
    ang1=-60.
    ang2=-90.
end
6: begin
    MainTitle      '-120!Uo!N < clock angle < -90!Uo!N', (2)
    FILE = 'IMFH2.eps'
    ang1=-90.
    ang2=-120.
end
7: begin
    MainTitle      '60!Uo!N < clock angle < 90!Uo!N', (3)
    FILE = 'IMFH3.eps'
    ang1=90.
    ang2=60.
end
8: begin
    MainTitle      '90!Uo!N < clock angle < 120!Uo!N', (4)
    FILE = 'IMFH4.eps'
    ang1=120.

```

```

        ang2=90
    end
    9  begin
        MainTitle      'Duskward IMF, 45'Uo'N < clock angle < 135'Uo'N'
        FILE = 'IMFDusk eps'
        ang1=135
        ang2=45
    end
    10 begin
        MainTitle      'Dawnward IMF, -135'Uo'N < clock angle < -45'Uo'N'
        FILE = 'IMFDawn eps'
        ang1=-45
        ang2=-135
    end
    11 begin
        MainTitle = '-120'Uo'N < clock angle < -60'Uo'N'
        FILE = 'IMFH5 eps'
        ang1=-60
        ang2=-120
    end
    12 begin
        MainTitle      '60'Uo'N < clock angle < 120'Uo'N'
        FILE = 'IMFH6 eps'
        ang1=120
        ang2=60
    end
endcase
,----- Settings for Averaging Grid Preparation -----
XRange  [-5 0, 15 0] , [-5 ,15 ]
YRange  [0 0,15 0]
ZRange  [0 0, 20 0] , [0 0,20 0]

YZangle  25

stepx    3 , 0 3 Re
stepz    3

Nx  fix((XRange(1)-XRange(0))/stepx+0 5)
Nz  fix((ZRange(1)-ZRange(0))/stepz+0 5)

stepx =(XRange(1)-XRange(0))/Nx
stepz =(ZRange(1)-ZRange(0))/Nz

Value  fltarr(Nx,Nz)
N_value = intarr(Nx,Nz)

, *****
,  LOAD HERE YOUR COLOR TABLE
,
,  loadct, 38, FILE=getenv("DDLIB")+ "DDcolors.tbl"
, *****
, dnc 'D N_COLORS < 256

,----- Earth, Field and Plot Setup -----

plot,cos(findgen(40)*'PI/40 ),sin(findgen(40)*'PI/40 ),xrange=XRange, $
    yrange=ZRange, xtitle=XTitle(0),ytitle=YTitle(0),title=MainTitle, $
    xthick=2, ythick=2, thick th, charsize 15, color= dnc-1, xstyle - 1,
    ystyle 1, $
    charthick = ch

,----- Plot Reference Frame and precalculated T96 field lines
,  All orbital data have been converted into this frame
,  Conditions
,      DATE      2001-07-01 10 34 00
,      RamPressure 1 5 nPa
,      IMF 0 0, 2 0, -0 1 nT
,      Dst -10nT

```

```

,-----
    plotnormallines, 'XZ', dnc-1, lth

for scnum=1,4 do begin, chooses cluster spacecraft
scnums=string(scnum, 'i1'), spacecraft number, string
if norm eq 'n' then RESTORE, 'C'+scnums+'_P'+strtrim(string(hrnum),2)+'_HR_2 sav', /
    VERBOSE else RESTORE, 'C'+scnums+'_P'+strtrim(string(hrnum),2)+'_HR_norm2 sav', /
    VERBOSE, not normalized vs normalized data
,----- Main Definitions -----

StartTime      ' '
TimeIntAll     ' '
TimeInt='0000000001000000'

Start          ''

,-----
, for data from cond* asc files
,-----
    ParRet      fltarr(4) , RamPressure, IMF[3]
    SW_PAR      fltarr(4) , Np, Vp, alpha ratio, Tp[K]

    dst        0 0
    delay       0 0

,-----
, for data from orb* asc files
,-----

TimeOrb = dblarr(5) , UNIX time   secs from 1970-01-01
XYZ = fltarr(3,5) , orbit cusp-normalised frame
XYZ_GSM = fltarr(3,5) , orbit gsm
XYZ_SM = fltarr(3,5) , orbit sm
B_T96_gsm = fltarr(3,5) , model T96 field for real condition
,-----

B_IMF = fltarr(3)
,----- Start Reading Files -----
, *****
, RES_DIR => put name of directory where you keep
, cond* and orb* files
, *****
    RES_DIR = 'sc'+scnums+'hr/',
if seldate eq 'y' then begin
    if preent eq 'n' then READ, date, PROMPT='Enter Date to Process, format  yyyydoy
    ,
    FileNames = FindFile(RES_DIR+'cond_'+date+' asc', count=NFiles)
endif else FileNames = FindFile(RES_DIR+'cond_* asc', count=NFiles)
,-----
    for FN = 0, NFiles -1 do begin

        openr, COND, FileNames[FN], /GET_LUN
        openr, ORB, RES_DIR+'orbY_'+STRMID(FileNames[FN], STRLEN(RES_DIR)+5, 7)+'
            asc_with_sm', /GET_LUN

        readf, COND, StartTime
        , print, StartTime
,-----
, stop
pwrarr = powerarray[FN]
Bp = pwrarr(p,*)
Bpsize=Bpsizep[FN]
if saveorigval ne 'y' then savValue = valuearr[p, plotn-1, hrnum]
,----- Read Files 10 min portions -----
cnt = -1

```

```

,print,Bpsize
if (plotn eq 4) then begin
    while (not EOF(COND)) do begin
        readf, COND, Start
        readf, ORB, Start
        readf, COND, dst
        readf, COND, delay
        readf, COND, SW_PAR
        readf, COND, ParRet
        readf, COND, Delta_Theta

        B_IMF   ParRet[1:3]

        for jj 0, 4 do begin
            readf, ORB, TTime, XX, YY, ZZ
            readf, ORB, Xgsm, Ygsm, Zgsm
            readf, ORB, Xsm, Ysm, Zsm
            readf, ORB, BT96x, BT96y, BT96z

            TimeOrb[jj] - TTime
            XYZ[0, jj] - XX
            XYZ[1, jj]  YY
            XYZ[2, jj]  ZZ
            XYZ_GSM[0, jj] Xgsm
            XYZ_GSM[1, jj] Ygsm
            XYZ_GSM[2, jj] Zgsm
            XYZ_SM[0, jj] Xsm
            XYZ_SM[1, jj] Ysm
            XYZ_SM[2, jj] Zsm
        endfor
    ,=====
    ,                               IMF Conditions
    ,
    , YOU MAY PUT HERE SOME FILTER. PROCESS DATA ONLY FOR HORIZONTAL IMF, fr
    ,=====

    if (abs(atan(B_IMF[1],B_IMF[2])) lt 120.*!pi/180. and abs(atan(B_IMF[1],B_IMF
    [2])) gt 60.*!pi/180.) then begin

    ;-----

    for jj 0, 4 do begin , orbital points every 2 min => so 5 points for 10
        min interval

        if(abs(atan(XYZ_SM[1, jj],XYZ_SM[2, jj]))*180./!pi le YZangle) then begin

    ,----- Making Averaging -----

        ix = fix((XYZ[0, jj]-XRange(0))/stepx)
        iz = fix((sqrt(total(XYZ[1:2, jj]^2))-ZRange(0))/stepz)

        if ((ix ge 0) and (ix le Nx-1) and (iz ge 0) and (iz le Nz-1)) then
            begin
                cnt  cnt +1
            if cnt ge Bpsize then break
                if Bp(cnt) ne -1e31 then begin
                    N_value(ix,iz)  N_value(ix,iz)+1
                    if saveorigval eq 'y' then Value(ix,iz)  Value(ix,iz) + Bp
                        (cnt) else Value(ix,iz)  Value(ix,iz) + ((Bp(cnt)-
                        savValue(ix,iz))^2)
                endif
            endif else begin
                cnt - cnt + 1 ,data not within plot region
            if cnt ge Bpsize then break
            endelse
            endif else begin, If YZ angle not too large
                cnt = cnt+1
            if cnt ge Bpsize then break

```

```

        endelse
        endfor , for jj 0, 4
    endif else begin, IMF conditions
        cnt = cnt + 5
    if cnt ge Bpsize then break
    endelse, IMF Conditions
    endwhile , EOF COND FILE

    endif else begin

if (plotn eq 2) then begin , plotn NOT EQ 4
    while (not EOF(COND)) do begin
        readf, COND, Start
        readf, ORB, Start
        readf, COND, dst
        readf, COND, delay
        readf, COND, SW_PAR
        readf, COND, ParRet
        readf, COND, Delta_Theta

        B_IMF   ParRet[1.3]

        for jj 0, 4 do begin
            readf, ORB, TTime, XX, YY, ZZ
            readf, ORB, Xgsm, Ygsm, Zgsm
            readf, ORB, Xsm, Ysm, Zsm
            readf, ORB, BT96x, BT96y, BT96z

            TimeOrb[jj]   TTime
            XYZ[0, jj] = XX
            XYZ[1, jj]   YY
            XYZ[2, jj]   ZZ
            XYZ_GSM[0, jj] = Xgsm
            XYZ_GSM[1, jj] = Ygsm
            XYZ_GSM[2, jj] = Zgsm
            XYZ_SM[0, jj] = Xsm
            XYZ_SM[1, jj] = Ysm
            XYZ_SM[2, jj] = Zsm
        endfor
, =====
,                               IMF Conditions
,
, YOU MAY PUT HERE SOME FILTER PROCESS DATA ONLY FOR SOUTHWARD IMF, f1
, =====
        if (abs(atan(B_IMF[1], B_IMF[2])) gt ang1*'pi/180 ) then begin
, -----

        for jj = 0, 4 do begin , orbital points every 2 min => so 5 points for 10
            min interval

            if(abs(atan(XYZ_SM[1, jj], XYZ_SM[2, jj]))*180./'pi le YZangle) then begin
, ----- Making Averaging -----

            ix = fix((XYZ(0, jj)-XRange(0))/stepx)
            iz = fix((sqrt(total(XYZ(1.2, jj)^2))-ZRange(0))/stepz)

            if ((ix ge 0) and (ix le Nx-1) and (iz ge 0) and (iz le Nz-1)) then
                begin
                    cnt   cnt +1
        if cnt ge Bpsize then break
                    if Bp(cnt) ne -1e31 then begin
                        N_value(ix, iz) = N_value(ix, iz)+1
                        if saveorigval eq 'y' then Value(ix, iz) = Value(ix, iz) + Bp(
                            cnt) else Value(ix, iz) = Value(ix, iz) + ((Bp(cnt)-savValue
                                (ix, iz))^2)
                    endif
                end

```

```

endif else begin
    cnt    cnt + 1 ,data not within plot region
if cnt ge Bpsize then break
endif else begin, If YZ angle not too large
    cnt    cnt+1
if cnt ge Bpsize then break
endif else begin, IMF conditions
    cnt = cnt + 5
if cnt ge Bpsize then break
endif else, IMF Conditions
endwhile , EOF COND FILE

endif else begin , plotn NOT EQ 2 or 4
while (not EOF(COND)) do begin
    readf, COND, Start
    readf, ORB, Start
    readf, COND, dst
    readf, COND, delay
    readf, COND, SW_PAR
    readf, COND, ParRet
    readf, COND, Delta_Theta

    B_IMF    ParRet[1:3]

    for jj    0, 4 do begin
        readf, ORB, TTime, XX, YY, ZZ
        readf, ORB, Xgsm, Ygsm, Zgsm
        readf, ORB, Xsm, Ysm, Zsm
        readf, ORB, BT96x, BT96y, BT96z

        TimeOrb[jj]    TTime
        XYZ[0,jj] = XX
        XYZ[1,jj] = YY
        XYZ[2,jj] = ZZ
        XYZ_GSM[0,jj]    Xgsm
        XYZ_GSM[1,jj]    Ygsm
        XYZ_GSM[2,jj]    Zgsm
        XYZ_SM[0,jj]    Xsm
        XYZ_SM[1,jj]    Ysm
        XYZ_SM[2,jj]    Zsm
    endfor
, =====
,
,           IMF Conditions
,
, YOU MAY PUT HERE SOME FILTER  PROCESS DATA ONLY FOR NORTHWARD IMF, fr
, =====

if((atan(B_IMF[1],B_IMF[2])) lt ang1*!pi/180. and (atan(B_IMF[1],B_IMF[2])) gt ang2*!
pi/180.) then begin
, -----

    for jj = 0, 4 do begin , orbital points every 2 min => so 5 points for 10
min interval

        if(abs(atan(XYZ_SM[1,jj],XYZ_SM[2,jj]))*180./!pi le YZangle) then begin
, ----- Making Averaging -----

            ix    fix((XYZ(0,jj)-XRange(0))/stepx)
            iz    fix((sqrt(total(XYZ(1:2,jj)^2))-ZRange(0))/stepz)

            if ((ix ge 0) and (ix le Nx-1) and (iz ge 0) and (iz le Nz-1)) then
begin

```

```

        cnt = cnt + 1
if cnt ge Bpsize then break
        if Bp(cnt) ne -1e31 then begin
            N_value(1x,1z) = N_value(1x,1z)+1
            if saveorigval eq 'y' then Value(1x,1z) = Value(1x,1z) + Bp(
                cnt) else Value(1x,1z) = Value(1x,1z) + ((Bp(cnt)-savValue
                (1x,1z))^2)
            endif
        endif else begin
            cnt = cnt + 1 ,data not within plot region
if cnt ge Bpsize then break
        endelse
            endif else begin, If YZ angle not too large
                cnt = cnt+1
if cnt ge Bpsize then break
        endelse
            endfor , for jj = 0, 4
            endif else begin, IMF conditions
                cnt = cnt + 5
if cnt ge Bpsize then break
endelse, IMF Conditions
        endwhile , EOF COND FILE
        endelse
endelse

close,/file
FREE_LUN, COND, ORB

endfor , all files are processed, FN
endfor , end of the data for this spacecraft, see scnum

,----- Drawing -----
,----- Weighting a Result-----
        Value_Min_1=Value_Max ,Setup for finding min value

        for i = 0, Nx-1 do for j = 0, Nz-1 do if (N_value[i,j] ne 0) then begin
            if saveorigval ne 'y' then Value[i,j] = (Value[i,j]/N_value[i,j])^0.5 else
                Value[i,j]=Value[i,j]/N_value[i,j]
            if (Value[i,j] lt Value_Min_1) then Value_Min_1 = Value[i,j]
        endif
        if (plotcol2 eq 'y') then Value_Min = Value_Min_1

        Value_Max_1 = MAX(Value)
        if (plotcol1 eq 'y') then if (Value_Max_1 ne Value_Min) then Value_Max = Value_Max_1

        XGRID = XRange[0] + indgen(Nx)*stepx + stepx
        ZGRID = ZRange[0] + indgen(Nz)*stepz + stepz

        KF = float(dnc - 2)/(Value_Max-Value_Min)
, stop
, print, Value_Max, Value_Min
if saveorigval eq 'y' then begin
savValue=Value
*valuearr[p,plotn-1,hrnum]=savValue
endif
if savstddev eq 'y' then begin
savstddev=Value
*stddevarr[p,plotn-1,hrnum]=savstddev
endif
,----- Linear Scale
,----- Cell Size is independent on N_value[i,j]
pfillstx = stepx/39
pfillstz = stepz/39
if plotsc eq 'y' then begin , Make plot square proportional to # samples<-----
    for i = 1, Nx-1 do for j = 1, Nz-1 do if (N_value[i,j] ne 0) then begin
        col = (Value[i,j]-Value_Min)*KF < (dnc-2) , > Max in RED
        col = col > 1
    
```

```

if N_value[i,j] lt 20 then begin
    ,print,N_value[i,j]
    ,print,'value',Value[i,j]
POLYFILL, $
[XGRID[i-1]+(20.-N_value[i,j])*pfillstx, XGRID[i-1]+(20.-N_value[i,j])*pfillstx,
 XGRID[i]-(20.-N_value[i,j])*pfillstx, XGRID[i]-(20.-N_value[i,j])*pfillstx, XGRID
 [i-1]+(20.-N_value[i,j])*pfillstx], $
[ZGRID[j-1]+(20.-N_value[i,j])*pfillstz, ZGRID[j]-(20.-N_value[i,j])*pfillstz, ZGRID[j]
 -(20.-N_value[i,j])*pfillstz, ZGRID[j-1]+(20.-N_value[i,j])*pfillstz, ZGRID[j]
 -1]+(20.-N_value[i,j])*pfillstz], $
color col
endif else begin
    ,print,N_value[i,j]
    ,print,'value',Value[i,j]
    POLYFILL, [XGRID[i-1],XGRID[i-1],XGRID[i],XGRID[i],XGRID[i-1]], $
              [ZGRID[j-1],ZGRID[j],ZGRID[j],ZGRID[j-1],ZGRID[j-1]], $
              color = col
    endwhile
    endif ,N_value ne 0
endif else begin, begin plotsc eq n below, Do NOT make plot square proportional to #
samples<-----
for i = 1, Nx-1 do begin
    for j = 1, Nz-1 do begin
        if (N_value[i,j] ne 0) then begin
            col (Value[i,j]-Value_Min)*KF < (dnc-2) , > Max in RED
            col col > 1
        ,print,col
        ,print,Value[i,j]
        POLYFILL, [XGRID[i-1],XGRID[i-1],XGRID[i],XGRID[i],XGRID[i-1]], $
                  [ZGRID[j-1],ZGRID[j],ZGRID[j],ZGRID[j-1],ZGRID[j-1]], $
                  color = col
        endif
    endwhile
    ,stop ; include this stop to plot column by column
endfor
    endwhile, plotsc eq n
    ,----- Color Scale -----
    , COLOR SCALE HERE
    if plotcoli eq 'y' then pcl ' ' else if Value_Max lt 1 then pcl = ' >' else pcl
    '>'
    loc [0.96, 0.87, 0.97, 0.97]
    bar REPLICATE(1B, 10) # BINDGEN(256)
    xsize (loc(2) loc(0)) * !D.X_VSIZE
    ysize (loc(3) loc(1)) * !D.Y_VSIZE
    placehelp = [0.3, 0.65, 1]
    placehelp2 = [0.98, 0.6, 0.2]
    if multicolorbar eq 'y' then begin
        multibarx=placehelp[p]
        multibary=placehelp2[plotn-1]
    endif else begin
        multibarx=1
        multibary=1
    endwhile
    xstart = loc(0) * !D.X_VSIZE * multibarx
    ystart = loc(1) * !D.Y_VSIZE * multibary
    ,print,xstart,ystart
    ,stop
    bar = BYTSCl(bar, TOP=dnc-1)
    IF !D.NAME EQ 'PS' THEN $
TV, bar, xstart, ystart, XSIZE=xsize, YSIZE=ysize ELSE $
    TV, CONGRID(bar, xsize, ysize), xstart, ystart
    xtext (loc(0)-0.1) * !D.X_VSIZE * multibarx
    XYOUTS,xtext,ystart,string(Value_Min,FORMAT='(F10 1)')+ ' nT!U2!N',/DEVICE,COLOR=255
    XYOUTS,xtext,ystart+ysize*0.225,string(Value_Max*0 25+Value_Min*0 75,FORMAT='(F10 1)'
    )+ ' nT!U2!N',/DEVICE,COLOR=255
    XYOUTS,xtext,ystart+ysize*0.450,string((Value_Max+Value_Min)*0.50,FORMAT='(F10 1)')+
    ' nT!U2!N',/DEVICE,COLOR=255

```



```

XYOUTS, xtext, ystart+ysize*0.675, string(Value_Max*0.75+Value_Min*0.25, FORMAT='(F10.1)'
      )+' nT!U2!N', /DEVICE, COLOR=255
XYOUTS, (loc(0)-0.08)*!D.X_VSIZE*multibarx, ystart+ysize*0.900, pci+STRTRIM(string(
      Value_Max, FORMAT='(F10.1)'))+1)+' nT!U2!N', /DEVICE, COLOR=255
;stop
;-----
;   Overplotting reference frame
;-----
plotnormallines, 'XZ', dnc-1

endfor; IMF condition loop, plotn

CASE hrnum OF
'0': freq1=1./(2.*60.*0.5)
'1': freq1=1./(2.*60.*0.5)
'2': freq1=1./(2.*60.*0.5)
'3': freq1=1./(2.*60.*0.5)
'4': freq1=1.0
'5': freq1=0.1
'6': freq1=1./(6.*60.)
'7': freq1=0.1
endcase
CASE hrnum OF
'0': freq2=0.1
'1': freq2=1./(2.*4.)
'2': freq2=1.
'3': freq2=10.
'4': freq2=10.
'5': freq2=10.
'6': freq2=10.
'7': freq2=1.
endcase

XYOUTS, -0.025, 0.007, string(freq1, '(F10.4)')+ '-' +strtrim(string(freq2, '(F10.3)'), 1)+'
      Hz', /normal, COLOR=255
;-----
endfor, power type loop (m, t, p)
if (dev eq 'PS') then DEVICE, /close_file
endfor; see plotsenum
endfor; see hrnum above, loop through different frequency ranges
if saveorigval eq 'y' then save, valuearr, FILENAME='averagepower.sav', DESCRIPTION='
      Valuearr is a 3x3x8 pointer array that saves the average power value for each
      grid point of the plot for column(power m, t, p), row(n, s, a imf), and depth(hrnum
      0-7)'
if savestddev eq 'y' then save, stddevarr, FILENAME='stddev.sav', DESCRIPTION='stddevarr
      is a 3x3x8 pointer array that saves the standard deviation value for each grid
      point of the plot for column(power m, t, p), row(n, s, a imf), and depth(hrnum 0-7)'
end

```

## A.3 Supporting Functions

**readfgmhr.pro** Adapted from code courtesy of Katariina Nykyri. Reads the data files.

```

Pro readfgmhr, namefgm, ntot, time, b
openr,1,namefgm
i=(LINDGEN(1))(0)

minutesarr=FLTARR(1604000)
hoursarr=FLTARR(1604000)
secondsarr=FLTARR(1604000)
timearr=FLTARR(1604000)
bxarr=FLTARR(1604000)
byarr=FLTARR(1604000)
bzarr=FLTARR(1604000)

dash=''
hour=10
minutes=10
seconds=10.422
bx1=-300.22222
by1=-300.22222
bz1=-300.22222
x1=11739.6
y1=11739.6
z1=11739.6
year=2000
month=12
day=20

while not eof(1) do begin
readf,1,$
FORMAT = '(I4,A1,I2,A1,I2,A1,I2,A1,I2,A1,F7.3,A1,F9.4,F9.4,F9.4,F10.1,F10.1,F10.1)',
year,dash,month,dash,day,dash,hour,dash,minutes,dash,seconds,dash,$
bx1,by1,bz1,x1,y1,z1

minutesarr(i)=minutes
hoursarr(i)=hour
secondsarr(i)=seconds
timearr(i)=hour*60.*60. + minutes*60. + seconds
bxarr(i)=bx1
byarr(i)=by1
bzarr(i)=bz1

i=i+1
endwhile

ntot=1
time=FLTARR(ntot)
b=FLTARR(3,ntot)
jind=(LINDGEN(1))(0)
for j=jind, ntot-1 do begin
time(j)=timearr(j)/60
b(0,j)=bxarr(j)
b(1,j)=byarr(j)
b(2,j)=bzarr(j)
endfor

close,1
return
end

```

**datagapfillhr.pro** Adapted from code courtesy of Katarina Nykyri Interpolates data gaps and bad data points.

```

PRO datagapfillhr, n,time,array,ctmin,ctmax,timenew,arraynew,newn,stime
openu,gaps,'DataGapsOver2min.txt',/append,/GET_LUN,,,,,,,,,,,,,
printf,gaps,stime,,,,,,,,,,,,,
, time comes in with units of [min], ctmin and ctmax in [hr]
, this program does calculations in [sec]
, FIND DATA GAPS and linearly interpolate across the gap
arraynew=FLTARR(3,2*n)
timenew=FLTARR(2*n)
, critical dt in seconds between t_i and t_{i+1} so that it is considered as a gap
, check dt from the data
dt=1/22.4
critint = 2*dt
time=60*time,convert to [sec]
ctmin=3600*long(ctmin),convert to [sec]
ctmax=3600*long(ctmax),convert to [sec]
i=(lindgen(1))(0) & j=(lindgen(1))(0)

nn=n
while i lt nn-1 do begin
  if (time(i) lt ctmin) or (time(i) gt ctmax) then begin ,outside of cusp interval
    timenew(j)=time(i)
    arraynew(*,j)=array(*,i)
    j=j+1
  endif else begin

    if (time(i+1)-time(i) le critint) then begin
      timenew(j)=time(i)
      arraynew(*,j)=array(*,i)
      j=j+1
    endif else begin

      ,filling the time data gaps
      if time(i+1)-time(i) gt critint then begin
if time(i+1)-time(i) gt 120 then begin,print to file if gap is larger than 2 min
printf,gaps,time(i)/60.,time(i+1)/60.,(time(i+1)-time(i))/60.,,,,,,,,,,
endif
        npoints=round((time(i+1)-time(i))/dt)
        for k=0l,npoints-1 do begin
          timenew(j+k)=time(i)+k*dt
          arraynew(*,j+k)=-1e31
          if (k eq 0) then begin
            arraynew(*,j+k)=array(*,i)
          endif
        endfor
        j=j+npoints
      endif
    endelse

    endelse
    i=i+1
  endwhile
  timenew(j) = time(i)
  arraynew(*,j)=array(*,i)

for ii=0,2 do begin
  a = where((arraynew(ii,*) ne -1e31) and (timenew ne 0),count)
  if timenew(0) eq 0 then begin
    kk = fltarr(count+1)
    for kkk = 0L, count-1 do begin
      kk(kkk+1) = a(kkk)
    endfor
    a = kk
  endif
endif

```

```
arraynew_1  arraynew(11,a)
timenew_1   timenew(a)
arrayint    interpol(arraynew_1, timenew_1, timenew)
arraynew(11,*)=arrayint
endfor

helpind=where(timenew ne 0,count)
if timenew(0) eq 0 then begin
  kk  fltarr(count+1)
  for kkk  0L, count-1 do begin
    kk(kkk+1)  helpind(kkk)
  endfor
  helpind = kk
endif
helptimearr=timenew(helpind)
helparraynew=arraynew(*,helpind)

timenew=helptimearr/60
arraynew=helparraynew
time    time/60
ctmin   ctmin/3600
ctmax   = ctmax/3600
newn    j+1
close,gaps,,,,,,,,,,,,,
FREE_LUN, gaps,,,,,,,,,,,,,
return
end
```

**hindbd.pro** Code courtesy of Katarina Nykyri Determines the beginning and ending of the cusp interval

```
Pro hindbd,min,max,n,time,its,ite

its=(LINDGEN(1))(0)
ite=(LINDGEN(1))(0)

  while ((time(its) lt min) and (its lt n-1)) do its=its+1
  ite=n-1 & while ((time(ite) gt max) and (ite gt 0)) do ite=ite-1
  if ite lt its then begin
    ite=its+1
  endif

return
end
```

**detrendb2.pro** Code courtesy of Katarina Nykyri. Subtracts background field (linear fit).

```
Pro detrendb2, dtime,arrayin,ibs,ibe,arrayout

arrayout=FLTARR(4,ibe-ibs+1)
for i=0,3 do begin
  signal=arrayin(i,ibs.ibe)
  , linear least square fit
  yfit=0
  yband=0
  sigma=0
  a0=0
  dsignal=0
  lfit=POLY_FIT(dtime,signal,1,yfit,yband,sigma,a0)
  , y=b+kx, lfit(0)=b and lfit(1)=k
  , signal after extracting the linear least square fit from it
  dsignal=signal-yfit
  arrayout(i,*)=dsignal
endfor

return
end
```

## Appendix B

# Unnormalized Integrated Power with Different Windowing

The integrated power for different frequency ranges (0.008-10 Hz, 0.017-10 Hz, and 0.025-10 Hz), Hanning window  $\alpha$  values ( $\alpha = 0.5, 0.75, 1.0$ ), and NIMF, SIMF, and AIMF are shown in this Appendix. The mean and perpendicular power plots are shown here. Mean power is shown in Figures B.1-B.3. Perpendicular power is shown in Figures B.4-B.6. The total power plots are shown in Section 3.2. The power in this Appendix is unnormalized.

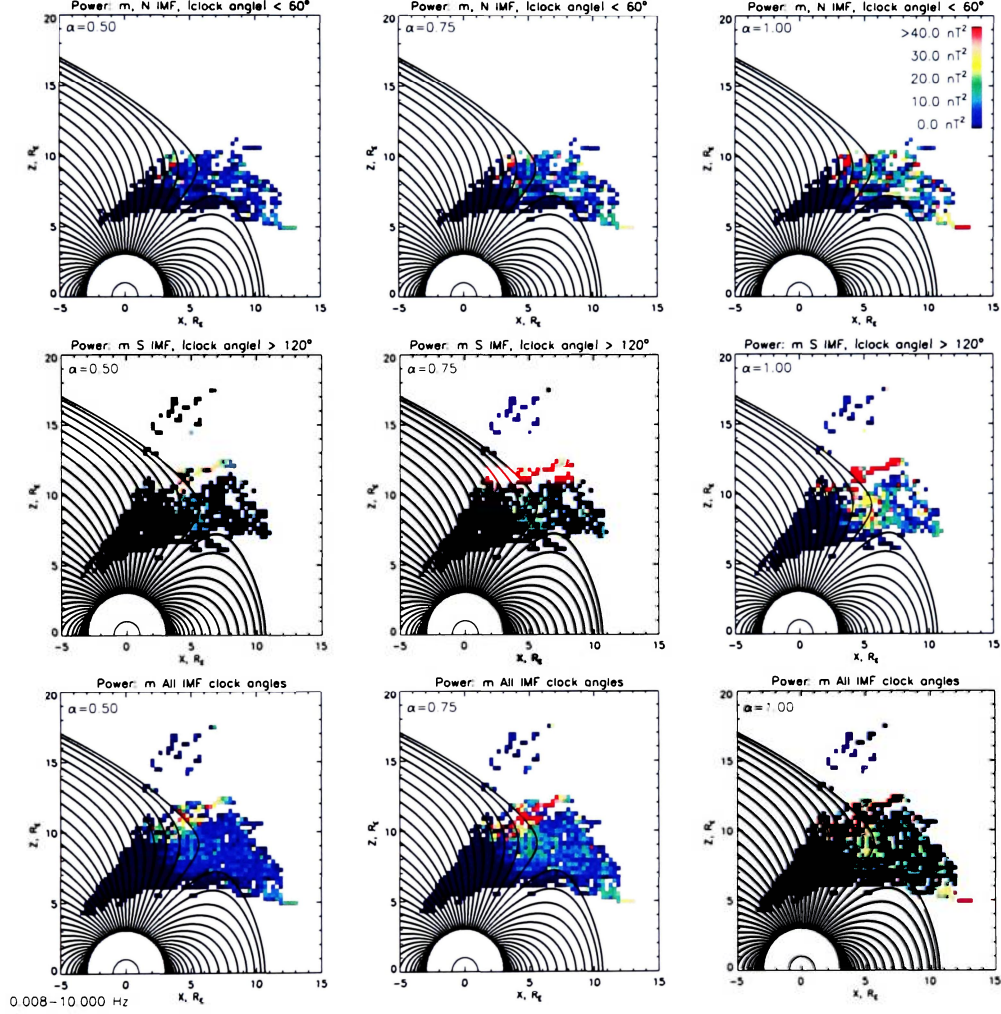


Figure B.1: Mean integrated power for the magnetic field fluctuations of the 0.008-10 Hz frequency range for NIMF, SIMF, and AIMF (rows) and Hanning window with  $\alpha = 0.5, 0.75, \text{ and } 1$  (columns).



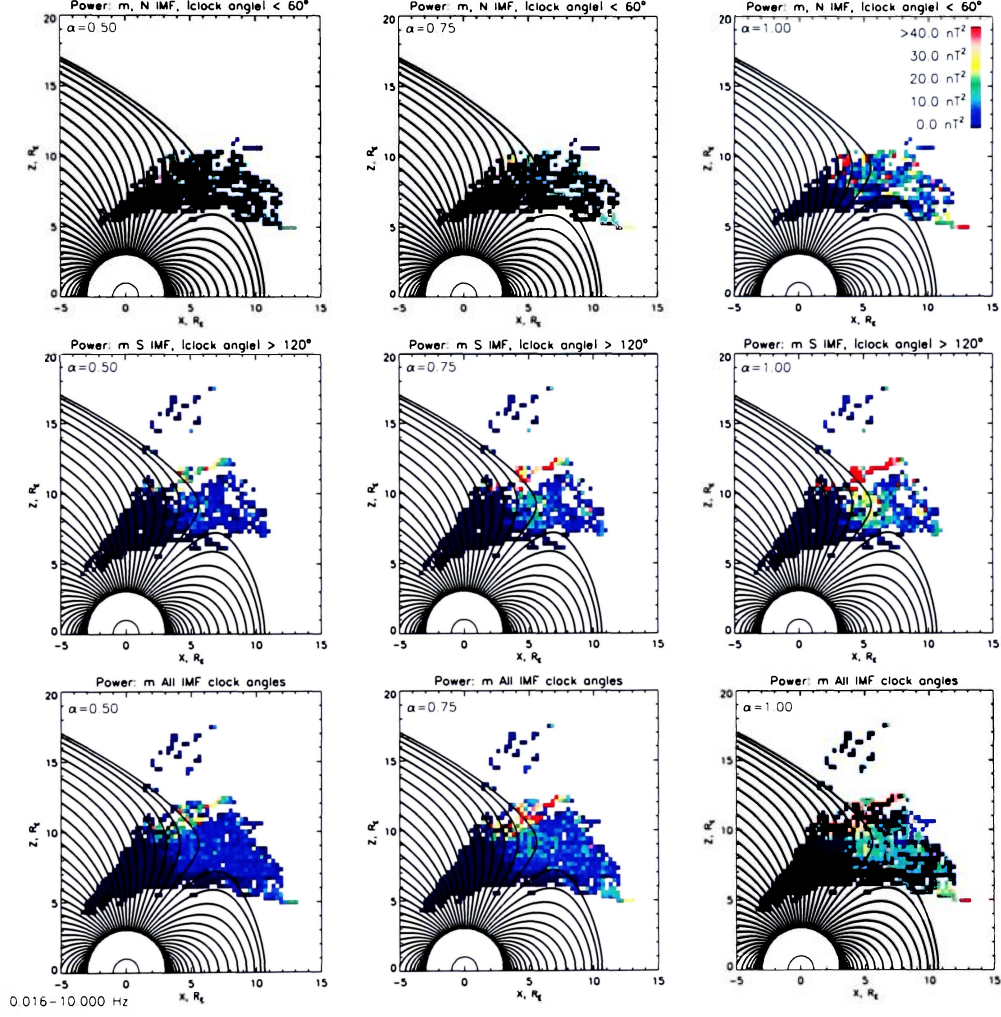


Figure B.2: Mean integrated power for the magnetic field fluctuations of the 0.017-10 Hz frequency range for NIMF, SIMF, and AIMF (rows) and Hanning window with  $\alpha = 0.5, 0.75$ , and 1 (columns).

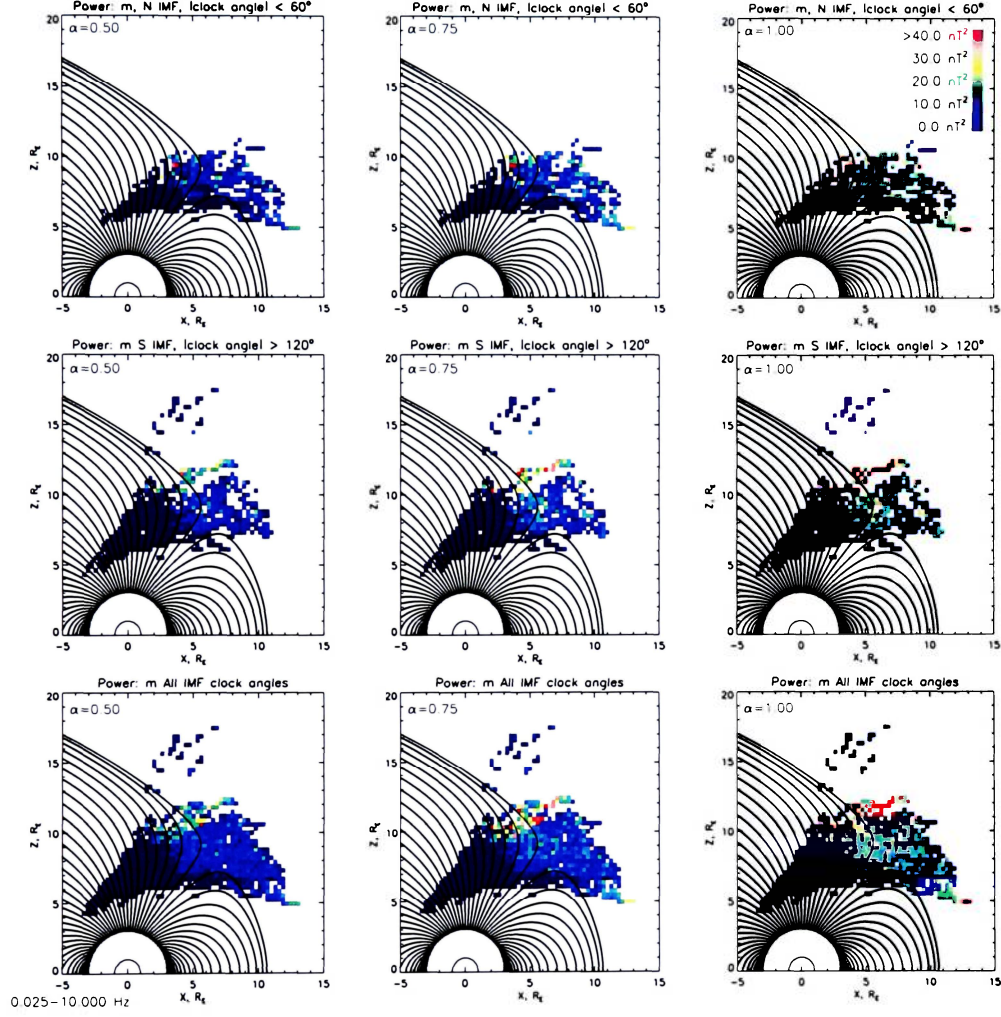


Figure B.3: Mean integrated power for the magnetic field fluctuations of the 0.025-10 Hz frequency range for NIMF, SIMF, and AIMF (rows) and Hanning window with  $\alpha = 0.5, 0.75$ , and 1 (columns).

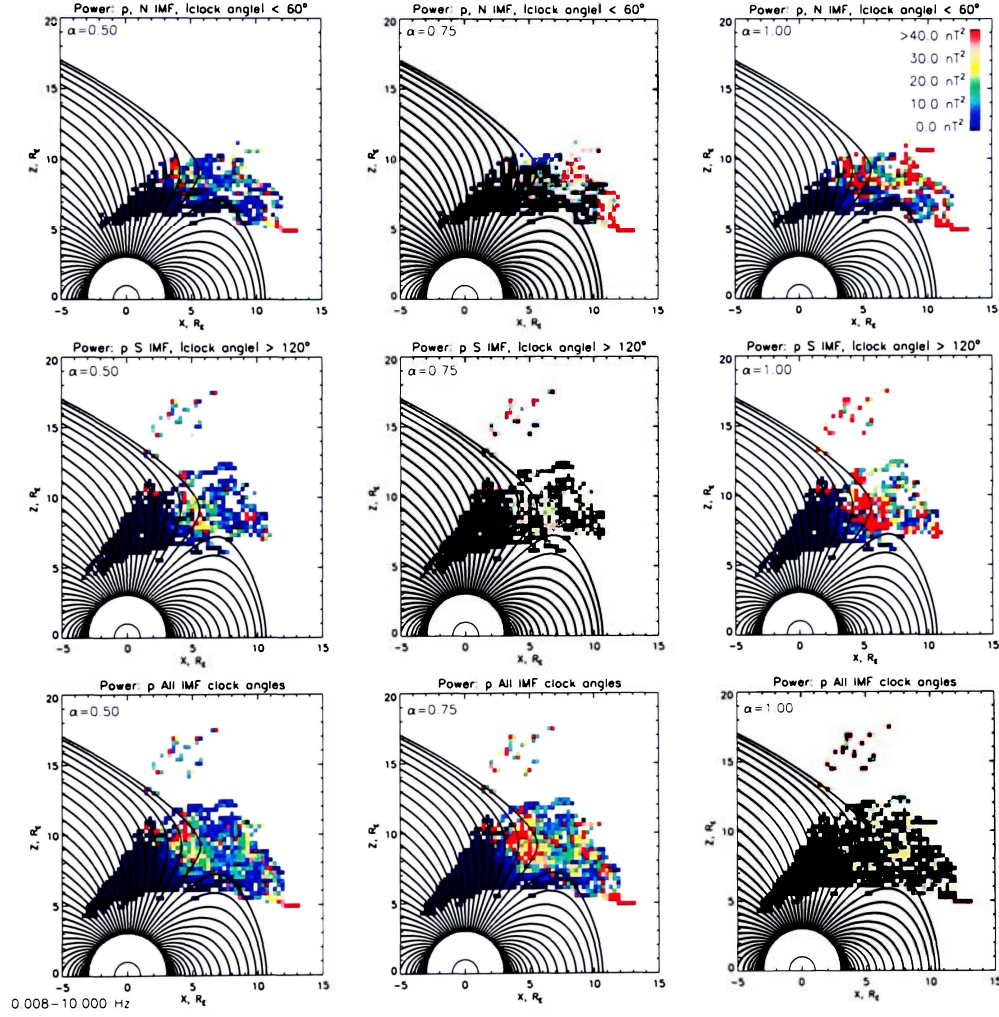


Figure B.4: Perpendicular integrated power for the magnetic field fluctuations of the 0.008-10 Hz frequency range for NIMF, SIMF, and AIMF (rows) and Hanning window with  $\alpha = 0.5, 0.75$ , and  $1$  (columns).



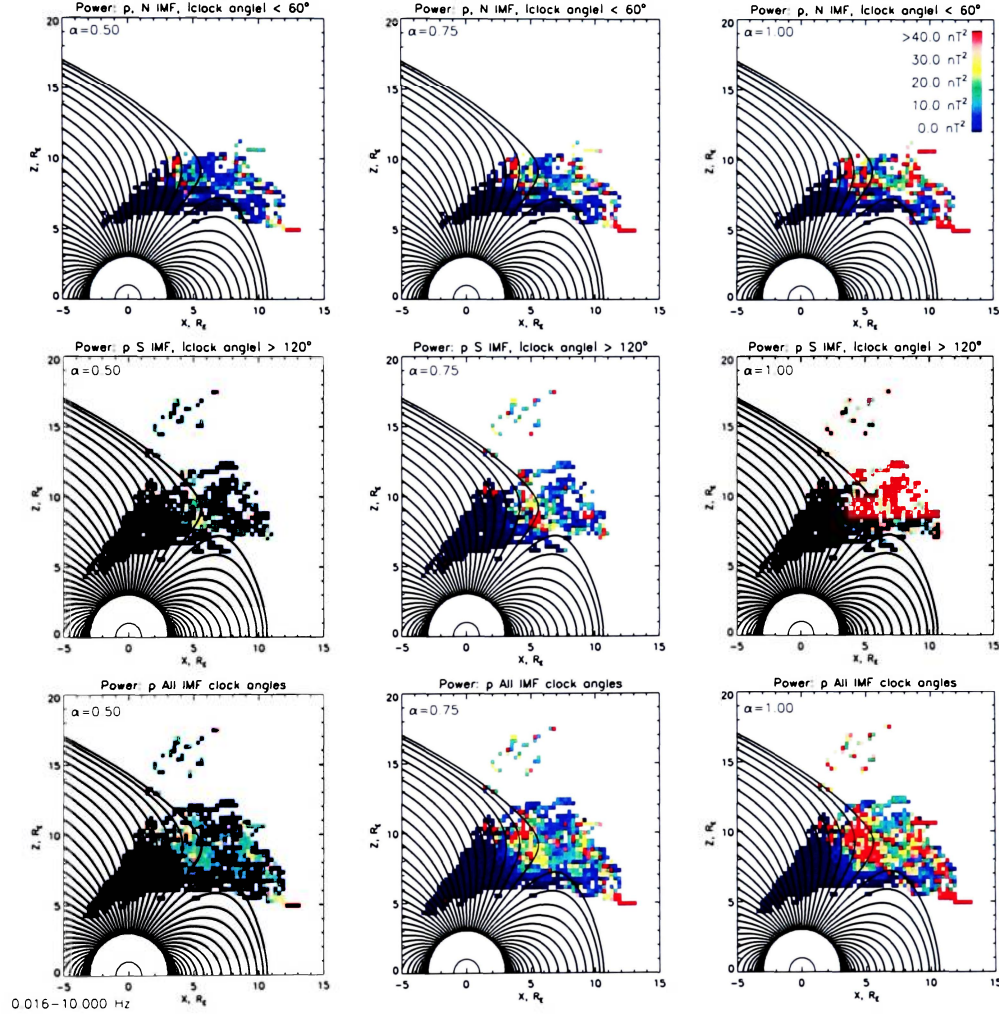


Figure B.5: Perpendicular integrated power for the magnetic field fluctuations of the 0.017-10 Hz frequency range for NIMF, SIMF, and AIMF (rows) and Hanning window with  $\alpha = 0.5$ ,  $0.75$ , and  $1$  (columns).

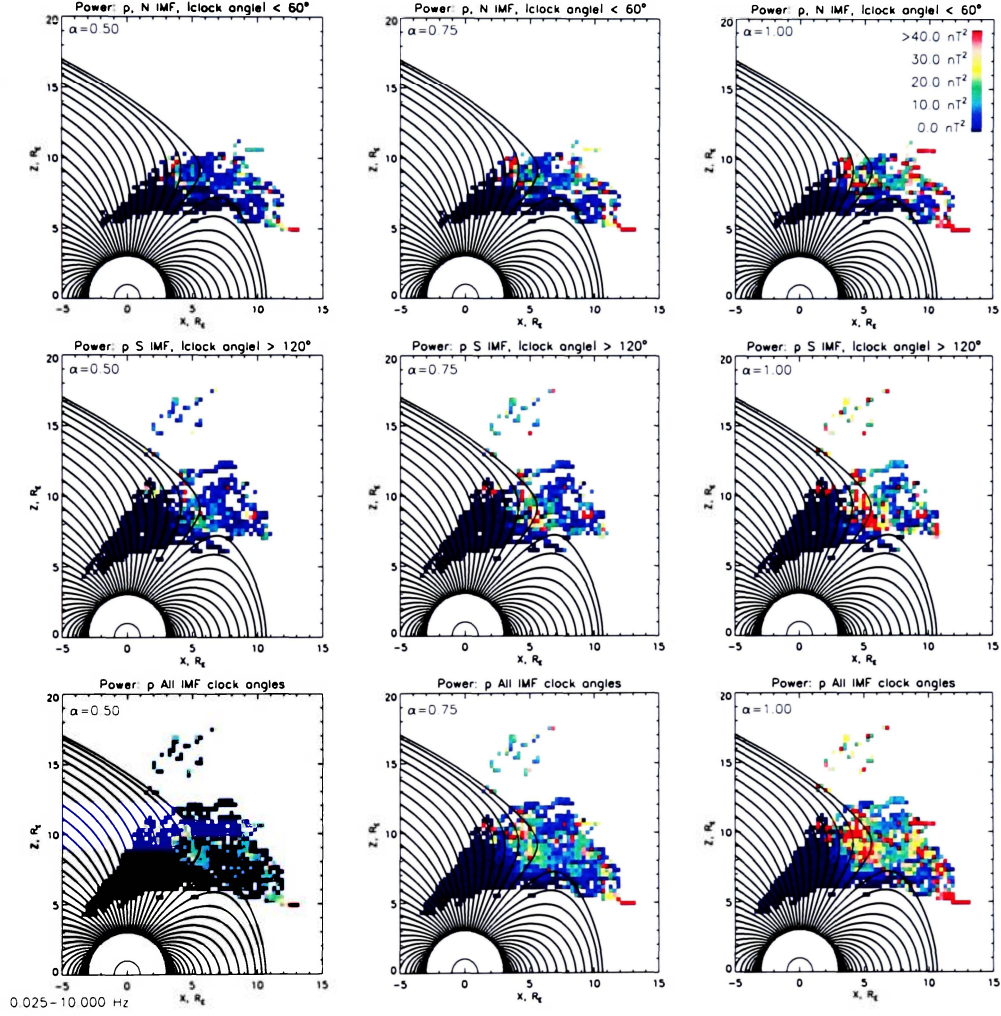


Figure B.6: Perpendicular integrated power for the magnetic field fluctuations of the 0.025-10 Hz frequency range for NIMF, SIMF, and AIMF (rows) and Hanning window with  $\alpha = 0.5, 0.75$ , and 1 (columns).

# Appendix C

## Unnormalized Integrated Power

The normalization process is described in Chapter 3 and the normalized power is described in Chapter 4. Without the normalization process, the data would appear as shown below in Figures C.1-C.3. The figures show the unnormalized mean, total, and perpendicular integrated power for NIMF, SIMF, and AIMF. Figure C.1 shows 0.017-10 Hz, Figure C.2 shows 0.017-0.1 Hz, and Figure C.3 shows 0.1-10 Hz.

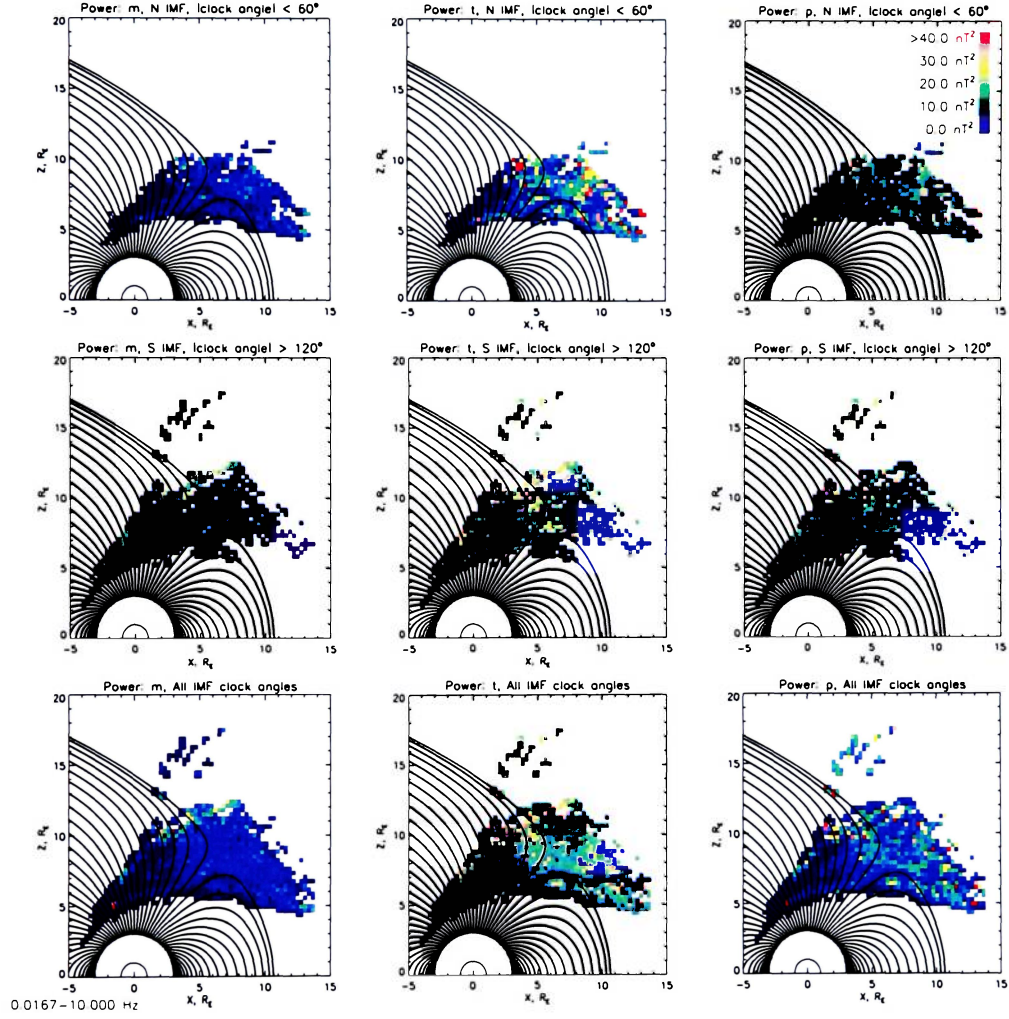


Figure C.1: Unnormalized integrated mean, total, and perpendicular power in the magnetic field fluctuations of the 0.017-10 Hz frequency range for NIMF, SIMF, and AIMF.



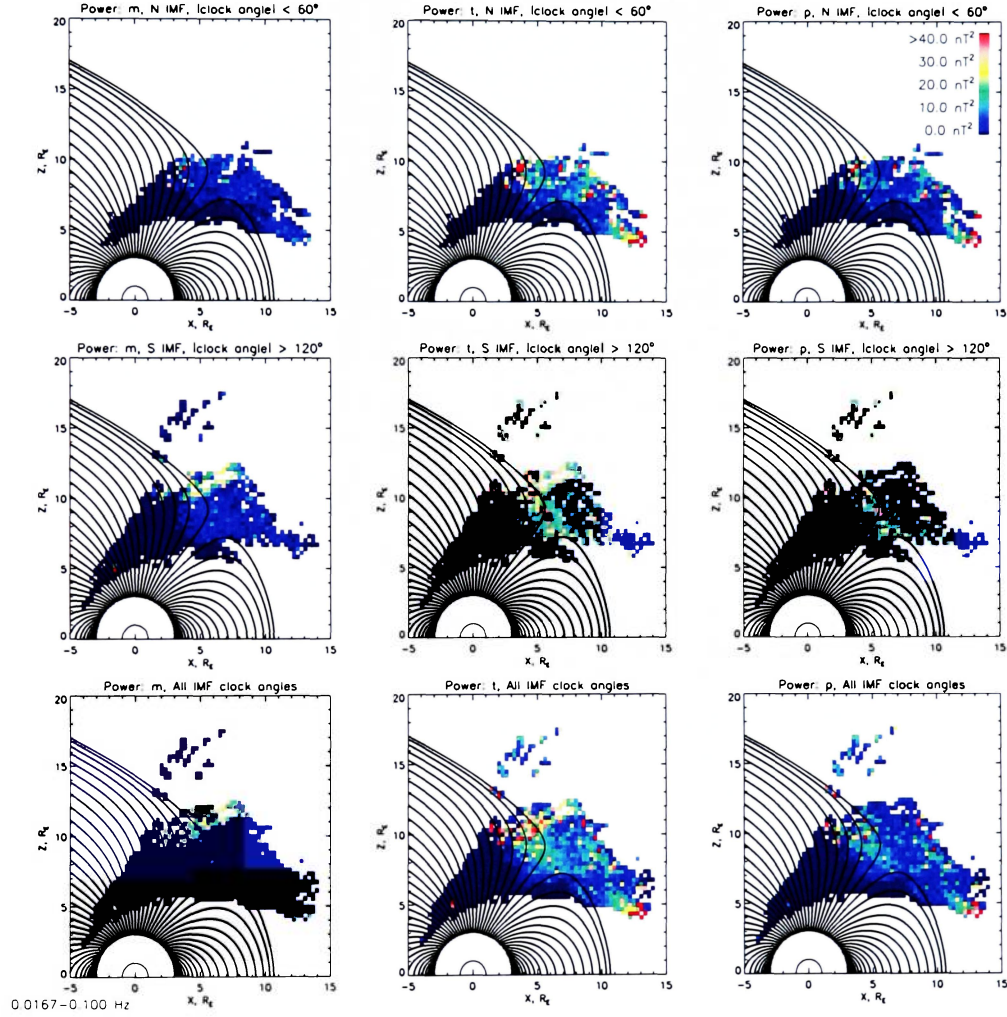


Figure C.2: Unnormalized integrated mean, total, and perpendicular power in the magnetic field fluctuations of the 0.017-0.1 Hz frequency range for NIMF, SIMF, and AIMF.



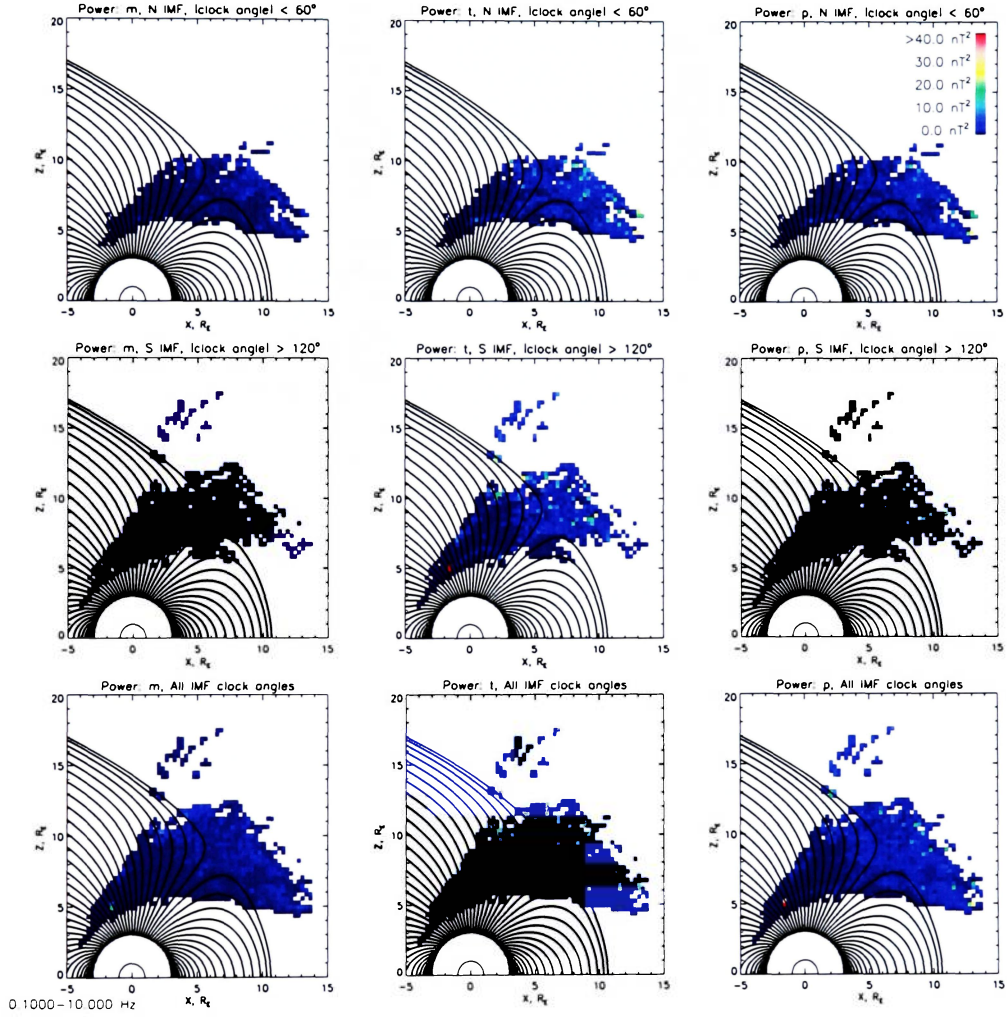


Figure C.3: Unnormalized integrated mean, total, and perpendicular power in the magnetic field fluctuations of the 0.1-10 Hz frequency range for NIMF, SIMF, and AIMF.

## Appendix D

### Integrated Power Figures: Size Scaled by Number of Data Points Averaged

Each data square in the power figures before this appendix represents  $0.3 R_e \times 0.3 R_e$  unless otherwise stated. In order to depict the number of data points averaged in each  $0.3 R_e \times 0.3 R_e$  region of space, each colored square in this Appendix has been scaled according to the number of data points averaged, with size saturation of  $0.3 R_e$  at 20 or more data points [Lavraud *et al.* 2004, 2005]. These figures show the normalized mean, total, and perpendicular integrated power for NIMF, SIMF, and AIMF. Figure D.1 show 0.017-10 Hz. Figure D.2 shows 0.017-1 Hz. Figure D.3 shows 0.1-10 Hz.

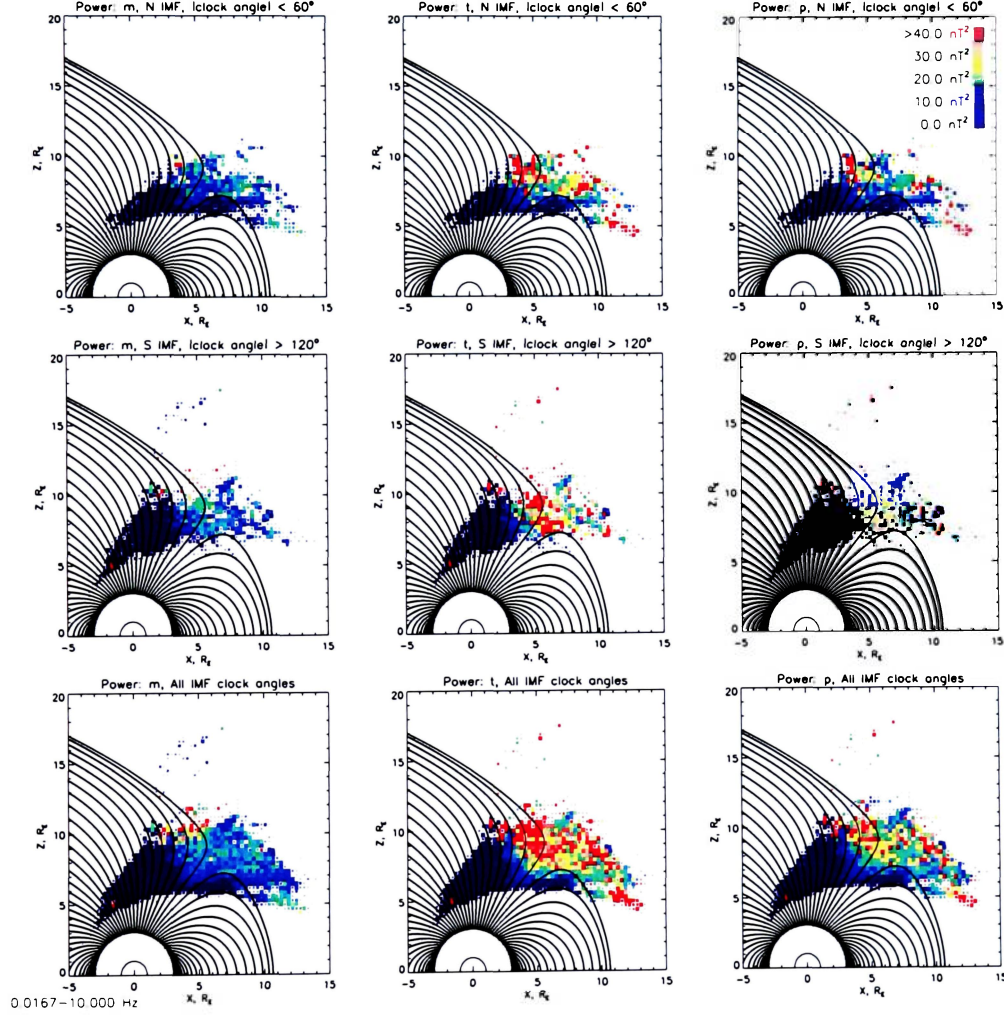


Figure D.1: Normalized integrated power, with size scaled to the number of data points averaged, for the mean, total, and perpendicular power in the magnetic field fluctuations of the 0.017-10 Hz frequency range for NIMF, SIMF, and AIMF.

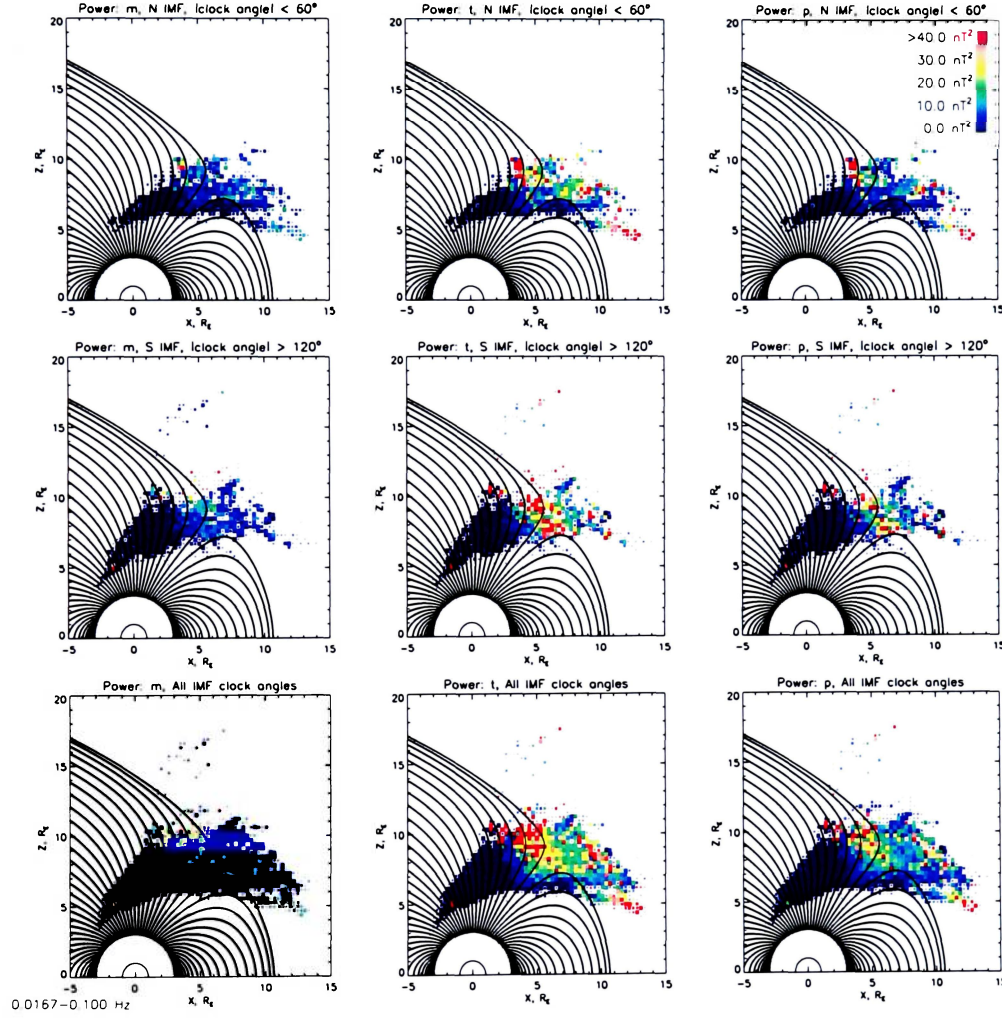


Figure D.2: Normalized integrated power, with size scaled to the number of data points averaged, for the mean, total, and perpendicular power in the magnetic field fluctuations of the 0.017-0.1 Hz frequency range for NIMF, SIMF, and AIMF.



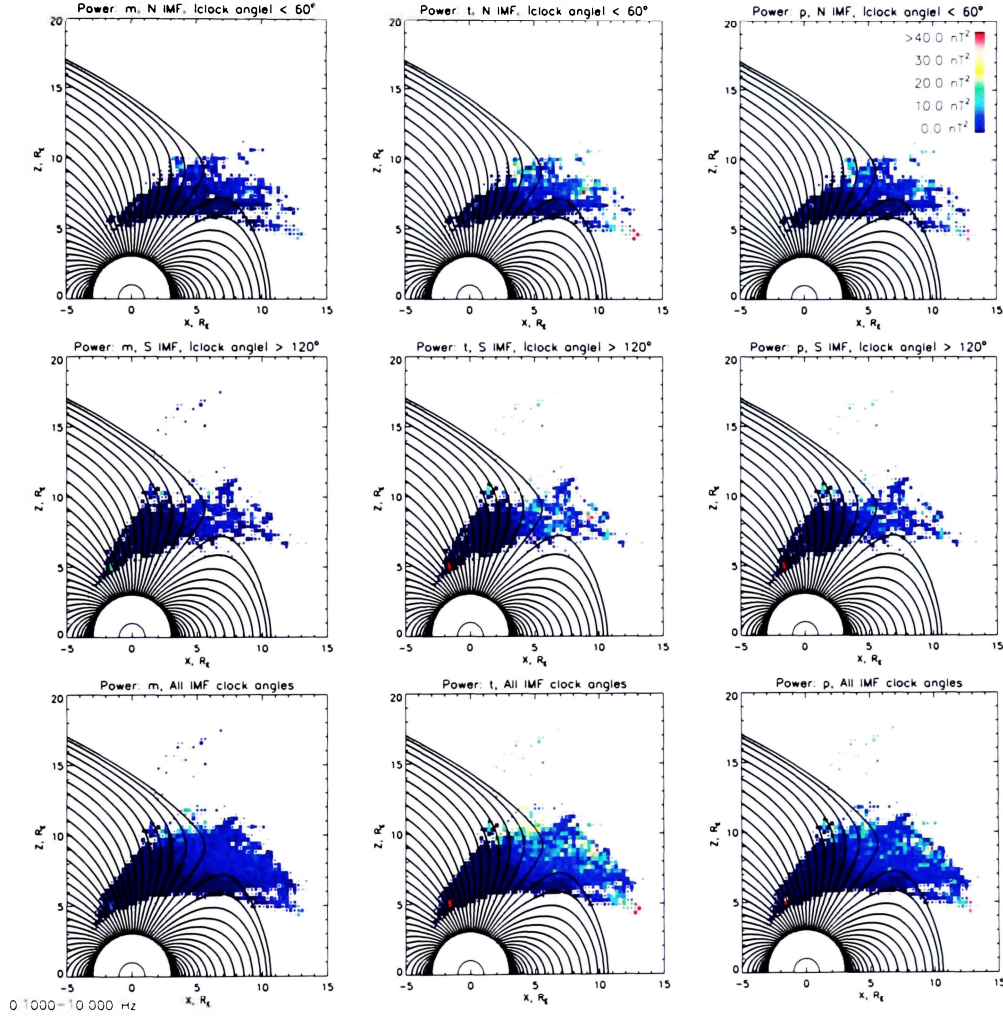


Figure D.3: Normalized integrated power, with size scaled to the number of data points averaged, for the mean, total, and perpendicular power in the magnetic field fluctuations of the 0.1-10 Hz frequency range for NIMF, SIMF, and AIMF.

# Bibliography

- Asikainen, T., and K. Mursula, Energetic particle fluxes in the exterior cusp and the high-latitude dayside magnetosphere: statistical results from the Cluster/RAPID instrument, *Annales Geophysicae*, *23*, 2217–2230, 2005.
- Asikainen, T., and K. Mursula, Reconnection and energetic particles at the edge of the exterior cusp, *Annales Geophysicae*, *24*, 1949–1956, 2006.
- Balogh, A., C. M. Carr, M. H. Acuña, M. W. Dunlop, T. J. Beek, P. Brown, K.-H. Fornacon, E. Georgescu, K.-H. Glassmeier, J. Harris, G. Musmann, T. Oddy, and K. Schwingenschuh, The cluster magnetic field investigation: overview of in-flight performance and initial results, *Annales Geophysicae*, *19*, 1207–1217, 2001.
- Cargill, P., M. Dunlop, B. Lavraud, R. Elphic, D. Holland, K. Nykyri, A. Balogh, I. Dandouras, and H. Rème, CLUSTER encounters with the high altitude cusp: boundary structure and magnetic field depletions, *Annales Geophysicae*, *22*, 1739–1754, 2004.
- Carozzi, T., B. Thidé, and T. Leyser, Full polarimetry measurements of stimulated electromagnetic emissions: First results, *Journal of Geophysical Research*, *106*, 21,395–21,407, 2001.
- Chang, S., J. D. Scudder, S. A. Fuselier, J. F. Fennell, K. J. Trattner, J. S. Pickett, H. E. Spence, J. D. Menietti, W. K. Peterson, R. P. Lepping, and R. Friedel, Cusp energetic ions: A bow shock source, *Geophysical Research Letters*, *25*, 3729–3732, 1998.

- Chapman, S., and V. C. A. Ferraro, A New Theory of Magnetic Storms, *Nature*, *126*, 129–130, 1930.
- Chen, J., Evidence for particle acceleration in the magnetospheric cusp, *Annales Geophysicae*, *26*, 1993–1997, 2008.
- Chen, J., and T. A. Fritz, Correlation of cusp MeV helium with turbulent ULF power spectra and its implications, *Geophysical Review Letters*, *25*, 4113–4116, 1998.
- Denton, R. E., S. P. Gary, X. Li, B. J. Anderson, J. W. Labelle, and M. Lessard, Low-frequency fluctuations in the magnetosheath near the magnetopause, *Journal of Geophysical Research*, *100*, 5665–5679, 1995.
- Dungey, J. W., Interplanetary magnetic field and the auroral zones, *Physical Review Letters*, *6*, 47–48, 1961.
- Dungey, J. W., The structure of the exosphere or adventures in velocity space, in *Geophysics: The Earth's Environment*, edited by C. Dewitt, J. Hieblot, and A. Lebeau, pp. 526–536, Gordon and Breach, New York, 1963.
- Dunlop, M. W., P. J. Cargill, T. J. Stubbs, and P. Woolliams, The high-altitude cusps: HEOS 2, *Journal of Geophysical Research*, *105*, 27,509–27,518, 2000.
- Frank, L. A., and K. L. Ackerson, Observations of charged particle precipitations into the auroral zone, *Journal of Geophysical Research*, *76*, 3612–3643, 1971.
- Fuselier, S. A., D. M. Klumpp, and E. G. Shelley, On the origins of energetic ions in the earth's dayside magnetosheath, *Journal of Geophysical Research*, *96*, 47–56, 1991.
- Harris, F. J., On the use of windows for harmonic analysis with the discrete fourier transform, *Proceedings of the IEEE*, *66*, 51–83, 1978.
- Hasegawa, A., Drift mirror instability of the magnetosphere., *Physics of Fluids*, *12*, 2642–2650, 1969.

- Heikkilä, W. J., and J. D. Winningham, Penetration of magnetosheath plasma to low altitudes through the dayside magnetospheric cusps, *Journal of Geophysical Research*, **76**, 883–891, 1971
- Imperial College Cluster Fluxgate Magnetometer Image, [http://www3.imperial.ac.uk/spat/research/missions/space\\_missions/clusterhomepage/cluster\\_magnetometer\\_instrument](http://www3.imperial.ac.uk/spat/research/missions/space_missions/clusterhomepage/cluster_magnetometer_instrument), 2000
- Kessel, R. L., S. Chen, J. L. Green, S. F. Fung, S. A. Boardsen, L. C. Tan, T. E. Eastman, J. D. Craven, and L. A. Frank, Evidence of high-latitude reconnecting during northward IMF Hawkeye observations, *Geophysical Research Letters*, **23**, 583–586, 1996
- Lavraud, B., M. W. Dunlop, T. D. Phan, H. Rème, J. Bosqued, I. Dandouras, J. Sauvaud, R. Lundin, M. G. G. T. Taylor, P. J. Cargill, C. Mazelle, C. P. Escoubet, C. W. Carlson, J. P. McFadden, G. K. Parks, E. Moebius, L. M. Kistler, M. Bavassano-Cattaneo, A. Korth, B. Klecker, and A. Balogh, Cluster observations of the exterior cusp and its surrounding boundaries under northward IMF, *Geophysical Research Letters*, **29**, 2002
- Lavraud, B., A. Fedorov, E. Budnik, A. Grigoriev, P. J. Cargill, M. W. Dunlop, H. Rème, I. Dandouras, and A. Balogh, Cluster survey of the high-altitude cusp properties: a three-year statistical study, *Annales Geophysicae*, **22**, 3009–3019, 2004
- Lavraud, B., A. Fedorov, E. Budnik, M. F. Thomsen, A. Grigoriev, P. J. Cargill, M. W. Dunlop, H. Rème, I. Dandouras, and A. Balogh, High-altitude cusp flow dependence on IMF orientation: A 3-year cluster statistical study, *Journal of Geophysical Research*, **110**, 2005
- Le, G., X. Blanco-Cano, C. T. Russell, X. Zhou, F. Mozer, K. J. Trattner, S. A. Fuselier, and B. J. Anderson, Electromagnetic ion cyclotron waves in the high altitude cusp: Polar observations, *Journal of Geophysical Research*, **106**, 19,067–19,080, 2001



- Lin, N., C. A. Cattell, M. J. Engebretson, R. P. Lepping, R. P. Lin, and S. Kokubun, Substorm associated magnetotail field and plasma fluctuations: a case study, in *Fifth International Conference on Substorms*, edited by A. Wilson, pp. 623–626, 2000.
- Ma, Z. W., L. C. Lee, and A. Otto, Generation of field-aligned currents and Alfvén waves by 3D magnetic reconnection, *Geophysical Research Letters*, *22*, 1737–1740, 1995.
- Martin, G., *Introduction to Sound Recording*, 2007.
- NASA, Magnetosphere image, <http://sec.gsfc.nasa.gov/popscise.jpg>.
- Newell, P. T., C. Meng, D. G. Sibeck, and R. Lepping, Some low-altitude cusp dependencies on the interplanetary magnetic field, *Journal of Geophysical Research*, *94*, 8921–8927, 1989.
- Niehof, J. T., T. A. Fritz, R. H. W. Friedel, and J. Chen, Size and location of cusp diamagnetic cavities observed by Polar, *Journal of Geophysical Research (Space Physics)*, *115*, 2010.
- Nykyri, K., P. J. Cargill, E. A. Lucek, T. S. Horbury, A. Balogh, B. Lavraud, I. Dandouras, and H. Rème, Ion cyclotron waves in the high altitude cusp: CLUSTER observations at varying spacecraft separations, *Geophysical Research Letters*, *30*, 2003.
- Nykyri, K., P. Cargill, E. Lucek, T. Horbury, B. Lavraud, A. Balogh, M. Dunlop, Y. Bogdanova, A. Fazakerley, I. Dandouras, and H. Rème, Cluster observations of magnetic field fluctuations in the high-altitude cusp, *Annales Geophysicae*, *22*, 2413–2429, 2004.
- Nykyri, K., B. Grison, P. J. Cargill, B. Lavraud, E. Lucek, I. Dandouras, A. Balogh, N. Cornilleau-Wehrin, and H. Rème, Origin of the turbulent spectra in the high-altitude cusp: Cluster spacecraft observations, *Annales Geophysicae*, *24*, 1057–1075, 2006.

- Nykyri, K., A. Otto, E. Adamson, B. Lavraud, E. Dougal, and J. Mumme, Cluster observations of a cusp diamagnetic cavity: Structure, size, and dynamics, 2010a, submitted to the Journal of Geophysical Research.
- Nykyri, K., A. Otto, E. Adamson, and A. Tjulin, On the origin of fluctuations in the cusp diamagnetic cavity, 2010b, submitted to the Journal of Geophysical Research.
- Paschmann, G., G. Haerendel, N. Sckopke, H. Rosenbauer, and P. C. Hedgecock, Plasma and magnetic field characteristics of the distant polar cusp near local noon The entry layer, *Journal of Geophysical Research*, *81*, 2883–2899, 1976.
- Richards, G., A middle riemann sum of  $x^3$  over  $[0,2]$  using 4 subdivisions, <http://en.wikipedia.org/wiki/File:MidRiemann2.svg#file>.
- Russell, C. T., The Polar Cusp, *Advances in Space Research*, *25*, 1413–1424, 2000.
- Sandahl, I., B. Popielawska, E. Budnick, A. Fedorov, S. Savin, J. Safrankova, and Z. Nemecek, The Cusp as seen from Interball, in *Cluster-II Workshop Multiscale / Multipoint Plasma Measurements*, edited by R. A. Harris, vol. 449 of *ESA Special Publication*, 2000.
- Savin, S., L. Zelenyi, N. Maynard, I. Sandahl, H. Kawano, C. T. Russell, S. Romanov, E. Amata, L. Avanov, J. Blecki, J. Buechner, G. Consolini, G. Gustafsson, S. Klimov, F. Marcucci, Z. Nemecek, B. Nikutowski, J. Pickett, J. L. Rauch, J. Safrankova, A. Skalsky, V. Smirnov, K. Stasiewicz, P. Song, J. G. Trotignon, and Y. Yermolaev, Multi-spacecraft tracing of turbulent boundary layer, *Advances in Space Research*, *30*, 2821–2830, 2002.
- Savin, S., L. Zelenyi, S. Romanov, I. Sandahl, J. Pickett, E. Amata, L. Avanov, J. Blecki, E. Budnik, J. Büchner, C. Cattell, G. Consolini, J. Fedder, S. Fuselier, H. Kawano, S. Klimov, V. Korepanov, D. Lagoutte, F. Marcucci, M. Mogilevsky, Z. Nemecek, B. Nikutowski, M. Nozdrachev, M. Parrot, J. Rauch, V. Romanov, T. Romantsova, C. Russell, J. Safrankova, J. Sauvaud, A. Skalsky, V. Smirnov, K. Stasiewicz, J. Trotignon, and Y. Yermolaev, Magnetosheath-cusp interface. *Annales Geophysicae*, *22*, 183–212, 2004.

- Savin, S. P., S. A. Romanov, A. O. Fedorov, L. Zelenyi, S. I. Klimov, Y. I. Yermolaev, E. Y. Budnik, N. S. Nikolaeva, C. T. Russell, X. Zhou, A. L. Urquhart, and P. H. Reiff, The cusp/magnetosheath interface on May 29, 1996: Interball-1 and polar observations, *Geophysical Research Letters*, *25*, 2963–2966, 1998.
- Schwartz, S. J., D. Burgess, and J. J. Moses, Low-frequency waves in the Earth's magnetosheath: present status, *Annales Geophysicae*, *14*, 1134–1150, 1996.
- Shannon, C. E., Communication in the presence of noise, *Proceedings of the Institute of Radio Engineers*, *37*, 10–21, 1949.
- Shue, J., J. K. Chao, H. C. Fu, C. T. Russell, P. Song, K. K. Khurana, and H. J. Singer, A new functional form to study the solar wind control of the magnetopause size and shape, *Journal of Geophysical Research*, *102*, 9497–9512, 1997.
- Sibeck, D. G., R. W. McEntire, A. T. Y. Lui, R. E. Lopez, and S. M. Krimigis, Energetic magnetospheric ions at the dayside magnetopause - Leakage or merging?, *Journal of Geophysical Research*, *92*, 12,097–12,114, 1987.
- Sonnerup, B. U. Ö., and M. Scheible, Minimum and Maximum Variance Analysis, *Analysis Methods for Multi-Spacecraft Data / Götz Paschmann and Patrick Daly (eds.). ISSI Scientific Reports Series, ESA/ISSI, Vol. 1. ISBN 1608-280X, 1998, p. 185-220, 1*, 185–220, 1998.
- Soucek, J., and E. Lucek, Properties and evolution of magnetosheath mirror mode structures observed by cluster, 2010, GEM conference powerpoint obtained from personal communication.
- Soucek, J., E. Lucek, and I. Dandouras, Properties of magnetosheath mirror modes observed by Cluster and their response to changes in plasma parameters, *Journal of Geophysical Research (Space Physics)*, *113*, 2008.
- Sundkvist, D., A. Vaivads, M. André, J. Wahlund, Y. Hobara, S. Joko, V. V. Krasnoselskikh, Y. V. Bogdanova, S. C. Buchert, N. Cornilleau-Wehrlin, A. Fazakerley,

- J. Hall, H. Rème, and G. Stenberg, Multi-spacecraft determination of wave characteristics near the proton gyrofrequency in high-altitude cusp, *Annales Geophysicae*, *23*, 983–995, 2005.
- Trattner, K. J., S. A. Fuselier, W. K. Peterson, S. Chang, R. Friedel, and M. R. Aellig, Origins of energetic ions in the cusp, *Journal of Geophysical Research*, *106*, 5967–5976, 2001.
- Tsyganenko, N. A., Modeling the Earth’s magnetospheric magnetic field confined within a realistic magnetopause, *Journal of Geophysical Research*, *100*, 5599–5612, 1995.
- Tsyganenko, N. A., Effects of the solar wind conditions in the global magnetospheric configurations as deduced from data-based field models (Invited), in *International Conference on Substorms*, edited by E. J. Rolfe & B. Kaldeich, vol. 389 of *ESA Special Publication*, 1996.
- University of Sheffield Space Systems Team, Cluster II Satellites Prelaunch Image, [http://www.ssg.group.shef.ac.uk/pictures/photos/cluster\\_sc\\_large.gif](http://www.ssg.group.shef.ac.uk/pictures/photos/cluster_sc_large.gif), 2000.
- Vonrat-Reberac, A., J. M. Bosqued, M. G. G. T. Taylor, B. Lavraud, D. Fontaine, M. W. Dunlop, H. Laakso, N. Cornilleau-Werhlin, P. Canu, and A. Fazakerley, Cluster observations of the high-altitude cusp for northward interplanetary magnetic field: A case study, *Journal of Geophysical Research (Space Physics)*, *108*, 2003.
- Yamauchi, M., R. Lundin, and T. A. Potemra, Dynamic response of the cusp morphology to the interplanetary magnetic field changes: An example observed by Viking, *Journal of Geophysical Research*, *100*, 7661–7670, 1995.
- Zhou, X., C. T. Russell, G. Le, S. A. Fuselier, and J. D. Scudder, The polar cusp location and its dependence on dipole tilt, *Geophysical Research Letters*, *26*, 429–432, 1999.

- 
- Zhou, X. W., C. T. Russell, G. Le, S. A. Fuselier, and J. D. Scudder, Solar wind control of the polar cusp at high altitude, *Journal of Geophysical Research*, 105, 245–252, 2000.